Optimization of Dissolved Air Flotation for Drinking Water Treatment

by

Benjamin James Bickerton

Submitted in partial fulfilment of the requirements
for the degree of Master of Applied Science

at

Dalhousie University
Halifax, Nova Scotia
August 2012

DALHOUSIE UNIVERSITY

DEPARTMENT OF CIVIL AND RESOURCE ENGINEERING

The undersigned hereby certify that they have read and recommend to the Faculty of Graduate Studies for acceptance a thesis entitled "Optimization of Dissolved Air Flotation for Drinking Water Treatment" by Benjamin James Bickerton in partial fulfilment of the requirements for the degree of Master of Applied Science.

Dated: August 10, 2012

Supervisor: _____

Readers: _____

_____

DALHOUSIE UNIVERSITY

DATE: August 10, 2012

AUTHOR: Benjamin James Bickerton

TITLE: Optimization of Dissolved Air Flotation for Drinking Water Treatment

DEPARTMENT OR SCHOOL: Department of Civil and Resource Engineering

DEGREE: MASc. CONVOCATION: October YEAR: 2012

_____

Signature of Author

Table of Contents

List of Tables

List of Figures

Abstract

The use of dissolved air flotation (DAF) for drinking water treatment has steadily grown in popularity in Atlantic Canada for the treatment of low turbidity water supplies with high levels of algae or dissolved organic matter. Runoff from high intensity rainfall events may cause a rapid increase in turbidity and dissolved organic matter in rivers and lakes used for drinking water.

A technical evaluation of a DAF water treatment plant (WTP) was conducted to determine the contributing factors to clearwell turbidity increases resulting from increased raw water turbidity and colour during intense rainfall and runoff events. The effect of chemical and operational factors on treatment of a low turbidity and colour water source as well as a high turbidity and colour water source were examined, including coagulant dose, coagulation pH, polyaluminum chloride (PACl) coagulant basicity and DAF recycle rate.

In response to deteriorating water quality, it was found that increased coagulant addition inadvertently caused the loss of coagulation pH control in a full-scale DAF WTP, resulting in potentially elevated dissolved aluminum residuals entering the clearwell. This would have led to excessive aluminum hydroxide precipitation in the clearwell, and resulted in turbidity increases above the acceptable limit of 0.2 NTU.

Turbidity was found to be better removed, and dissolved aluminum residuals minimized, when coagulation pH was set to the pH of minimum aluminum solubility vs. a lower pH of 6.0 during bench-scale DAF testing. A higher dose of coagulant was required to produce optimal removal of turbidity and dissolved organics at the pH of minimum solubility. The difference in bench-scale DAF treatment performance was found to be minimal when comparing sulphated PACl coagulants with 50 and 70+ % basicity. Charge analysis parameters zeta potential and streaming current were found to have a strong correlation in bench-scale testing, though the relationship between the two was affected by the coagulation pH. The results suggest that utilizing streaming current for coagulant dose control at a full-scale WTP would be best accomplished by establishing a consistent relationship between raw water quality, pH and other factors with streaming current experimentally before relying streaming current targets for dose control.

Equivalent or improved DAF efficacy for solid-liquid separation was found when the recycle rate was lowered from 12 to 6 % in bench-scale tests and 12 to 8% in full-scale tests. The results suggested that maintaining an optimum air:solids ratio improved treatment performance, possibly by providing adequate bubble contact opportunities while minimizing excess shearing of the sludge blanket.

The most significant finding of this research was that maintaining the coagulation pH in WTPs utilizing PACl coagulants is of utmost importance during source water quality deterioration in order to optimize treatment performance as well as prevent excess dissolved and precipitated aluminum from entering a public drinking water supply.

List of Abbreviations and Symbols Used

%	percent
°C	degrees Celsius
ρ	density
σ	surface tension of water
Al	aluminum
$Al(OH)_3$	aluminum hydroxide
alum	aluminum sulphate; $Al_2(SO_4)_3$
ANC	acid neutralizing capacity
ANOVA	analysis of variance
aq	aqueous; dissolved
$B(OH)_4$	borate
BBWTP	Brierly Brook Water Treatment Plant
$Ca(OH)_2$	lime
$CaCO_3$	calcium carbonate
CaO	quicklime
CCC	chlorine contact chamber
C_d	coefficient of discharge in orifice equation
CFU/100 mL	colony forming units per 100 millilitres
cm	centimeter
CO_2	carbon dioxide
CO_3	carbonate
cts/mL	counts per millilitre
CU	colour units
DAF	dissolved air flotation
D_b	bubble diameter
DBP	disinfection by-product
D_{cb}	critical bubble diameter
D_{fb}	floc-bubble aggregate diameter
DLVO	Deryagin-Landau-Verway-Overbeek
DOC	dissolved organic carbon

E. coli	*Escherichia coli*
g	gravitational constant, 9.81 m/s^2
GCDWQ	Guidelines for Canadian Drinking Water Quality
G-value	velocity gradient
H_2CO_3	carbonic acid
H_2O	water
HAA	haloacetic acid
HB	high basicity
HCO_3	bicarbonate
HLR	hydraulic loading rate
h	hour
ICP-MS	inductively coupled plasma mass spectrophotometer
kPa	kilopascals
L	litre
LB	low basicity
m	meter
m^3/h	cubic meters per hour
MAC	maximum acceptable concentration
MCL	maximum contaminant level
meq/L	milliequivalents per litre
MFI	MicroFlow Imaging
mg/L	milligrams per litre
min	minute
mm	millimeter
mV	millivolts
µeq/L	microequivalents per litre
µL	microlitre
µm	micrometer; micron
µS/cm	microsiemens per centimeter
μ_w	dynamic viscosity of water
Na(OH)	sodium hydroxide; caustic soda; caustic
Na_2CO_3	sodium carbonate; soda ash

$NaHCO_3$	sodium bicarbonate
ng	nanogram
NH_3	ammonia
nm	nanometer
NO_3	nitrate
NOM	natural organic matter
NTU	nephelometric turbidity units
OH	hydroxide
PACl	polyaluminum chloride
PO_4	phosphate
polyDADMAC	polydiallyldimethylammonium chloride
ppb	parts per billion
Q	flowrate
RO	reverse osmosis
rpm	revolutions per minute
RR	recycle rate
s	second
SC	streaming current
SCADA	supervisory control and data acquisition
SCM	streaming current meter
SO_4	sulphate
SUVA	specific ultraviolet absorbance
THM	trihalomethane
TOC	total organic carbon
USEPA	United States Environmental Protection Agency
UV_{254}	ultraviolet absorbance at 254 nanometer wavelength
WTP	water treatment plant
ZP	zeta potential
ZPC	zero point of charge

Acknowledgements

I would like to thank Dr. Margaret Walsh for her continual guidance, beginning from my initial decision to pursue graduate studies and continuing all the way through to the completion of this thesis.

I would also like to thank Dr. Graham Gagnon and Dr. Rob Jamieson for reviewing this thesis and providing valuable insight.

The Natural Sciences and Engineering Research Council of Canada provided funding for this project, which could not have been completed without the collaboration of Antigonish Town Engineer Ken Proctor and Brierly Brook Water Treatment Plant operators Wayne March and Joe Landry.

I would like to acknowledge research assistant Monica McVicar and laboratory manager Heather Daurie for their contributions to my work in the Dalhousie Clean Water Laboratory, as well as my colleagues in Dr. Walsh's and Dr. Gagnon's research groups.

Chapter 1: Introduction

Dissolved air flotation (DAF) is a solid-liquid separation process utilized in drinking water treatment. The use of DAF in the clarification stage of drinking water treatment plants (WTPs) originated in the 1960s and has become common in systems treating low turbidity water sources, and is highly effective for the removal of algae and organic matter (Haarhoff, 2008). DAF is used as an alternative to settling or sedimentation clarification which is more effective for high turbidity water sources, particularly those where turbidity is derived from mineral, rather than organic, sources (Valade *et al*., 2010). Like sedimentation, DAF requires coagulation-flocculation pretreatment to perform effectively (AWWA, 1997). DAF works by first dissolving air into water at high pressures and injecting the water into the bottom of a DAF clarifier. The subsequent drop in pressure forces microbubbles to form, which attach to flocs as they rise to the surface of the clarifier, where they are removed (Edzwald, 2010).

Since DAF is most effective in treating source water with specific characteristics, rapid deterioration of source water quality due to rainfall and runoff events may be detrimental to treatment performance. As global climate models project warmer temperatures and more frequent high intensity storm events, optimizing DAF performance during these challenging conditions is critical to ensuring no deterioration of treated water quality occurs (Bates *et al.*, 2008). The experiments and analyses performed as part of this research study were founded on the hypothesis that optimizing coagulation chemistry and operations in the DAF process can improve treatment performance during challenging source water conditions.

1.1 Objectives

Three research phases were completed in this thesis to reach the following objectives:

1. Conduct a comprehensive technical assessment of a DAF WTP to determine the potential impacts of rapid deterioration of source water quality during intense rainfall events on treatment performance;
2. Evaluate key chemical parameters related to DAF treatment at the bench-scale;
3. Examine the effect of recycle rate on DAF performance at both bench and full-scale.

1.2 Thesis Organization

Chapter 2 contains a detailed literature review outlining relevant background information for drinking water treatment, particularly pertaining to DAF treatment plants using polyaluminum chloride (PACl) coagulants. Chapter 3 describes the materials and methods utilized to complete this study. Chapter 4 summarizes a technical assessment conducted at the Brierly Brook Water Treatment Plant (BBWTP), including examination of treatment processes and historical data for raw and treated water quality, with special focus on conditions leading to poor performance. Chapter 5 presents results and discussion of bench-scale DAF testing, focusing on the impacts of varying pH and coagulant basicity on treatment performance. Chapter 6 outlines the results of changing the recycle rate in bench-scale DAF trials as well as full-scale trials conducted at the BBWTP on DAF treatment performance. Chapter 7 concludes this work by summarizing the major findings of the study and presents recommendations for future research.

1.3 Originality of Research

There has been much research evaluating the efficacy of DAF clarification for drinking water treatment while examining the effect of a multitude of factors, such as alternative coagulants, coagulation and flocculation mixing gradients, hydraulic loading rates and raw water characteristics (Valade *et al*., 2009; Haarhoff, 2008; Edzwald, 2007; Teixeira & Rosa, 2006; Bunker *et al*., 1995, Edzwald & Wingler, 1990). DAF as a technology for drinking water treatment has only existed in Canada within the past two decades, however, and much research aimed at optimizing DAF in water treatment plants does not consider factors such as low temperatures, pH and alkalinity found in Atlantic Canada surface waters. Furthermore, little research has been done on optimizing the coagulation-flocculation-DAF process on rapidly changing source water quality conditions which exist due to rainfall and runoff, quickly adding high amounts of turbidity or dissolved organics to an otherwise high quality water supply. Considering that most climate models project an increase in high intensity storm events in the future (Bates *et al.*, 2008), it is prudent to investigate how DAF treatment performance is affected under these circumstances using typical Atlantic Canada source water.

Chapter 2: Literature Review

An extensive literature review has been conducted investigating issues related to drinking water treatment in Nova Scotia as well as contaminants of concern in drinking water, coagulation and flocculation in drinking water treatment, dissolved air flotation (DAF) and its application in drinking water treatment plants, and the combined effects of factors within each of these topics.

2.1 Drinking Water Treatment in Nova Scotia

A breakdown of the population served by these municipal water utilities is provided in Figure 2.1, showing the population served and number of utilities (shown above columns) using direct filtration, conventional sedimentation, DAF and membrane filtration (Mosher, 2012). Of the 76 municipal water utilities producing drinking water for approximately 60 % of Nova Scotians, 39 draw from surface water supplies.

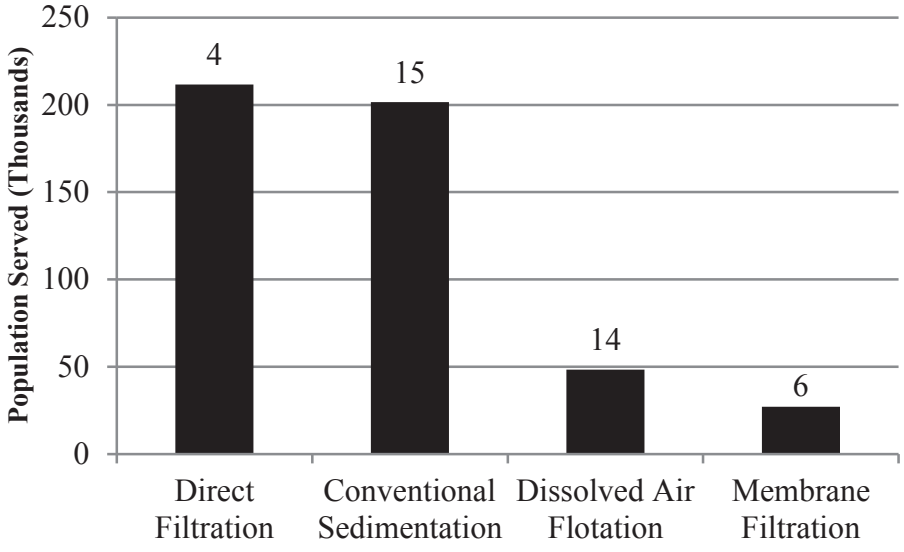

Figure 2.1. Breakdown of populations served by number and type of municipal drinking water supply.

The degree to which two large facilities exceed the treatment capacity of all other WTPs in the province can be seen in Figure 2.2. A large percentage of surface water treated in Nova Scotia passes through the J. D. Kline Water Supply Plant in Halifax, NS. Omitting this single water treatment plant (WTP), it becomes clear that conventional treatment plants (coagulation-flocculation, sedimentation and media-filtration) are the most common and largest type of WTPs in number and capacity in Nova Scotia. The Lake Major Water Supply Plant in Dartmouth accounts for over half of the conventional water treatment in the province.

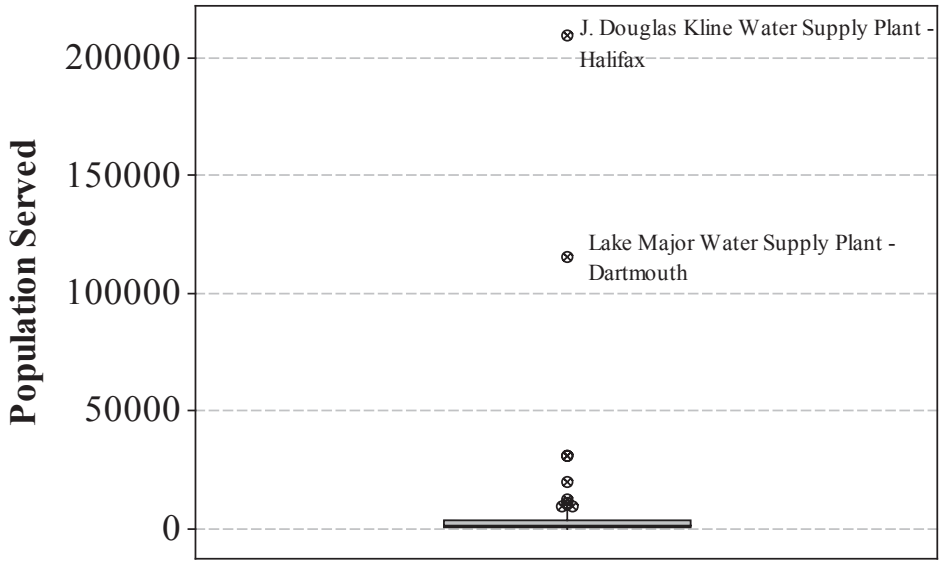

Figure 2.2. Boxplot of Nova Scotia water treatment plants by population served

Omitting the Lake Major facility, there are 14 conventional sedimentation plants and 14 DAF plants in Nova Scotia, although on average the sedimentation plants tend to be larger, and supply water for 77 % more people than DAF plants. DAF technology is

relatively new in Canada as the first drinking WTP utilizing DAF was commissioned in Port Hawkesbury, NS in 1996.

When considering which type of treatment technology research is most important in Nova Scotia, an argument could be made for each of these five major areas. However, when factoring in the bodies of research already available for more established fields such as sedimentation, direct filtration and groundwater treatment, DAF and membrane technology present the most obvious need for examination in Nova Scotia. As DAF currently serves a higher population in Nova Scotia with more treatment facilities, it was chosen to be the topic for this thesis.

2.1.1 Regulatory Bodies in Nova Scotia

The Nova Scotia Treatment Standards for Municipal Drinking Water Systems was approved on March 12, 2012 by the NS Department of Environment and replaces several other documents regarding guidelines for treatment and monitoring of drinking water in the province. The document refers to the latest version of Health Canada's Guidelines for Canadian Drinking Water Quality (GCDWQ) (Health Canada, 2010) and adopts the water quality standards outlined there as its own (Nova Scotia Environment, 2012).

2.1.2 Impact of Global Climate Change on Surface Water in Nova Scotia

Difficulty in the treatment of surface water is often due to weather events causing an upset in raw water quality used by water plants. A study by Schuster *et al*. (2005) concluded that infectious waterborne disease outbreaks in Canada from 1974 to 2001 were either caused or exacerbated by severe weather events as well as treatment malfunctions, predominately occurring in summer months or periods of heightened snowmelt.

Over half of waterborne disease outbreaks in the United States from 1948 to 1994 followed an extreme precipitation event (Curriero *et al*., 2001). The frequency of severe weather events due to global warming is expected to trend upward, with rainfall intensity increasing during these events (Bates *et al.*, 2008). The general finding in soil erosion studies is that an increase in rainfall intensity leads to an increase in turbidity and other contaminants in surface water systems due to enhanced soil fluvial erosion (Leemans & Kleidon, 2002; Bates *et al.*, 2008). In addition, the shift in winter precipitation from less erosive snow to more erosive rainfall due to increasing temperatures will also increase the number of runoff events during this season, and the decrease in snow storage may lead to further depression of summer low-flows in river systems, amplifying the effect of erosion during rainfall events (Barnett *et al.*, 2005). Under normal conditions, increased water level in streams due to runoff causes increased erosion of soil along the stream banks. Charron *et al.* (2004) state that every region in Canada is likely to be affected by climate change, with waterborne illness risk increasing due to coastal erosion and flooding, as well as periods of drought followed by heavy rainfall. The study concludes that decreased effectiveness of water treatment due to these events is considered to be a major risk factor.

2.2 Raw Water Contaminants

A variety of contaminants, introduced by natural or anthropogenic sources, is present in most raw water sources. Visually, the clarity and colour of water represent obvious indications as to its quality. However, there are many other raw water quality concerns which are less visually apparent. Natural surface waters are contaminated with pathogenic microorganisms (pathogens) which can cause waterborne disease outbreaks if not removed or inactivated in drinking water systems. In both surface and groundwater, nuisance metals such as iron and manganese may be abundant, along with more concerning elements such as arsenic, lead, mercury, radon and others depending on the area geology. Anthropogenic contributions to raw water contamination can cover a broad range of pollutants: organic and inorganic chemicals such as pesticides and polychlorinated biphenyls, pathogens from wastewater treatment or agriculture, metals from mining or industrial activity as well as a host of others.

2.2.1 Pathogens

A list of diseases and pathogens which may be spread via the feco-oral transmission route is shown in Table 2.1. The primary goal for municipal drinking water treatment is to mitigate waterborne illnesses spread by pathogens which may be present as viruses, bacteria or protozoans. There are a multitude of pathogens which may be present in waters contaminated with fecal matter, therefore indicator organisms such as *E. coli*, which are present in the fecal matter of warm-blooded animals, are used to determine whether contamination has occurred (Droste, 1997).

Table 2.1 Pathogens and diseases spread by contaminated water (Droste, 1997; Schoenen, 2002; EPA 2012).

Bacterial	Viral	Protozoan
Cholera	Poliomyelitis	Amoebiasis
Typhoid fever	Hepatitis A and E	Giardiasis
Paratyphoid fever	Enterovirus	Cryptosporidiosis
Salmonellosis	Rotavirus	Toxoplasmosis
Shigellosis	Adenovirus	Entamoeba histolytica
Yersiniosis	Norwalk-like virus	Balantidium coli
Campylobacter enteritis	Coxsackie A and B viruses	
E. coli	Echoviruses	
Leptospirosis	Reoviruses	

The GCDWQ require that there to be no detectable *E. coli* or total coliforms in public drinking water systems (Health Canada, 2010). No maximum acceptable concentration (MAC) has been established for protozoan or viral pathogens due to detection and characterization difficulties, however, a 3-log reduction of protozoans and 4-log reduction in viruses is required in WTPs treating surface waters susceptible to these pathogens (Health Canada, 2010). Fecal-contaminated surface waters cannot be easily replicated when evaluating chemical disinfectants in laboratory settings due to confounding factors such as pathogen distributions and other impurities in the water. Many viral pathogens are non-culturable in a laboratory setting, and therefore the efficacy of chemical disinfectants on these species has not been well established, and some populations such as *Cryptosporidium parvum* show no adverse effects when exposed to normal concentrations of disinfectant (Schoenen, 2002).

2.2.2 Turbidity

Turbidity is a general measure of the clarity or the water, as determined by the degree of light scattering by suspended particles. Turbidity measurements are affected by the number, size, shape and colour of particles (Gregory, 2006). Turbidity may be caused

by mineral sources, such as alumina-silicate clay particles, or non-mineral organic sources such as algae (Valade *et al*., 2010). Turbidity levels in filter effluents of WTPs are regulated under the GCDWQ and may also be monitored in the finished water supply (clearwell) and distribution system (Health Canada, 2010). Excess turbidity in filtered water indicates a process deficiency or disruption, and may reduce the effectiveness of disinfection processes by shielding pathogens (Droste, 1997; Schoenen, 2002; AWWA, 2003). In addition, particles may chemically react with disinfectants, thereby reducing disinfectant concentrations along with physically shielding pathogens (Schoenen, 2002: AWWA, 2003).

2.2.3 Natural Organic Matter and Disinfection By-Product Precursors

Natural organic matter (NOM) is a colloquial term for a broad array of complex organic material found in natural water systems. A major component of NOM is "humic" material, which is originated primarily from the decomposition of plant and animal matter, as well as microbial excretions (Duan & Gregory, 2003). NOM concentration can be approximated by measuring total and dissolved organic carbon (TOC and DOC), colour, or ultraviolet absorbance at 254 nanometers (UV_{254}) which is absorbed by the double-bonds in organic molecules. NOM has been identified as the primary precursor for organic disinfection by-products (DBPs) (Stevens *et al.*, 1976; Babcock & Singer, 1979; Christman *et al.,* 1983). A list of regulated DBPs in shown in Table 2.2. As DBPs form in the disinfection stage at a WTP, which is at the end of the treatment train, utilities are not capable of further treatment to remove these contaminants. Also, DBPs may continue to form in the distribution system after leaving the WTP. Therefore, the removal of DBP precursors prior to disinfection is the most

effective treatment practice, and coagulation practices now focus on NOM removal in conjunction with turbidity. Regulated DBPs include trihalomethanes (THMs) and haloacetic acids (HAAs); chlorinated compounds, some of which have been proven to increase cancer rates in exposed populations.

Table 2.2. Regulated DBPs.

	Trihalomethanes (THMs)	Haloacetic Acids (HAAs)
	Chloroform	Monochloroacetic acid
	Bromoform*	Dichloroacetic acid
	Dichlorobromomethane*	Trichloroacetic acid
	Dibromochloromethane*	Monobromoacetic acid*
		Dibromoacetic acid*
MAC (Canada)	100 µg/L (total)	80 µg/L (total)
MCL (U.S.)	80 µg/L (total)	60 µg/L (total)

*Only present when raw water supply contains bromine.

A Canadian study estimated the risk of cancer caused by THMs alone to be 45 cases per million in Nova Scotia, above the national average of 22 cases per million (Chowdhury *et al.*, 2011). The study only takes into account THMs, and suggests that cancer risk due to HAAs may be more severe. The total medical cost of all cancer cases due to THMs in Canada is estimated at $140 million annually. A maximum acceptable concentration (MAC) of 100 µg/L for THMs and 80 µg/L for HAAs in drinking water has been outlined in the GCDWQ (Health Canada, 2010).

2.3 Dissolved Air Flotation

DAF is a well-established alternative to sedimentation in the clarification stage of a WTP, with similar pretreatment processes (typically coagulation and flocculation) required for effective operation. DAF works by dissolving air into water at high pressure and injecting this solution into the bottom of a DAF clarifier tank. The subsequent drop in pressure causes the dissolved air to bubble out of solution and rise to the top of the clarifier. Along the way, these bubbles will attach to coagulated flocs, forming floc-bubble aggregates which collect at the top of the clarifier where they can be separated from the water. The modern application of DAF for drinking water was developed in the 1960s in Sweden and Finland, and also independently in Namibia and South Africa (Haarhoff, 2008).

DAF research has primarily focused on effects of pretreatment coagulation and flocculation processes (Valade *et al.*, 1996; Bunker *et al.*, 1995; Han & Lawler, 1992; Edzwald & Wingler, 1990), floc-bubble interactions and hydrodynamics (Haarhoff & Edzwald, 2004; Leppinen & Dalziel, 2004; Han *et al.*, 2002; Haarhoff & Edzwald, 2001; Haarhoff, 1997) and clarification basin configuration and hydraulic loading rates (HLRs) (Haarhoff, 2008; Edzwald, 2007; Dahlquist & Goransson, 2004; Edzwald *et al.*, 2004). DAF has been shown to be particularly effective in waters with low mineral turbidities and high natural colour and algae. Treatment of green algae by DAF vs. sedimentation has been shown to be increased by up to 2-log removal (Edzwald & Wingler, 1990). Cyanobacteria (blue-green algae) removal has been shown to improve from 70 to 94 % removal using sedimentation to 92 to 98 % when utilizing DAF (Teixeira and Rosa, 2006). Research has shown protozoan cyst (*Giardia lamblia* and *Cryptosporidium*

parvum) removal to be enhanced by using DAF over sedimentation (Edzwald *et al.*, 2000).

Turbidity removal efficacy of DAF is dependent on the composition of turbidity in the water. Raw water turbidities which can be effectively treated were analyzed in a North American study involving 400 WTPs by Valade *et al.* (2009). They recommended the average mineral turbidities in the source water to be no more than 10 NTU, with maximum mineral turbidity spikes no to be no greater than 50 NTU. DAF is recommended for water sources with non-mineral turbidities averaging 100 NTU or less, with spikes no greater than 200 NTU, and no upper limit on colour or TOC.

2.3.1 Dissolved Air Flotation Design

The hydraulic loading rate (HLR) is a practically important characteristic of unit operations in a WTP as it is directly related to the tank size required for the utility to meet water demand. The HLR for a DAF clarifier is calculated as shown in Equation 2.1.

$$HLR = \frac{\text{Treated Flow}}{\text{Total Clarifier Footprint}} \qquad \text{Equation 2.1}$$

where, HLR = hydraulic loading rate (m/h)
Treated Flow = clarifier effluent flow, not including recycle flow (m^3/h)
Total Clarifier Footprint = footprint area including contact and separation zones of clarifier (m^2)

DAF is a high-rate clarification process with nominal HLRs ranging from 5 to 40 m/h, as opposed to sedimentation loading rates which are 0.5 to 5 m/h, both depending on factors such as water quality, temperature and basin configuration (Droste, 1997; Edzwald, 2010). A typical DAF treatment train vs. conventional sedimentation is shown in Figure 2.3. Flocculation pretreatment for sedimentation clarification is

designed to produce large flocs, on the order of hundreds of microns, to facilitate faster settling speeds, which requires longer and gentler flocculation mixing processes; DAF is most effective with smaller flocs 25 to 50 microns in diameter (Edzwald, 2010). DAF clarification works well with a condensed flocculation stage, with modern DAF plants utilizing flocculation detention times as low as 5 to 10 minutes vs. 20 to 30 minutes in sedimentation plants (Edzwald, 2006; Haarhoff, 2008). Flocculation times for DAF as low as 2.5 minutes have been demonstrated to be effective at the bench-scale (Bunker *et al.*, 1995). Lower detention times in the flocculation/clarification stages allow DAF plants to have a smaller plant footprint, reducing capital costs for plant construction.

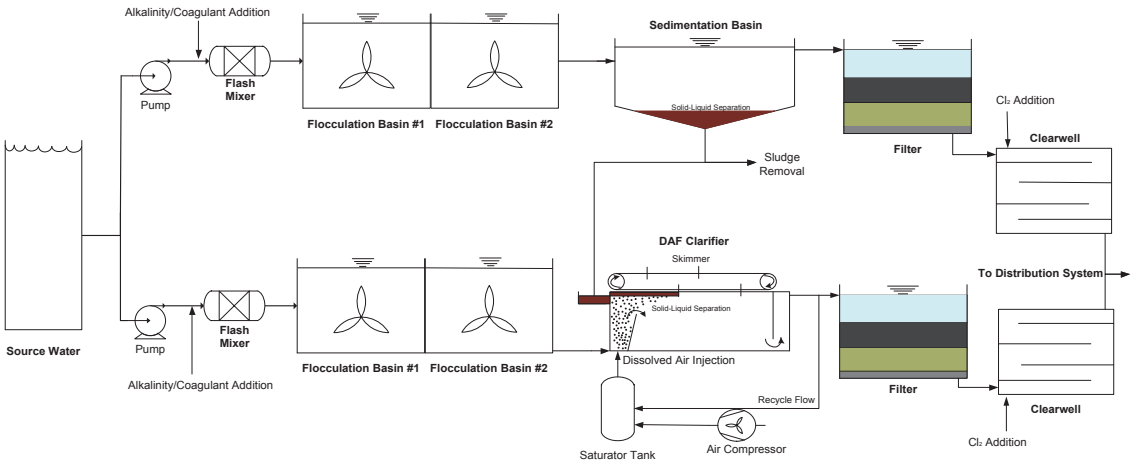

Figure 2.3. Sedimentation (above) vs. DAF (below) treatment train configuration.

The recycle flow shown in the figure is drawn from the clarifier effluent at a flowrate typically described in terms of percentage of total plant effluent, termed "recycle rate" (RR). The recycle flow may also be drawn from the filter effluent in alternative plant configurations. Other configurations for DAF followed by filtration exist, such as a single unit where the filter is at the bottom of the clarifier, further reducing plant footprint

and capital cost as well as improving filter performance by inducing perfectly even hydraulic flow into the filter (Haarhoff, 2008). The clarifier is divided into two distinct zones: the contact zone, where floc-bubble aggregates are formed, and the separation zone where these aggregates rise to the surface of the tank. The optimization of flow patterns in these zones allows HLRs to be increased to 30 to 40 m/h, with some research suggesting DAF tank modification will allow HLRs as high as 60 m/h (Haarhoff, 2008).

Temperature affects water viscosity, such that at warm temperatures higher rise velocities can be achieved. Theoretical floc-bubble aggregate rise rate has been derived from Stokes' Law (Equation 2.2) by Haarhoff and Edzwald (2004), and is shown below in Equation 2.3. Ensuring floc-bubble aggregate rise velocities are sufficient to reach the top of the clarifier before being drawn into the subnatant effluent flow is crucial to DAF performance.

$$v_b = \frac{g(\rho_w - \rho_b)d_b^2}{18\mu_w} \qquad \text{Equation 2.2}$$

$$v_{fb} = \frac{4g(\rho_w - \rho_b)d_{fb}^2}{3K\mu_w} \qquad \text{Equation 2.3}$$

where v_b = rise velocity of bubble
v_{fb} = rise velocity of floc-bubble aggregate
g = gravitational constant
ρ_w = density of water
ρ_b = density of air
μ_w = water dynamic viscosity
d_b = diameter of bubble
d_{fb} = diameter of floc-bubble aggregate
K = coefficient: varying from 24 for flocs < 40 microns to 45 for 170 microns

A stratified flow condition exists in DAF clarifiers due to strong density gradients within the separation zone. A diagram outlining stratified flow in a DAF clarifier is shown below in Figure 2.4. Short circuiting in the separation zone, where the return horizontal current is irregular and drawn towards the clarifier outlet, may be caused by a decreasing concentration of air in the separation zone. Early DAF designs assumed plug flow through the separation zone of the clarifier, leading to design HLRs considerably lower than typical floc-bubble aggregate rise velocities of 20 m/h. However, if stratified flow is achieved, Edzwald (2007) has shown that the effective surface area in the separation zone can be tripled, so that loading rates of 30 m/h are effectively reduced to 10 m/h, well below floc-bubble aggregate rise velocities.

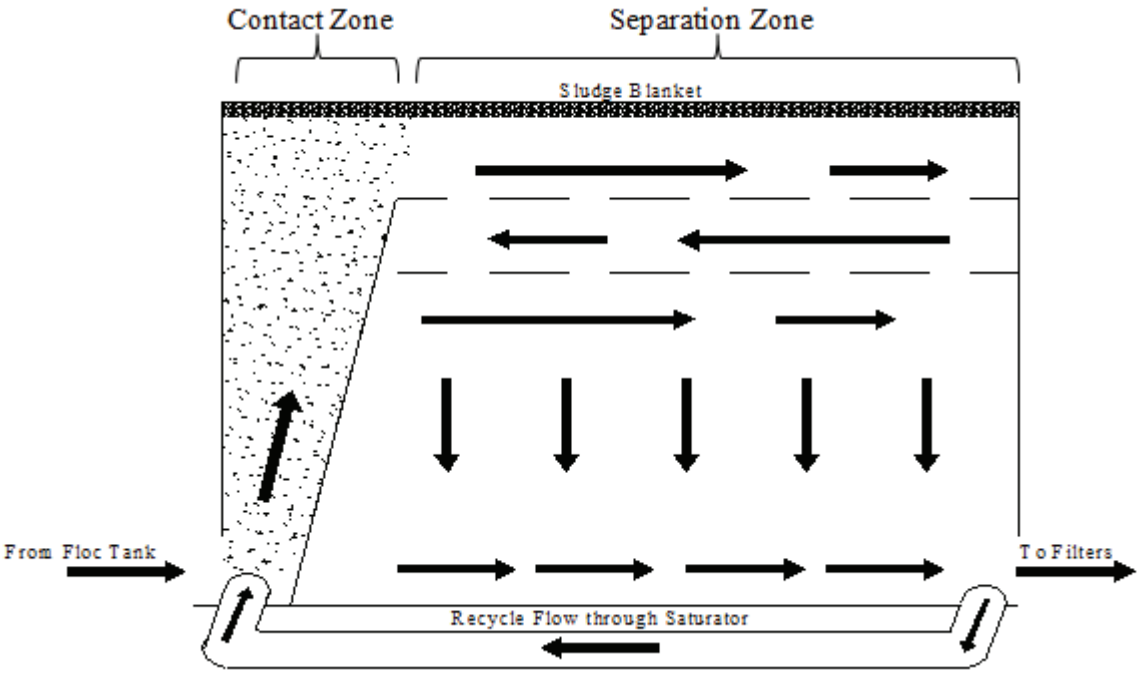

Figure 2.4. Stratified flow pattern in DAF clarifier.

There is a strong relationship between recycle rate, HLR and degree of short-circuiting, and the contributing role of clarifier depth, solids content and coagulant dosing requires further work. However limited precision in both mathematical models and empirical measurement of flow patterns in a nearly opaque suspension have hindered progress in this area (Haarhoff, 2008).

2.3.2 Bubble Introduction

A saturator tank connected to a recycle water line as well as an air compressor acts to dissolve air (according to Henry's law) into the water at pressures between 400 to 600 kPa (Haarhoff, 2008; Edzwald, 2010). The saturator tank may be packed or unpacked, typically running with higher efficiency if packed with media facilitating faster mixing of air and water. The recycle water is drawn from the outlet of the clarifier or from the filter effluent at a ratio of 6 to 12 % of the total plant output (Edzwald, 2010). The recycle water, saturated with air at 400 to 600 kPa, is injected at the bottom of the DAF tank, and the corresponding pressure drop forces the dissolved air to come out of solution, forming bubbles approximately 10 to 100 μm in diameter (Edzwald, 2010). The critical bubble diameter (D_{cb}), which is the diameter at which bubbles will form and rise in water and under which they will collapse and dissolve, is decreased with increasing pressure drop, and the relationship is shown in Equation 2.4 below. However, empirical research has shown that for saturator pressures from 350 to 500 kPa the bubbles showed no further decrease in size (Han *et al.*, 2002; Edzwald, 2010).

$$D_{cb}(\mathrm{m}) = \frac{4\sigma}{\Delta P} \qquad \text{Equation 2.4}$$

where σ = surface tension of the water (N/m)
ΔP = pressure drop across nozzle (Pa)

An approximate D_{cb} for conditions expected in a DAF WTP can therefore be calculated with this equation using the parameters shown Table 2.3. Calculations show that the D_{cb} of bubbles under normal operating conditions of WTPs is less than 1 μm. Bubbles will grow quickly after injection to the clarifier due to coalescence with other bubbles to a nominal diameter of 40 to 80 μm in the contact zone, with the uptake of dissolved air in the water and reduced hydrostatic pressure as the bubbles rise playing secondary roles in bubble growth (Edzwald, 2010).

Table 2.3. Critical bubble diameter calculation parameters and example result.

Temperature	σ	Saturator Pressure	Depth of Nozzles	Tank Pressure (3 m Depth)	ΔP	D_{cb}
10°C	0.074	350 kPa	3 m	30 kPa	320 kPa	0.93 μm

Nozzle type is also important to bubble formation. Lucas Van Vuuren, an early researcher of DAF for drinking water, unintentionally discovered that impinging nozzle flow with his finger resulted in the formation of smaller bubbles. Currently, projecting flows onto an obstructing surface is a common characteristic of all nozzle types (Haarhoff, 2008). Avoiding the formation of macro-bubbles (>150 μm) has become an important design consideration, and these bubbles have been especially problematic with the use of needle valve nozzles (Haarhoff, 2008). Macro-bubbles in the contact zone consume a large amount of dissolved air from solution and are also detrimental to DAF efficacy (Haarhoff, 1997; Leppinen & Dalziel, 2004).

2.4 Coagulation and Flocculation

Coagulation and flocculation is a required pretreatment for effective DAF clarification, and the optimization of this pretreatment is as important to DAF as the design of the clarifier itself (Haarhoff, 2008). Coagulation and flocculation are two terms often used interchangeably in water treatment literature. Coagulation occurs before flocculation, and is a process that allows discrete particles and dissolved components to precipitate and aggregate into larger complexes known as "flocs". Flocculation is the formation of larger floc aggregates which enables effective solid-liquid separation via clarification or filtration.

The agglomeration of colloids into small groups called microflocs or pinflocs and the formation of active coagulant species occurs quickly upon coagulant addition in a rapid mix stage, with slow mixing in the flocculation stage at a WTP allowing larger flocs to form. Practically, coagulation and flocculation occurs simultaneously in WTPs. Process design emphasis should ideally consider source water quality and desired coagulation-flocculation pathway for effective treatment, beginning with rapid mix design, coagulant type, additional chemicals required and dosing sequence, as well as mixing intensity and retention time throughout the process. Coagulation and flocculation is necessary for the removal of dissolved components such as NOM as well as colloidal particles (particles less than ~1 μm) which do not settle in a reasonable timeframe.

2.4.1 Coagulation

Coagulation and flocculation were first used in water treatment in ancient Egypt 4000 years ago, where crushed seeds were found to clarify water when mixed.

Aluminum sulphate (alum) was used by the Romans as far back as ca. 77 AD, and first used for the treatment of public water supplies in 1881 in England (Bratby, 2006).

2.4.1.1 Aluminum based coagulants

The highly charged nature of dissolved aluminum, being a trivalent cation, makes it a suitable coagulant for drinking water treatment where the common removal targets, particles and NOM, both carry negative charge. Alum ($Al_2(SO_4)_3 \cdot nH_2O$) is one of the most commonly used coagulants, and may be produced from the simple digestion of bauxite ore with sulfuric acid, making it relatively abundant and inexpensive (Bratby, 2006). However, alum performance deteriorates in cold temperatures, therefore (depending on climate) alum alone may not be ideal for coagulation in a WTP, and may require the use of an additional polymer to help alum performance in these challenging conditions (Duan & Gregory, 2003; Van Benschoten & Edzwald, 1990a).

Other aluminum based coagulants have been developed and have been found to be superior to alum not only in treatment performance but also in minimizing sludge production. There are several polyaluminum coagulants such as aluminum chlorohydrate, polyaluminum sulfate and polyaluminum chloride (PACl), all of which can vary in basicity and strength, and can have added elements such as sulphate, silica, and calcium (Pernitsky, 2001). The basicity of a PACl coagulant is a measure of the ratio of hydroxyl ions to aluminum ions present in the chemical structure of the coagulant. Basicity is calculated according to Equation 2.5, shown below. A higher basicity PACl has been hydrolyzed to a higher degree in production, and therefore there are fewer hydrolysis reactions occurring upon introduction to water.

$$\text{Basicity} = \frac{[OH^-]}{3[Al_T]} \times 100\% \qquad \text{Equation 2.5}$$

Common aluminum coagulant reactions occurring upon introduction to water are shown in Table 2.4. Dissolved Al^{3+} reacts with either NOM or inorganic ligands such as OH^-, or it is hydrolyzed by water to one of its active coagulant species. Pre-hydrolyzed coagulants such as PACl require less reaction time than alum to form active coagulant species upon introduction to water as many of these species are pre-formed.

Table 2.4. Common aluminum reactions in water (Pernitsky & Edzwald, 2003).

Reaction	Aluminum Species Formed
$Al^{3+} + 3OH^- \rightarrow Al(OH)_{3(am)}$	Amorphous (Solid)
$Al^{3+} + H_2O \rightarrow AlOH^{2+} + H^+$	Monomeric
$Al^{3+} + 2H_2O \rightarrow Al(OH)_2^+ + 2H^+$	Monomeric
$Al^{3+} + 4H_2O \rightarrow Al(OH)_4^- + 4H^+$	Monomeric
$13Al^{3+} + 28H_2O \rightarrow Al_{13}(OH)_{24}^{7+} + 32H^+$	Polymeric

High basicity PACl coagulants (up to a basicity of 70 %) have been found to produce a higher proportion of polymeric species upon introduction to water, such as the Al_{13} variety which has been found to be the dominant polymeric aluminum species (Van Benschoten & Edzwald, 1990a; Pernitsky, 2001).

2.4.2 Mechanisms of Coagulation-Flocculation Processes

Active coagulant species and mechanisms of removal for colloidal particles and NOM by alum and PACl coagulants have been summarized by Pernitsky (2001) in Figure 2.5.

The two main types of coagulation-flocculation are charge neutralization/destabilization and sweep flocculation. There are four major mechanisms by which coagulation and flocculation occur. Destabilization, complexation, enmeshment, and adsorption each play some role in coagulation-flocculation, but some will dominate depending on raw water quality and coagulant used.

While all particles in a given water source have the same surface charge, smaller particles have proportionately larger surface areas which causes charge interactions to be the most important force acting on the particle. Colloidal particles are generally defined as having an equivalent spherical diameter between 1 nm and 1 micron, which is a somewhat arbitrary but convenient classification, and is near where relative surface area becomes important for particle interactions (Gregory, 2006).

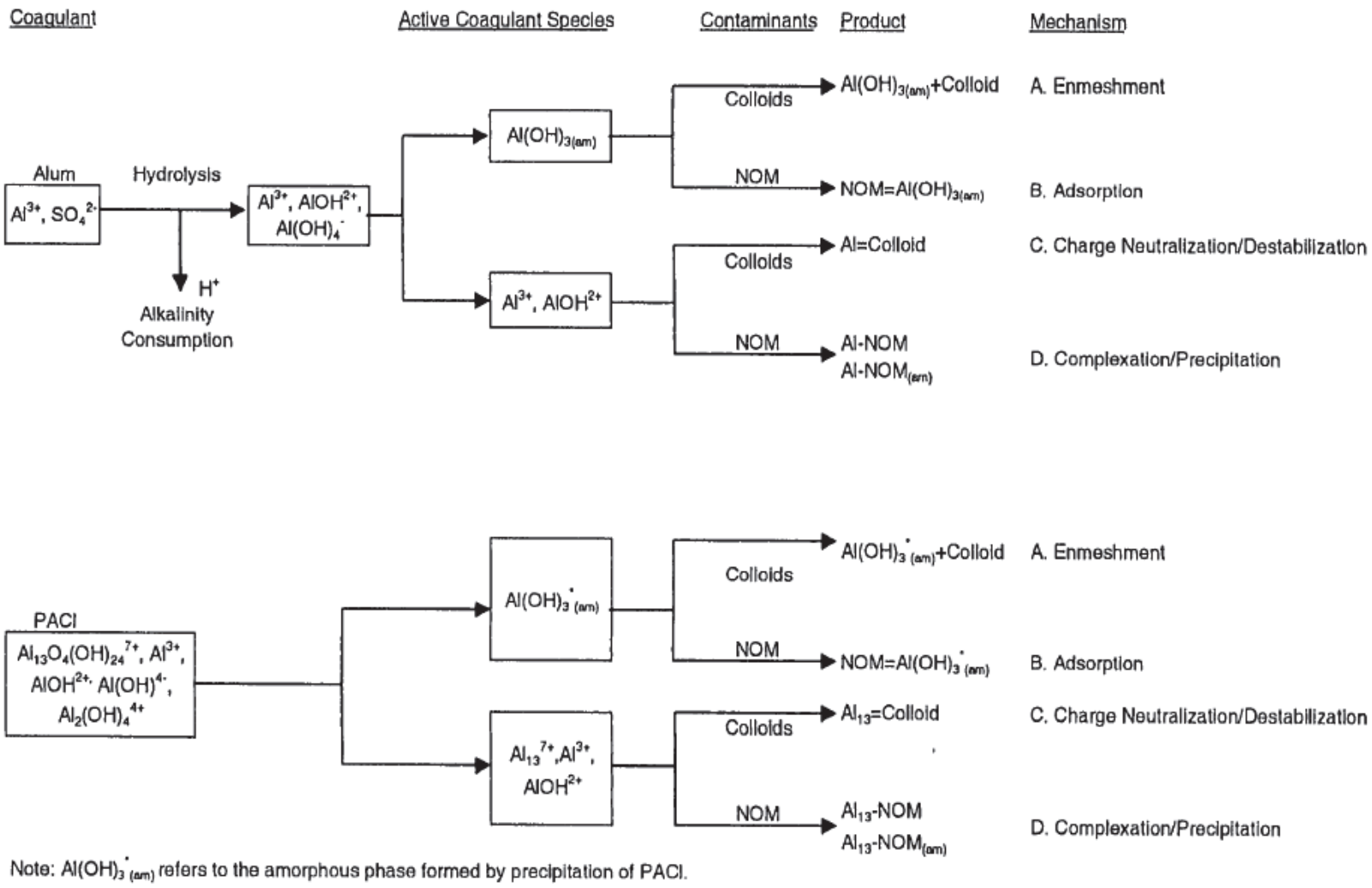

Figure 2.5. Conceptual view of coagulation reactions and removal mechanisms (Pernitsky, 2001)

2.4.2.1 Charge Neutralization and Destabilization of Colloidal Particles

There are several mechanisms by which coagulation occurs, but ideally the purpose of coagulant addition is to "destabilize" these discrete colloids. This is done through complex interactions between the coagulant in solution and the colloids, where the coagulant acts to neutralize the surface charge of the colloids to the point where collisions between two colloids produce enough energy to overcome the repulsion and allow Van der Waal's forces to hold the colloids together (Gregory, 2006; Droppo *et al.*, 2005). An example of an energy barrier between colloids which must be overcome to allow coagulation to occur via the charge neutralization/destabilization mechanisms is shown in Figure 2.6. These collisions are facilitated by mixing in the flocculation stage of a water treatment plant. This mechanism is commonly known as the DLVO theory after the authors of two papers where it was first described (Deryagin & Landau, 1941; Verway & Overbeek, 1948).

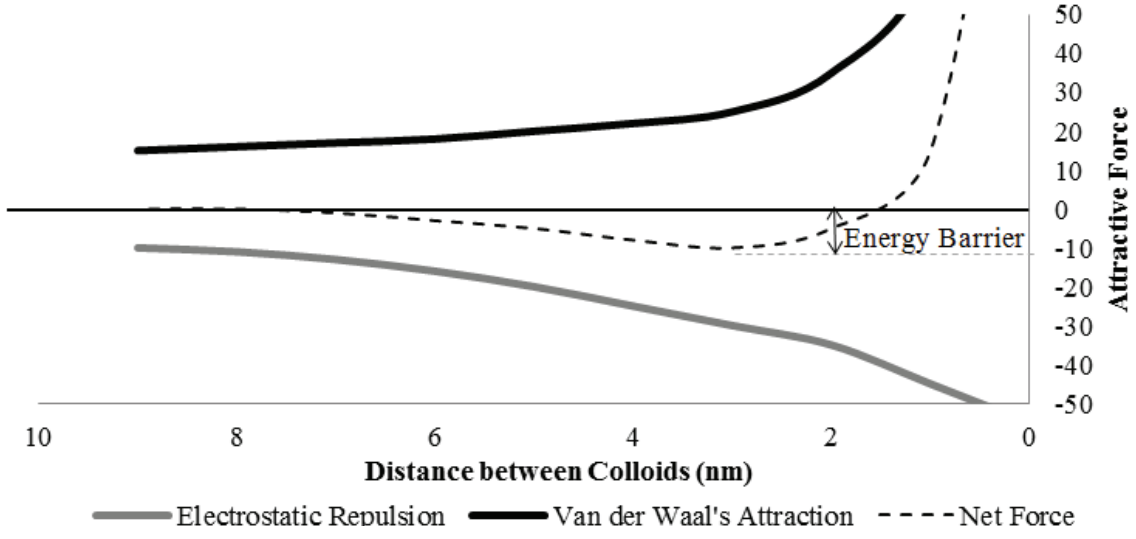

Figure 2.6. DLVO theory forces on two colloids in suspension.

The energy barrier can be overcome by the kinetic energy of particles and flocs during flocculation, which is dependent on the bodies' speed and mass. The addition of a coagulant reduces the energy barrier to near zero, where collisions will easily result in the agglomeration of the particles. The hydrophobicity of the particles is also important, as hydrophobic surfaces will minimize hydrodynamic repulsion effects between particles, which may be significant under sub-nanometer distances (Droppo *et al.*, 2005).

2.4.2.2 The Double Layer Theory

The DLVO theory of electrostatic repulsion and Van Der Waal's attraction incorporates the electrical double layer theorem, first described by Gouy and Chapman independently in the early 1920's and later improved by Stern in 1924 (Gregory, 2006). The modern version of the double layer theory explains a colloid in suspension as having two distinct surrounding zones; the Stern layer, which is composed of positively charged counter-ions (counter to the typically negative charge found on the surfaces of colloids) surrounded by a Diffuse layer of counter-ions, which are attracted to the negative colloid surface but repelled by the counter-ions present in the Stern layer. The double layer model is presented in Figure 2.7, showing a colloid, the Stern and Diffuse layer, and the electric potential profile near the surface of the colloid. Zeta potential is a measurement often used to estimate the surface charge, although it is actually a measure of the electric potential at the boundary of the shear plane. The shear plane is the distance from the colloid within which ions are essentially fixed to the surface, and outside of which the weakly held counter-ions in the outer diffuse layer may be removed by shear forces due to fluid movement. The shear plane is located somewhere near the boundary between the

Stern and Diffuse layers, its exact location dependent on the surface charge and ions in the bulk solution (Gregory, 2005).

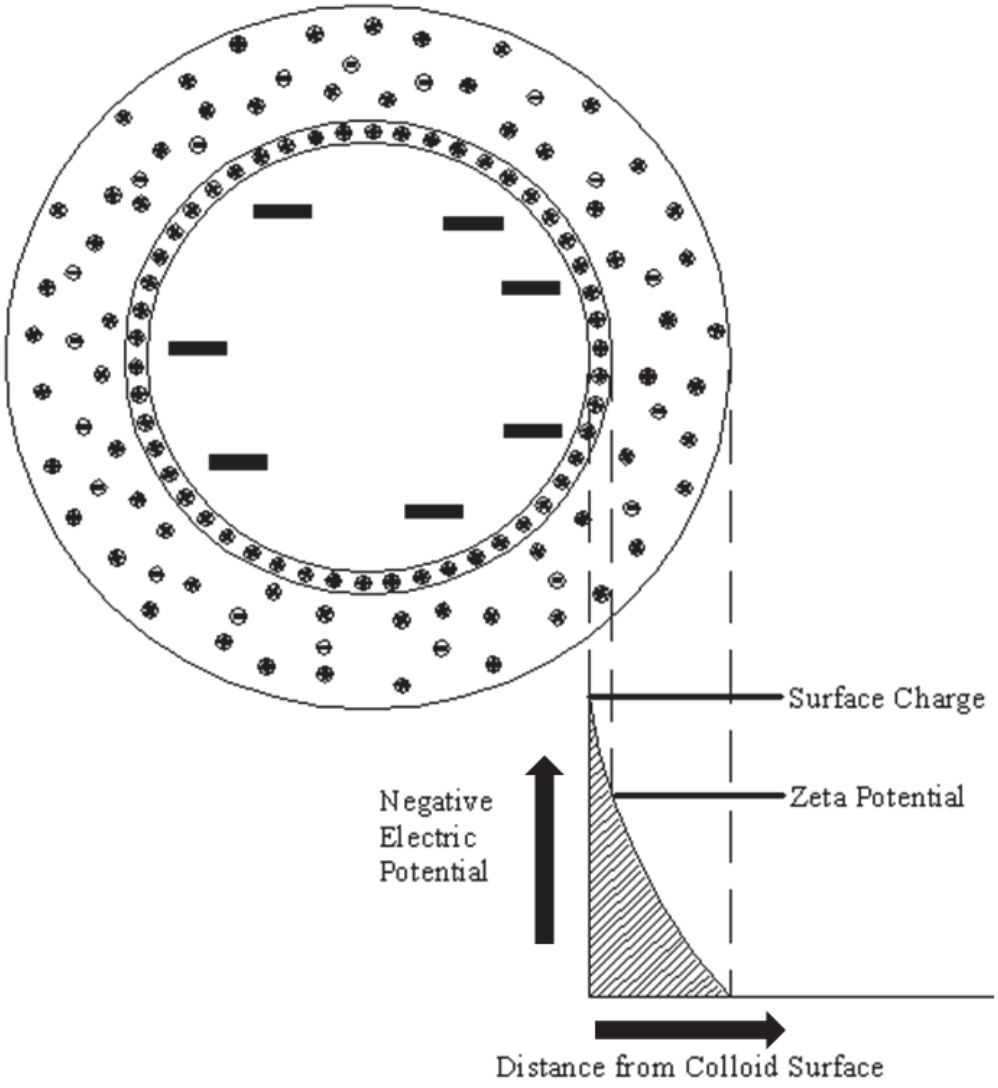

Figure 2.7. The Double Layer theory showing zeta potential measurement.

Highly charged Al^{3+} and other active coagulant species will add to or replace weaker counter-ions in the Stern layer, reducing the net negative electric potential near the surface of the colloid (Duan & Gregory, 2003).

2.4.2.3 Complexation/Precipitation

The negative charge density of NOM may range from 10 to 150 times that of colloidal clay particles in suspension, which explains why for many WTPs coagulant demand is driven by NOM rather than turbidity (Shin *et al.*, 2008; Tseng *et al.*, 2000; Edzwald, 1990). Complexation refers to the chemical bonding of positively charged coagulant with reactive functional groups such as carboxylic and phenolic present on NOM molecules, and direct precipitation of these complexes is an important removal pathway for these negatively charged compounds (Duan & Gregory, 2003). Aluminum coagulants can remove NOM by two main mechanisms: neutralization of NOM by complexation with dissolved aluminum followed directly by Al-NOM precipitate (known as complexation-precipitation), and the adsorption of NOM or Al-NOM complexes onto amorphous aluminum hydroxide precipitate (Van Benschoten & Edzwald, 1990a). Complexation/precipitation may also occur between aluminum and other suitable ligands dissolved in the water, such as bicarbonate (HCO_3^-), nitrate (NO_3^-) and sulphate (SO_4^{2-}) ions, which is will enhance sweep flocculation processes in waters where these ions are present in sufficient concentrations (Chowdhury *et al.*, 1991).

2.4.2.4 Sweep Flocculation: Adsorption and Enmeshment

Other coagulation mechanisms may play a major role in the removal of particles and NOM from the water column and into large flocs where they can be easily separated.

Chowdhury *et al.* (1991) described the incorporation of colloids into aluminum hydroxide ($Al(OH)_3$) floc as occurring via two pathways – homogeneous and heterogeneous. In heterogeneous coagulation, the colloid acts as the nucleation point for floc formation through charge neutralization of the colloid and subsequent attachment to

other particles. In homogeneous coagulation, $Al(OH)_3$ precipitate served as the nucleus for floc formation, with particle and NOM removal then occurring mainly through adsorption and enmeshment. It was also found that only one of these pathways will dominate, with heterogeneous coagulation preferred for the formation of compact flocs suitable for DAF clarification (Chowdhury *et al.*, 1991).

Sweep flocculation is a dominant mechanism in many WTPs, and is particularly effective in sedimentation plants where larger flocs are desirable for faster settling, and typically also provides better particle and NOM removal than DLVO coagulation (Duan & Gregory, 2003). Sweep flocculation refers to the phenomena of incorporating particles and NOM into flocs by physical enmeshment or by adsorption onto the surface of flocs. Sweep flocculation occurs at higher doses of coagulant than DLVO coagulation, typically beyond the charge reversal and restabilization point. The effect of increasing coagulant concentration on dominant coagulation mechanisms is presented in Figure 2.8. Sweep flocculation is increasingly effective to a point, at which no further contaminant removal will occur with increasing coagulant dose.

NOM with lower molecular weight is more likely to be removed by other processes, but NOM with high molecular weight can act as the nucleus for precipitate formation in a similar manner to the removal of negatively charged particles (Yan *et al*., 2008). Polymeric coagulants which are constituted of long molecular chains may follow a similar pattern of bridging flocculation at optimum doses and steric restabilization at higher doses, preventing flocculation. At still higher concentrations, dissolved non-adsorbing polymers will reside in the bulk solution, and concentrate particulate matter together, causing destabilization (Droppo *et al.*, 2005).

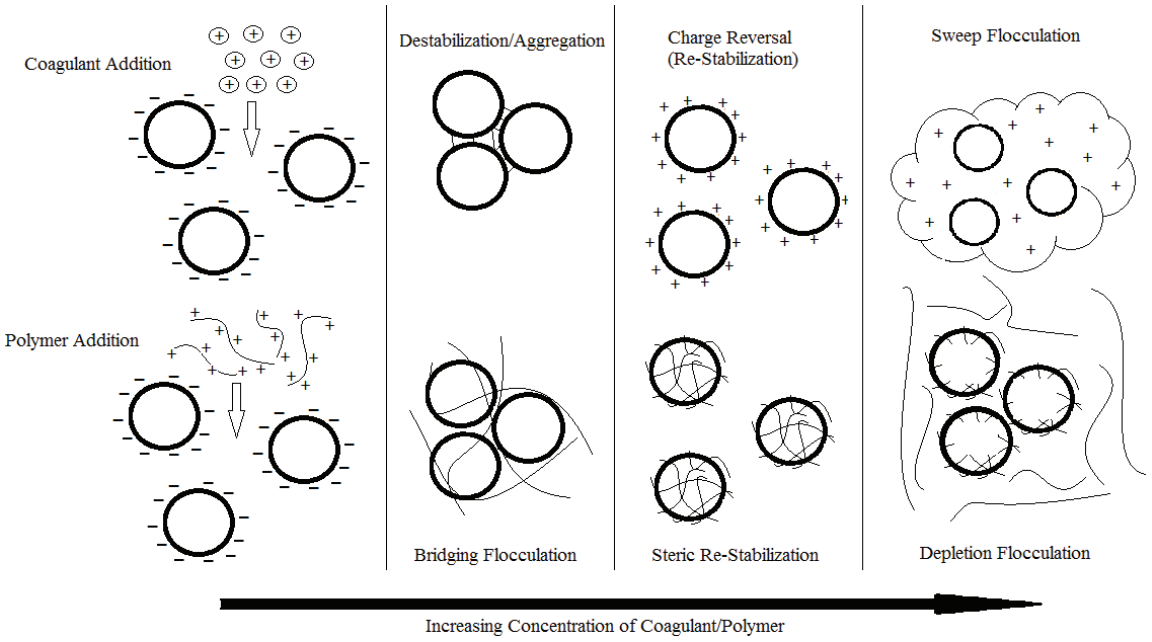

Figure 2.8. Four zones of coagulation for particles in suspension.

2.4.3 Rapid Mixing

Rapid mixing may play a significant role in coagulation-flocculation processes, particularly when the charge neutralization/destabilization mechanism is desired. The speed with which hydrolysis reactions of aluminum take place upon alum addition to water has been found to be on the order of microseconds, and the formation of polymeric species within 1 s. If destabilization coagulation is desired, the even dispersal of the coagulant will therefore be extremely important for the active coagulant species to attach to colloidal particles to destabilize them. For sweep flocculation, it is less so, with aluminum hydroxides forming in 1 to 7 s (Amirtharajah & Mills, 1982). The type of coagulation occurring was found to be related to the coagulant dose and pH, with rapid mixing intensity making a significant impact on final turbidity in alum-sedimentation tests. Rapid mixing intensity was not found to be important outside of charge

neutralization/destabilization type systems, which are more common where higher particle concentrations exist (Amirtharajah & Mills, 1982). Kan *et al.* (2002) found that when coagulating highly turbid waters, the quick dispersion of PACl in the rapid mix was a key factor for the effective destabilization removal of colloidal particles. The presence of sufficient amounts of anions such as bicarbonate, sulphate, nitrate and phosphate is shown to prevent restabilization of colloids at coagulant overdose conditions and promote Al-NOM complexation and/or sweep flocculation processes (Shin *et al.*, 2008; Chowdhury *et al.*, 1991; Amirtharajah & Mills, 1982).

In addition to rapid mix intensity and coagulant dispersion, the addition sequence of any other pH/alkalinity adjustment chemicals in the treatment process may also have an impact on coagulation mechanisms. If aluminum is added first, a resulting decrease in pH implies a low concentration of reactive hydroxide ions, which would drive coagulation processes to favour the charge neutralization/destabilization mechanism. Conversely, the addition of a base along with or prior to coagulant addition would mean a higher concentration of hydroxides, facilitating $Al(OH)_3$ formation and enhancing sweep flocculation processes (Van Benschoten & Edzwald, 1990b)

2.4.4 Alkalinity

It is suggested that pH is the most important factor in coagulation, and therefore the ability to control pH in a WTP is critical to maintaining optimum coagulation conditions and overall plant performance (Pernitsky, 2001; Amirtharajah & Mills, 1982). Since aluminum coagulants are acidic, the acid neutralizing capacity (ANC) of the raw water is of great importance. In natural surface waters within normal pH ranges, ANC is primarily determined by the concentration of carbonic acid (H_2CO_3) and its associated

ions carbonate (CO_3^-) and bicarbonate (HCO_3^-) as well as hydroxide (OH^-), although other ions such as sulphate (SO_4^{2-}) phosphates (PO_4^{3-}, HPO_4^{2-}, $H_2PO_4^-$), borates ($B(OH)_4^-$) and ammonia (NH_3) can also contribute. Carbonate ions in surface waters are derived from three main sources: (1) cellular respiration of aquatic organisms which produce carbon dioxide (CO_2), (2) dissolution of carbonate minerals such as limestone, calcite and dolomite, and (3) atmospheric dissolution of carbon dioxide (CO_2) according to Henry's Law. Typically sources (1) and (2) are most influential as surface waters tend to be oversaturated with CO_2 (Brezonik & Arnold, 2011).

In natural water systems where the carbonate family is dominant, ANC is referred to as alkalinity (Jensen, 2003). The alkalinity can be defined as the equivalent amount of acid needed before there are enough free protons in the solution to convert all carbonate and bicarbonate ions to carbonic acid. At this "pH endpoint", further addition of protons will result in a rapid decreasing of pH. Analytically, the alkalinity is the sum of titratable bases with strong acid to a defined endpoint which is dependent on the concentration of carbonate, at a pH between 4.3-4.9. This pH value is dependent on the total carbonate concentration, as higher concentrations yield lower pH endpoints (Jensen, 2003). The endpoint is the pH at which all carbonate ions in the system primarily exist as H_2CO_3 (Brezonik & Arnold, 2011). The relationship is between pH and dominant carbonate species is shown in Figure 2.9. It is apparent that at a neutral pH level, alkalinity is driven by HCO_3^-. From this figure it can also be seen that hydroxide, or caustic, concentration is not significant below a pH of ~10, carbonate concentration is not significant below pH ~8, and bicarbonate is insignificant below a pH of ~5.5.

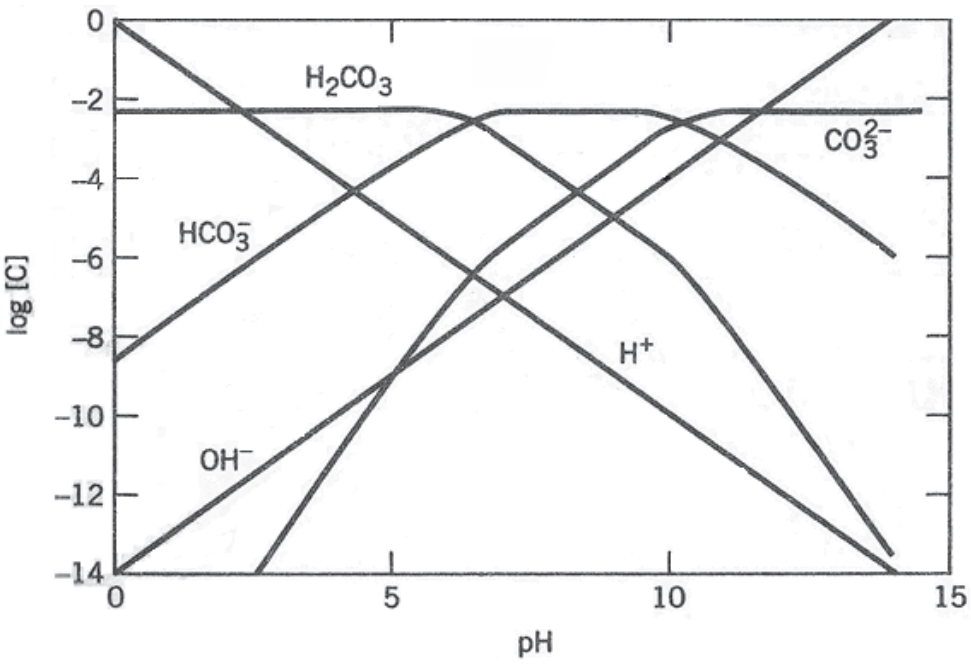

Figure 2.9. Carbonate species relative to pH (Droste, 1997).

An illustration of alkalinity vs. pH and total carbonate concentration is provided by Deffeyes and shown in Figure 2.10. Maintaining sufficient alkalinity in raw water has been shown to improve treatment performance with respect to turbidity and NOM removal in alum-sedimentation WTPs, and alkalinity along with organic carbon concentration in raw water have been found to be the primary determinants of coagulant demand (Shin *et al.*, 2008; Ye *et al.*, 2007; Tseng *et al.*, 2000; Gregory, 1998).

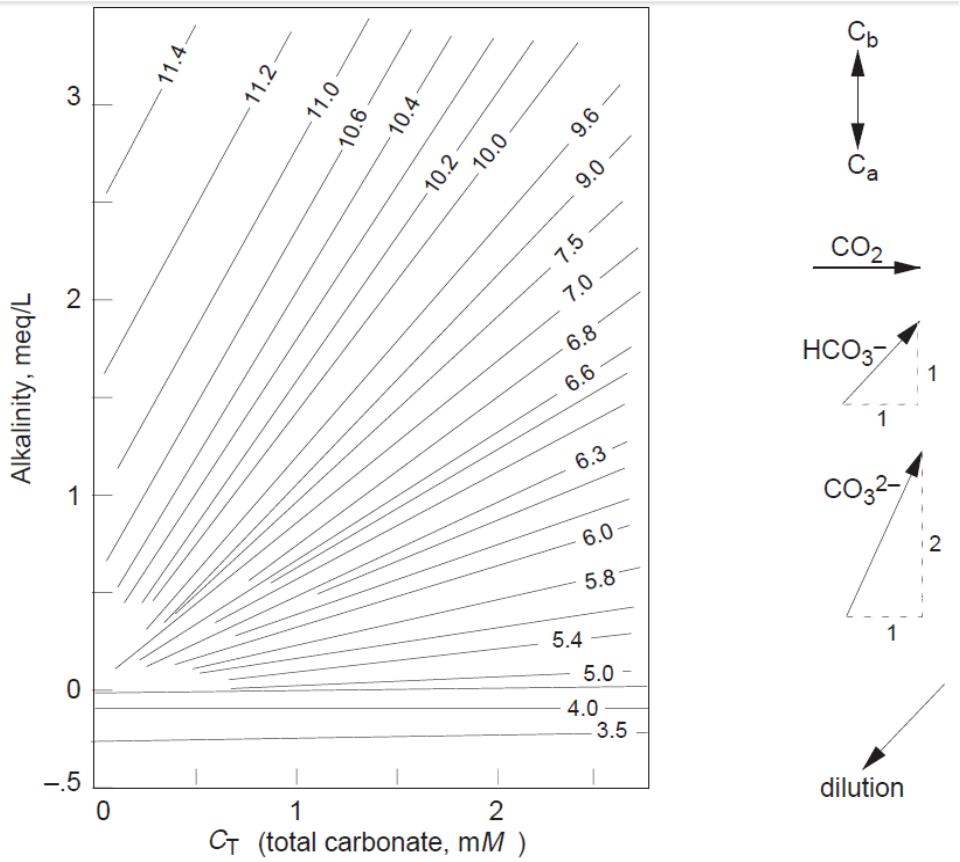

Figure 2.10. Deffeyes diagram, adapted from Stumm and Morgan (1995).

The Deffeyes diagram (Figure 2.10) shows the difficulty of elevating alkalinity levels at a lower pH value without the addition of substantial total carbonate by plotting lines of constant pH vs. alkalinity and carbonate. The lines shown on the right side of the figure show the effect of additional concentrated acids and bases, as well as carbonate family ions. For a WTP operating at pH less than 7 and low initial alkalinity, the chemical costs of boosting alkalinity to 30 mg/L or greater, as suggested by Tseng *et al.* (2000), may be prohibitive for normal operation, especially considering the increase in coagulant needed to reach optimum dose.

2.4.4.1 Carbonate and Caustic Alkalinity

An example of an acid titration on pure water buffered with sodium bicarbonate ($NaHCO_3$) and caustic (NaOH) is shown in Figure 2.11 below. It can be seen that the buffer capacity is equal for both solutions; however the buffer intensity across the titration, which is equal to the reciprocal of the slope of the titration, is quite different (Jensen, 2003). Since alkalinity is defined as the equivalent amount of acid that can be neutralized before the endpoint, the alkalinity determined for each solution in the graph is 0.001 eq/L (1 meq/L; 50 mg/L as $CaCO_3$). However, it can be seen that if targeting a neutral pH for applications such as coagulation, utilizing bicarbonate buffering will yield more accurate pH control. Alkalinity is reported in milliequivalents per liter or, most commonly, mg/L as calcium carbonate ($CaCO_3$), as it is a common source of alkalinity in nature (calcite dissolution) and its molecular weight (100 grams/mol) helps to simplify conversions (Jensen, 2003). As discussed earlier however, the source of this alkalinity may come from multiple sources other than calcite.

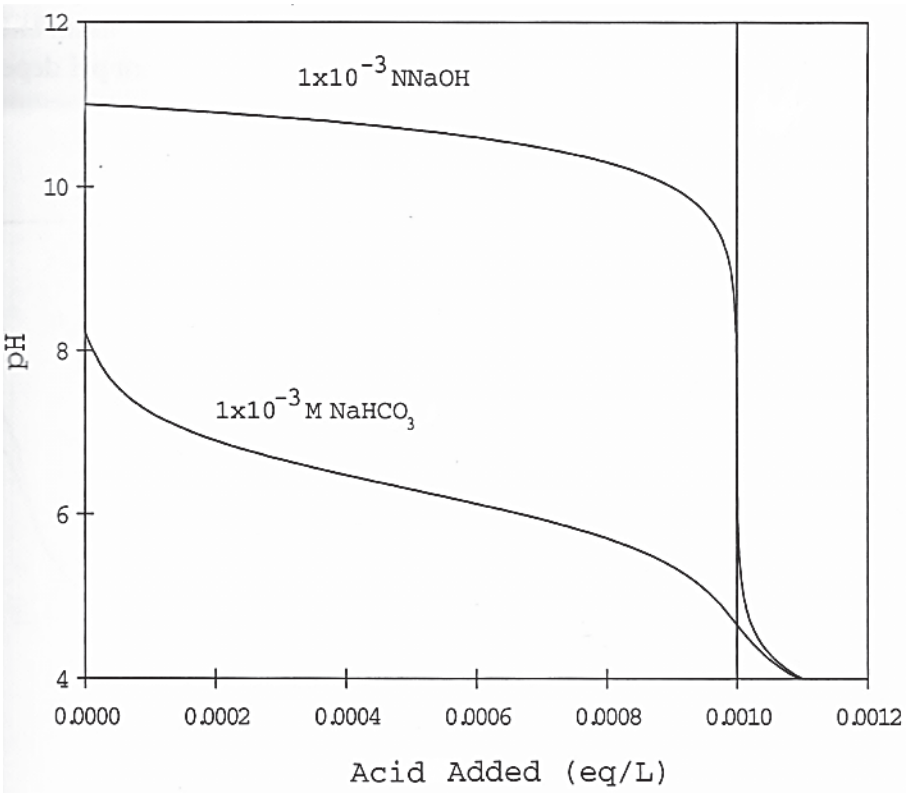

Figure 2.11. Acid titration curves into two buffers (Jensen, 2003).

Several alkalinity/pH adjustment chemicals may be used in WTPs. Lime, or hydrated calcium oxide, is typically the least expensive source of alkalinity (Droste, 1997). Quicklime rapid hydrolyzes when added to water, as shown below in Equation 2.6.

$$CaO_{(s)}\ (\text{quicklime}) + H_2O \rightarrow Ca(OH)_{2(aq)}\ (\text{lime}) \qquad \text{Equation 2.6}$$

Lime dissociates to produce calcium ions and hydroxide ions, shown in the Equation 2.7 below.

$$Ca(OH)_{2(aq)} \rightleftharpoons Ca^{2+} + 2OH^- \qquad \text{Equation 2.7}$$

From these equations it can easily be seen that quicklime and lime produce hydroxide or caustic alkalinity, and do not contribute to carbonate levels, with the exception that aqueous lime may react with any dissolved CO_2 present as shown Equation 2.8 below.

$$Ca(OH)_{2(aq)} + CO_{2(aq)} \rightarrow CaCO_{3(s)} + H_2O \qquad \text{Equation 2.8}$$

The $CaCO_3$ produced will precipitate or dissolve into solution depending on the pH, but typically at WTP pH levels it will dissolve and contribute to carbonate alkalinity. NaOH is a strong base, which is typically more expensive than other alkalinity sources and will dissociate completely to form sodium and hydroxide ions.

Caustic contributes to alkalinity in a similar manner as lime, raising pH and reacting with available CO_2 to form carbonate ions as shown in Equation 2.9 below. Soda ash (Na_2CO_3) contributes to carbonate alkalinity by dissociating as shown below in Equation 2.10.

$$2OH^- + CO_2 \rightarrow CO_3^{2-} + H_2O \qquad \text{Equation 2.9}$$

$$Na_2CO_3 \rightarrow 2Na^+ + CO_3^{2-} \qquad \text{Equation 2.10}$$

The contribution of carbonate ions will increase the pH by combining with H^+ ions and form bicarbonate at typical pH ranges between ~ 4.5 and 10.

Chapter 3: Materials and Methods

3.1 Data Acquisition at the Brierly Brook Water Treatment Plant

Data from continuous monitoring of 94 water quality and process parameters at the Brierly Brook Water Treatment Plant (BBWTP) is automatically compiled by a supervisory control and data acquisition (SCADA) system, which records measurements at either 1 h intervals, 30 s intervals or when a significant change in the measured value occurs, typically 1% of the set range. For example, the filter turbidimeters record values between 0 and 2 NTU, therefore they log a measurement every 1 h or when a change of 0.02 NTU occurs. Parameters such as coagulation pH, raw water turbidity, clarifier effluent turbidity and streaming current are automatically recorded every 30 s.

3.2 Bench-scale Dissolved Air Flotation Jar Testing Unit

Jar testing was carried out for bench-scale analysis discussed in Chapter 5 and Chapter 6. A bench-scale dissolved air flotation (DAF) batch jar tester unit (EC Engineering), which is shown in Figure 3.1, was used. The unit is operated analogous to a regular jar tester, using rotating paddles at variable rpm to control velocity gradients within the six jars. The unit also includes a DAF injection apparatus which has six nozzles, which can be controlled independently to operate between 0 and 10 s to allow manipulation of recycle flow.

Figure 3.1. EC Engineering dissolved air flotation batch tester apparatus.

The nozzle apparatus is connected to a pressurized saturator tank, which must be manually shaken to ensure reasonable saturation efficiency. Reverse osmosis (RO) filtered water was used for recycle water, pressured to 450 kPa in the saturator tank. The recycle rate was determined by the length of time the recycle valve was opened. This rate varied slightly between nozzles, and with changing saturator tank pressure (which dropped as the recycle valve remains open). Calibration of recycle flow, to ensure accurate and consistent recycle rates were reported, was done for each nozzle of the unit at pressures of 470 and 430 kPa, and the results are presented in Table 3.1.

Table 3.1. Recycle flow vs. operating time for each nozzle at 470 and 430 kPa saturator pressures.

	Saturator Pressure 470 kPa					Saturator Pressure 430 kPa				
Time (s)	2	4	6	8	10	2	4	6	8	10
Nozzle 1	32	72.5	112.7	158	176	34.5	72.5	108	140	170.5
Nozzle 2	33	68	108.8	150	176	30.5	67.5	102	141.5	168
Nozzle 3	30.5	73	120	155	181	31.5	71	112	149.5	173.5
Nozzle 4	32	71	120	155	181	28	71	110.5	154	171
Nozzle 5	32.5	70.5	121	152	174	31	73.5	111	149	172
Nozzle 6	32	74	118.5	156.5	184	32	73	111.5	153.5	176.5

3.3 Analytical Methods

All laboratory techniques and procedures used were done in accordance with *Standard Methods for the Examination of Water and Wastewater* (APHA, 2012). Procedures unavailable in this text were done in accordance to the equipment manufacturer description. Alkalinity was measured using method 2320B: potentiometric titration of low alkalinity (APHA, 2012). Turbidity was measured using a HACH 2100AN turbidimeter. pH was measured using variable temperature electrodes (accuFlow, Fisher Scientific) and an XL50 meter (Fisher Scientific). Dissolved aluminum was analyzed by filtering samples through a 0.45 µm paper filter (Whatman) and using inductively coupled plasma mass spectrophotometry (XSeries 2 ICP-MS, Thermo Scientific) with a detection limit 4 ppb. Total and dissolved organic carbon were measured using a total organic carbon analyzer (TOC-VCSH TOC Analyzer, Shimadzu), detection limit 0.6 mg/L. True colour and UV_{254} were measured on a HACH DR 5000 spectrophotometer. Particle count analysis was done using a Brightwell MicroFlow Imaging System (MFI), measuring particle diameters as low as 2 µm. Statistical analysis was done using Minitab 16 software (Minitab, Inc.).

Chapter 4: Evaluation of the Brierly Brook Water Treatment Plant

4.1 Introduction

The introduction of the Treatment Standard for Municipal Surface Source Water Treatment Facilities in 2002 prompted the construction or improvement of many water treatment facilities in order to comply with the provisions of the Treatment Standard by 2008 (Nova Scotia Environment, 2002).

In 1996, Port Hawkesbury, Nova Scotia built the first DAF WTP in Canada. Since then, 13 other DAF plants have been commissioned in the province, and at least 30 have been built in the Maritime provinces (Mosher, 2012; Edzwald, 2010). DAF technology is known for treating low turbidity water sources quite well. Typical Atlantic Canada surface water is low alkalinity, low pH and low turbidity with high colour, making DAF treatment a suitable choice (ACWWA, 2004).

Rainfall that produces runoff within the James River watershed contributes eroded particles and dissolved organic matter, which may cause a spike in colour and turbidity at the Brierly Brook Water Treatment Plant (BBWTP). This may result in treatment difficulties and occasionally deterioration of plant performance. Typically, the operating parameter used to determine plant performance on a continual basis is turbidity. From a regulatory standpoint, there are no set guidelines on NOM removal other than that the quarterly sampling average for trihalomethanes (THMs) and haloacetic acids (HAAs) must be below 100 µg/L and 80 µg/L, respectively (Nova Scotia Environment, 2012). Turbidity in the clearwell, however, must be below a threshold value of 0.2 as set out in the permit to operate (PTO) for the BBWTP. The Nova Scotia Treatment Standards for Municipal Drinking Water Systems requires that plants utilizing conventional filtration,

such as the BBWTP, shall have a filter effluent turbidity less than 0.2 NTU 95 % of the time and filter-to-waste capabilities to be used if filter effluent turbidity is higher than 0.2 NTU (Nova Scotia Environment, 2012). Online turbidimeters are monitored using a supervisory control and data acquisition (SCADA) system and are used to ensure this requirement is met.

4.2 Materials and Methods

The BBWTP is located in Antigonish, Nova Scotia, and serves a growing population of as many as 12,000. Site visits were conducted approximately bimonthly between May 2011 and June 2012 in order to collect data, observe plant processes, and discuss treatment issues with the plant operators.

All data used in this chapter was collected from the SCADA system, which records 94 parameters of raw water quality, plant operating conditions and hydraulic information. Large datasets were analyzed to identify relevant water quality and performance trends at the BBWTP.

4.2.1 Treatment Train

The BBWTP processes raw water drawn from a reservoir created by the damming of the James River, drawing from a watershed of approximately 40 km^2 and bypassing an older treatment plant which utilized coagulation and direct filtration followed by chlorination. A simplified process diagram showing the plant layout is displayed in Figure 4.1. The BBWTP was commissioned in 1996, and consists of a flash mixer/flow splitter tank, dual flocculation and DAF clarification trains, three anthracite-sand rapid rate filters, a chlorine contact chamber (CCC) and clearwell, along with all the necessary pumps and instrumentation required to control and monitor important hydraulic and physicochemical water quality characteristics in the plant. The plant is equipped with a SCADA system which allows online monitoring and manipulation of key plant processes.

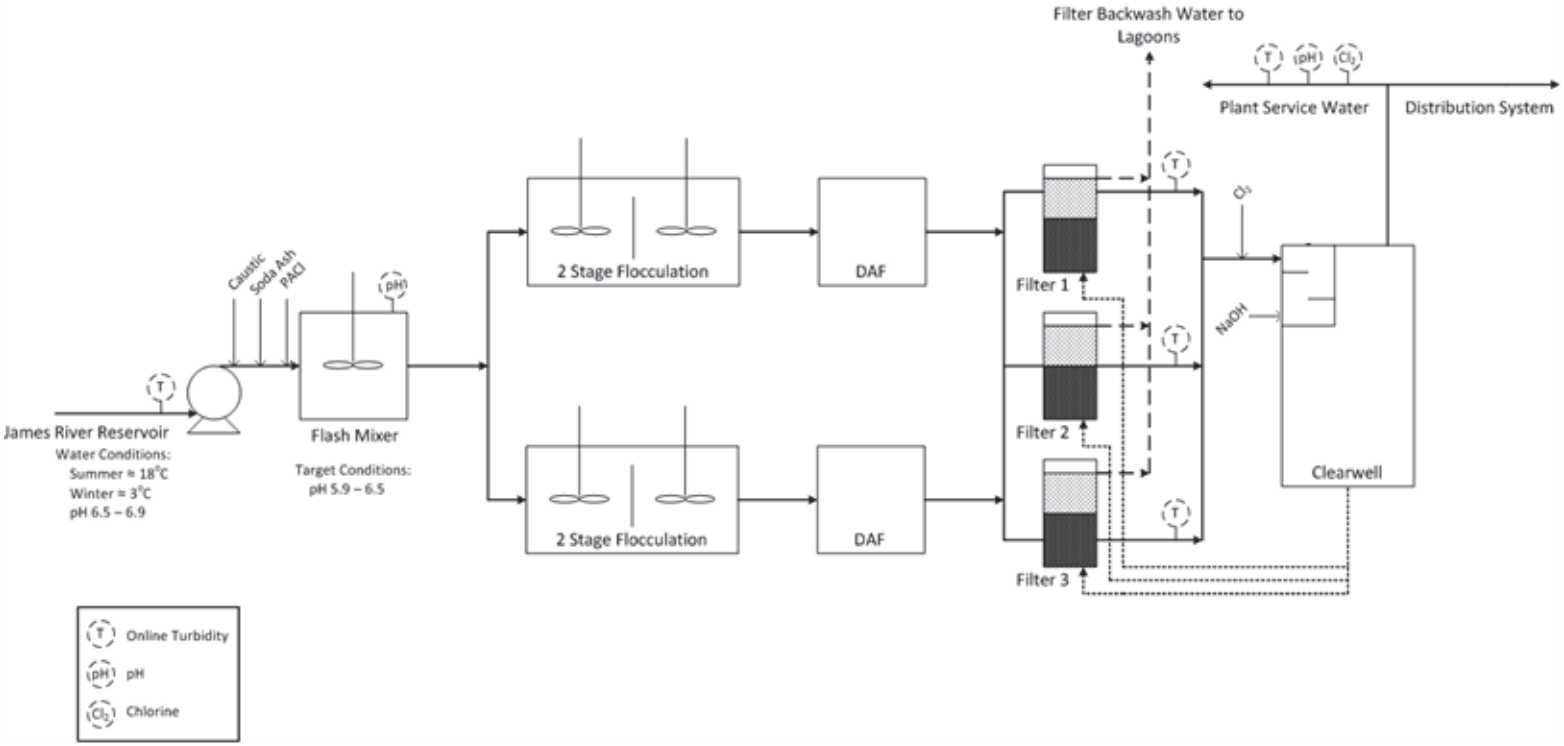

Figure 4.1. Simplified process diagram of the BBWTP.

4.3 Results and Discussion

The BBWTP utilizes a reservoir created by the James River dam which has a total capacity of 116 million liters. Figure 4.2 shows the dam at maximum capacity.

Figure 4.2. James River dam at maximum capacity.

4.3.1 Coagulation and Rapid Mix

Raw water is drawn from 7 meters below the top of the dam and enters the plant in a 16" diameter pipe which is connected to a flash mixer/flow splitter tank. The plant is equipped to add soda ash (Na_2CO_3) or caustic (NaOH) as buffering agents as well as a medium basicity polyaluminum chloride (PACl) coagulant near the base of the tank. Typical coagulant dosing ranges from 11 to 14 mg/L in the winter months (January to April) and 35 to 46 mg/L in summer (June to September). Monthly average coagulant doses with one standard deviation are shown in Figure 4.3.

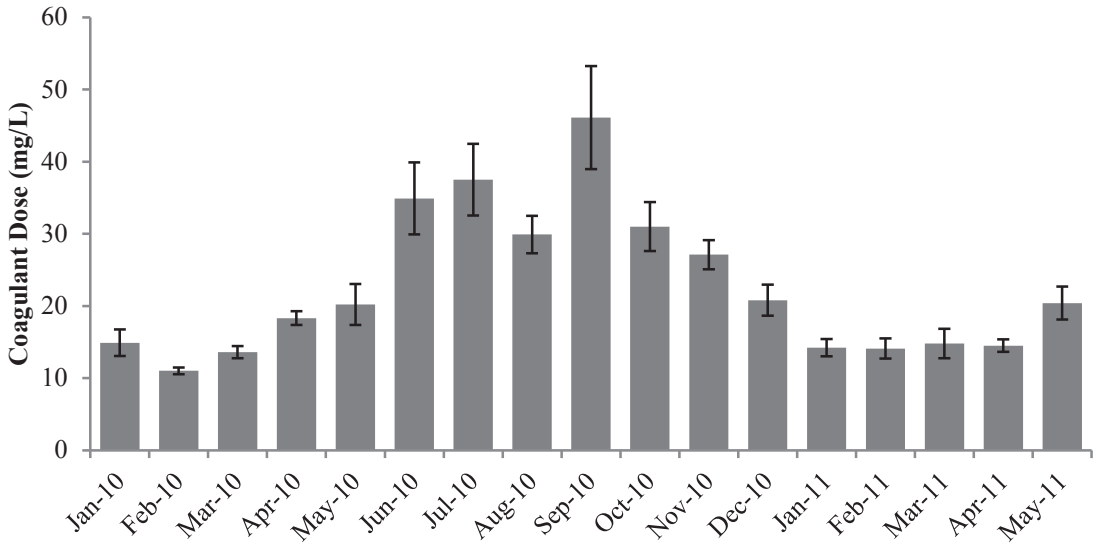

Figure 4.3. Monthly average coagulant dose at the BBWTP.

The rapid mix tank is 1.9 m^3 and achieves 30 s of retention time during normal plant flowrates and 20 s at the design flow. Mixing intensity is quantified by the velocity gradient (G-value, s^{-1}), which is calculated using the energy dissipation rate into the water as shown in Equation 4.1 (Droste, 1997).

$$G = \sqrt{\frac{P}{\mu V}} \qquad \text{Equation 4.1}$$

where G = velocity gradient (s^{-1})
P = net power dissipated into the mixing chamber
μ = dynamic viscosity of water (temperature dependent)
V = volume of the mixing chamber

The BBWTP utilizes a 2 horsepower flash mixer, therefore G-values between 600 to 800 s^{-1} are achieved at temperatures ranging from 0.5 to 20 °C assuming a mixer efficiency of 0.7 (AWWA, 2011). The recommended G-value for rapid mixing is 700 to

1000 s^{-1}, although this value is less important when sweep flocculation is used as the dominant mechanism of coagulation (Droste, 1997; Amirtharajah & Mills, 1982).

The water flows up from the bottom of the rapid mix tank and spills over the top of two weirs. The raw water inlet pipe and flash mixer tank are shown in Figure 4.4 and 4.5. There is a streaming current meter (SCM) placed downstream from the flash mixer, which acts as a feedback mechanism indicating whether sufficient charge neutralization is occurring, and is the first instrument notifying operators of a significant change in raw water quality. The streaming current (SC) is related to zeta potential, and is produced by water flowing past fixed particles, which causes diffuse counter-ions to be removed outside the shear plane, as discussed in Section 2.4.2.2. A current which results from the electric potential difference between the shear plane and the bulk solution is used to identify changes in particle surface charge, causing a change in required coagulant dosing. The pH is measured in the flash mixer, and the probe can be seen on the left side of Figure 4.5. From the flash mixer, water is piped to one of two DAF trains, each consisting of two flocculation basins and a DAF clarifier.

Figure 4.4. Raw water supply pipe leading to flash mixer tank.

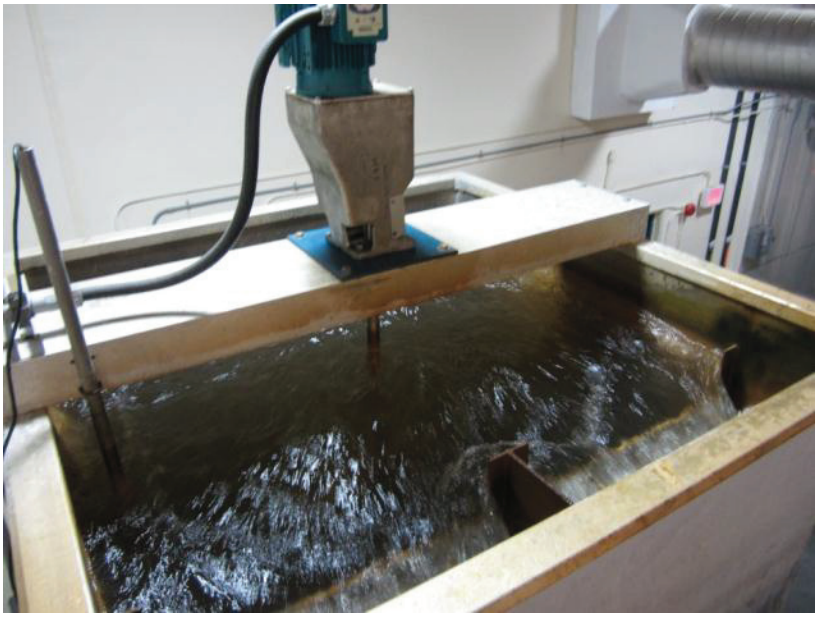

Figure 4.5. Flash mixer showing flow over weirs.

4.3.2 Flocculation

Turbulent flow over the flash mixer weirs results in air entrainment and consequently large bubbles which surface in the first floc basins, causing foam to collect at the surface. This can be seen in Figure 4.6 below.

Figure 4.6. First floc basin with bubbles and surface foam.

The flocculation basins utilize vertical axis paddles which are designed to induce tapering G-values to allow floc growth. The retention time in each basin at normal flowrates is approximately 12 minutes, with G-values reducing from approximately 65 s^{-1} to 35 s^{-1}. This falls into the normal range of velocity gradients for flocculation in DAF pretreatment, with tapered G-values from 50 to 100 s^{-1} in the first flocculation basin and 20 to 50 s^{-1} in the last flocculation basin (AWWA, 2011). Total retention times and G-values through the plant are shown in Table 4.1 for the maximum plant flowrate of 340 m^3/h and normal flowrate of 250 m^3/h.

Table 4.1. Retention times and G-values for unit operations at the BBWTP.

Stage	G-values		Retention Time		Gt/1000
	Winter	Summer	Normal Flow	Maximum Flow	
Rapid Mix	600 s^{-1}	800 s^{-1}	30 s	22 s	13 to 24
Floc Basin 1	60 s^{-1}	65 s^{-1}	21.1 mins	15.5 mins	41 to 61
Floc Basin 2	30 s^{-1}	35 s^{-1}	21.1 mins	15.5 mins	21 to 33
DAF Tank			32.6 mins	24 mins	
Filter			11.2 mins	8.2 mins	
Chlorine Contact Chamber			48 mins	38.3 mins	
Clearwell			4.8 hours	3.5 hours	
		Total	7.0 hours	5.2 hours	

4.3.3 DAF Clarification

After passing through the flocculation basins, the water flows into the bottom of the contact zone of the DAF clarification tank, where air saturated with water is injected to provide bubbles for floc attachment and flotation (a detailed description of the recycle/saturator system is provided in Chapter 6). The surface of the DAF clarifier at the contact zone and separation zone, showing both the rising whitewater (bubbles and floc-bubble aggregates) and accumulated sludge blanket (separated by the skimmer) can be seen in Figure 4.7.

Figure 4.7. Surface of DAF tank showing whitewater, skimmer and sludge blanket.

The skimmer rotates intermittently on operator adjusted timing and speed in order to allow thickening and prevent disruption of the sludge blanket. The floating sludge blanket is pushed into a waste trough and clarified water is drawn from perforated pipes spread along the bottom of the DAF tank. This water then overflows an exit weir into filter supply pipes. The DAF exit weir can be seen in Figure 4.8.

Figure 4.8. DAF tank exit weir overflowing to filter supply pipe.

4.3.4 Filtration

There are three rapid sand filters to provide sufficient filtering capability for high raw water flowrates even while backwashing. Each filter is composed of media as shown Table 4.2.

Table 4.2. BBWTP filter media composition listed from top to bottom.

Material	Material Size	Depth
Anthracite coal	1 mm	450 mm
Sand	0.45 mm	300 mm
Gravel	¾" x ½"	50 mm
Gravel	¼" x ¾"	50 mm
Gravel	$^{1}/_{8}$" x $^{1}/_{16}$"	50 mm
Gravel	¼" x $^{1}/_{8}$"	50 mm
Gravel	½" x ¼"	50 mm
Gravel	¾" x ½"	50 mm

Typical dual-media filter beds are composed of 0.46 to 0.76 m of anthracite coal atop 0.15 to 0.3 m of sand; therefore the BBWTP has a fairly thin layer of anthracite atop a fairly thick layer of sand (AWWA, 1997). The filters are equipped with nozzles along

the bed of the filter which allow for air scouring prior to backwash cycles. Typically air scouring is performed for 3 to 4 minutes before backwashing begins.

The relative removal of colour and turbidity from the DAF clarifier and filters can be seen in Figure 4.9, comparing a grab sample of raw water, DAF effluent and finished water from the plant during conditions of elevated raw water colour and turbidity where good plant performance was maintained. It can be seen that when the plant is performing well, a large percentage of turbidity and colour is removed in the DAF clarification stage with the filter acting as more of a polishing step. While filtration is often considered to be the most important unit operation in a WTP, it is apparent that well adapted chemical conditioning and DAF clarification will provide the majority of contaminant removal, allowing the filter to run for a longer period of time and reducing backwash water volume requirements.

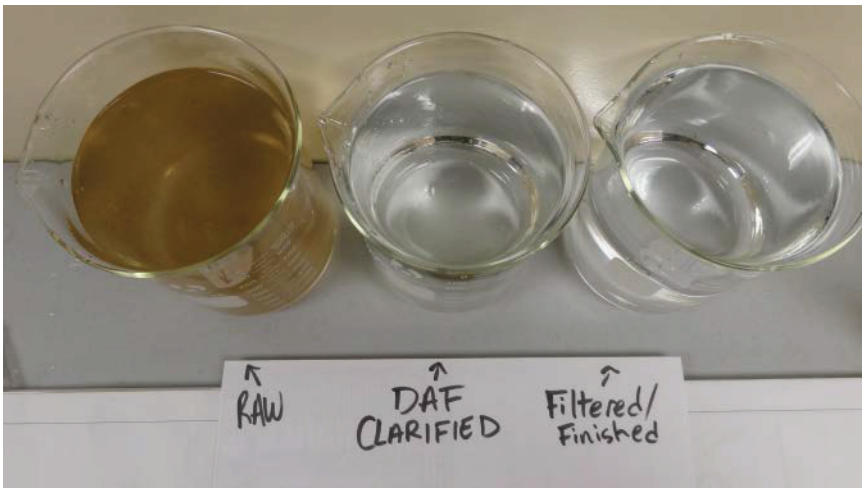

Figure 4.9. Visual comparison of raw water, DAF effluent and finished water.

4.3.5 Disinfection

After filtration, water is piped to the CCC where chlorine gas is injected at the inlet of the CCC and caustic soda is added at the outlet to increase the pH to within the Guidelines for Canadian Drinking Water Quality (GCDWQ) acceptable range of 6.5 to 8.5 (Health Canada, 2010).

According to the Nova Scotia Treatment Standards for Municipal Drinking Water Systems, the BBWTP distribution system must achieve a CT ratio of 1 as determined by a 0.5-log log inactivation of *Giardia* protozoans (Nova Scotia Environment, 2012). The CT concept is explained by Equations 4.2 and 4.3.

$$CT_{actual} = \text{Free Chlorine (mg/L)} \cdot \text{Retention Time (min)} \cdot \text{Baffling Factor} \quad \text{Equation 4.2}$$

$$\text{CT Ratio} = CT_{actual}/CT_{required} \quad \text{Equation 4.3}$$

The baffling factor is used in CT calculations to account for short circuiting within the chamber. Baffling factors range from 0.1 for an unbaffled basin with low length-to-width ratio to 1.0 for a plug flow basin with a length-to-width ratio greater than 10:1 (Nova Scotia Environment, 2012). The BBWTP CCC contains serpentine intra-basin baffles and an outlet weir, corresponding to a baffling factor of 0.7.

Using the CT tables provided in the Nova Scotia Treatment Standard for Municipal Drinking Water Systems (Nova Scotia Environment, 2012), which provide $CT_{required}$ values, along with the design specifications of the BBWTP CCC, Figure 4.10 illustrates the chlorine residual required at various pH levels at a minimum water temperature of 0.5° C.

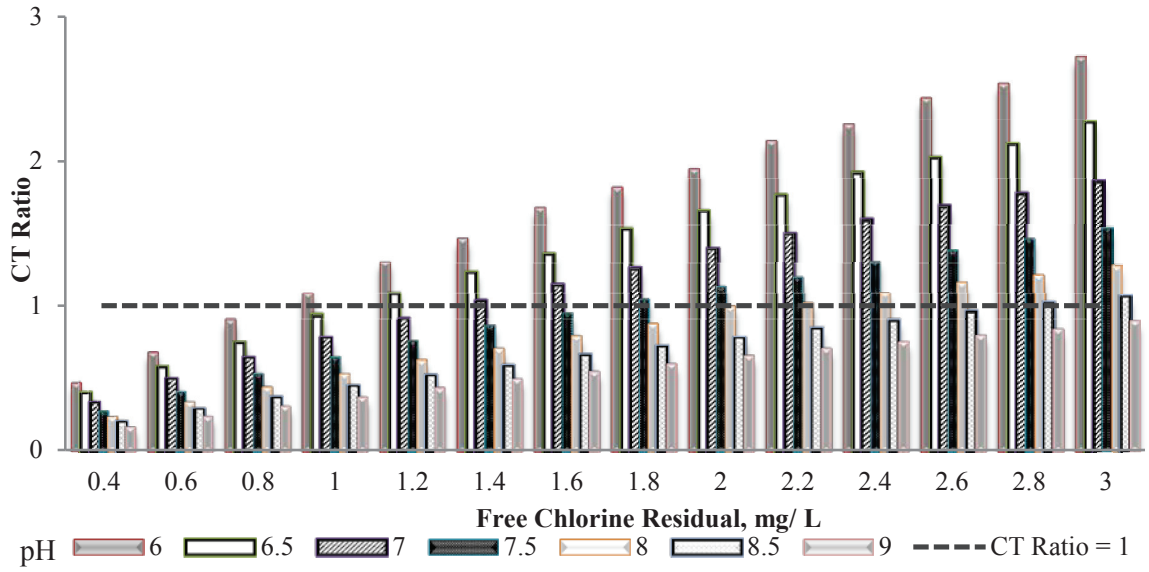

Figure 4.10. CT achieved in BBWTP chlorine contact chamber at 0.5 °C.

The typical pH in the CCC will be similar to the flash mixer pH, as there is no chemical addition in the unit operations between the flash mixer and contact chamber. The actual pH will likely be slightly less than the rapid mix pH, as the chlorine addition will slightly depress pH. Typically, the rapid mix pH in the plant is between 6.0 and 6.5, and so a free chlorine residual of 1.2 mg/L at the outlet of the CCC is required at a temperature of 0.5 °C. At warmer temperatures, this required concentration will decrease, as chlorine disinfection efficacy increases with water temperature.

Water exiting the CCC then flows to the clearwell, from which water is pumped to the distribution system or used in backwashing of the filters.

4.3.6 Source Water Quality

Data collected from online SCADA measurements, daily operator log sheets and quarterly general chemical analysis reports was used to analyze the normal raw water

quality, seasonal variation in water characteristics and, of particular interest, the typical rate and extent of raw water quality degradation during stormwater runoff events.

Monthly pH measurement averages of raw water, taken daily at the BBWTP, are shown in Figure 4.11.

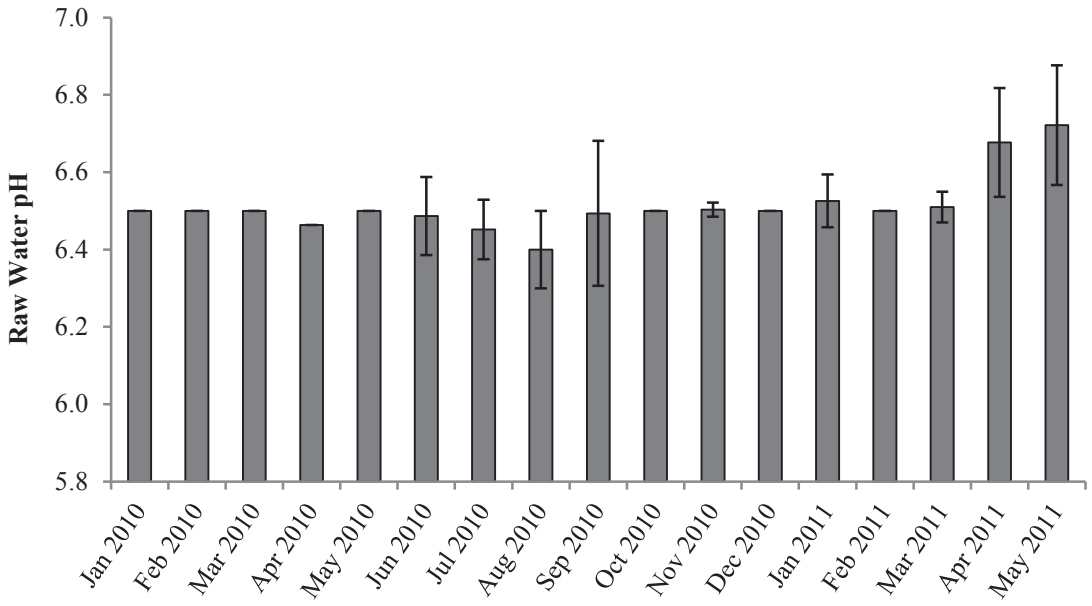

Figure 4.11. Monthly average raw water pH at the BBWTP, January 2010 to May 2011.

The raw water pH was found to remain relatively constant from 6.4 to 6.7 between January 2010 and May 2011. This source water to the BBWTP can be characterized as being slightly acidic, though this pH is actually above average for surface waters in Nova Scotia (Underwood *et al.*, 1987). Alkalinity titrations of samples taken from the BBWTP yielded values less than 10 mg/L as $CaCO_3$, which is extremely low and typical of most surface waters in Atlantic Canada.

Daily turbidity and apparent colour measurements taken from January 2010 to May 2011 are presented in Figure 4.12.

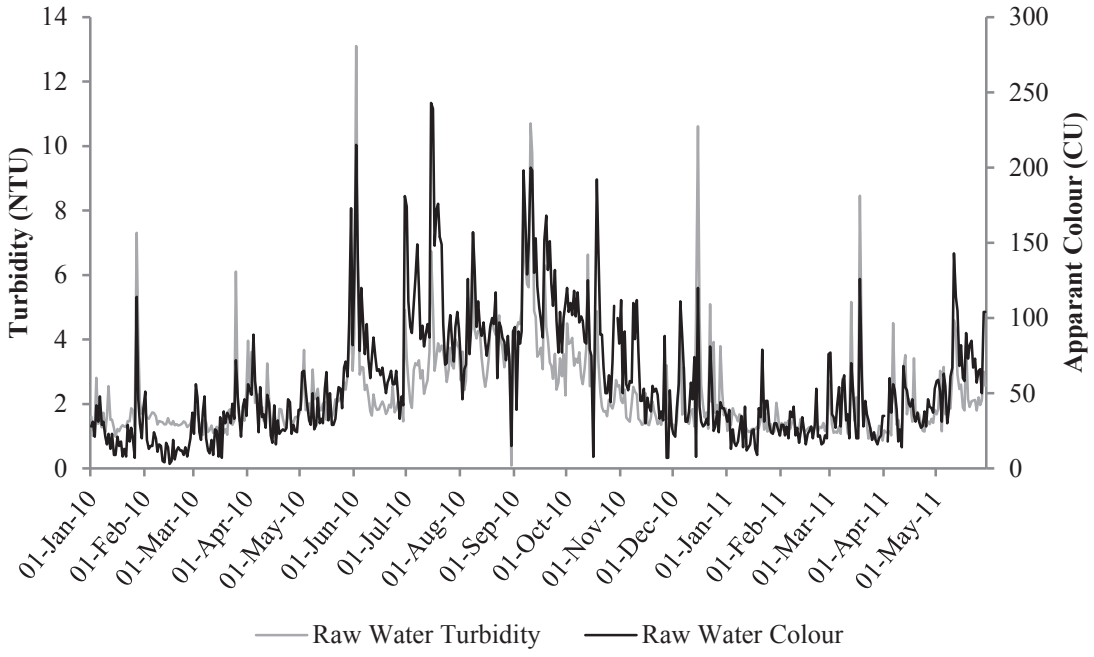

Figure 4.12. Daily raw water turbidity and apparent colour at the BBWTP, January 2010 to May 2011.

A similar pattern can be seen in turbidity and colour measurements, with the highest spikes in turbidity and colour occurring in the summer months. The correlation between turbidity and apparent colour was examined using Minitab. The Pearson correlation coefficient was found to be 0.777 ($p<0.01$). This shows a strong correlation between turbidity and colour, as was expected. Based on this data, collected over a 17 month period, both raw water turbidity and apparent color were found to be highest during the summer months (June to September) and lowest during the winter months (January to April). The monthly averages for apparent colour and turbidity are plotted

below in Figure 4.13 and confirm that average raw water turbidity and colour increase during the summer months, possibly due to rainfall/runoff events.

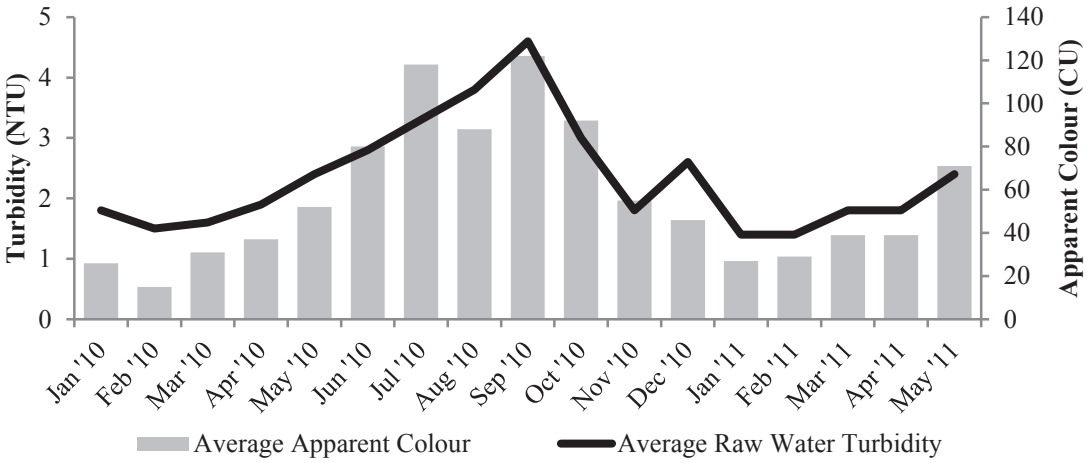

Figure 4.13. Monthly average raw water turbidity and apparent colour at the BBWTP, January 2010 to May 2011.

Results of quarterly chemical analysis of raw water at the BBWTP have been compiled in Table 4.3.

Table 4.3. BBWTP raw water general chemical analysis, 2006 to 2011.

Analyte	Unit	Result (# of tests)	Analyte	Unit	Result (# of tests)
Total Alkalinity as $CaCO_3$	mg/L	6.6 +/- 7 (19)	Nitrate	mg/L	0.12 +/- 0.1 (16)
Aluminum	µg/L	110 +/- 94 (18)	Nitrate + Nitrite	mg/L	0.12 +/- 0.1 (19)
Ammonia	mg/L	ND (4)	Nitrite	mg/L	ND (16)
Antimony	µg/L	ND (18)	Nitrogen	mg/L	ND (19)
Arsenic	µg/L	ND (18)	Orthophosphate	µg/L	0.5 +/- 5 (19)
Barium	µg/L	12.6 +/- 3.5 (18)	pH		6.8 +/- 0.4 (19)
Benzene	mg/L	ND (1)	Phosphorus	mg/L	ND (16)
Beryllium	µg/L	ND (18)	Potassium	mg/L	0.36 +/- 0.1 (19)
Bismuth	µg/L	ND (18)	Selenium	µg/L	ND (18)
Boron	µg/L	0.3 +/- 3 (18)	Silica (SiO2)	mg/L	4.85 +/- 1 (18)
Cadmium	µg/L	ND (18)	Silver	µg/L	ND (18)
Calcium	mg/L	2.9 +/- 1.9 (19)	Sodium	mg/L	4.2 +/- 1.19 (19)
Carbon Tetrachloride	µg/L	ND (1)	Strontium	µg/L	11.4 +/- 6.5 (18)
Chloride	mg/L	5.3 +/- 3 (18)	Sulphate (SO_4)	mg/L	1.2 +/- 2 (18)
Chlorobenzene	µg/L	ND (1)	Tetrachloroethene	µg/L	ND (1)
Chromium	µg/L	ND (18)	Thallium	µg/L	ND (18)
Cobalt	µg/L	ND (18)	Tin	µg/L	ND (18)
Colour	CU	20.8 +/- 19.5 (19)	Titanium	µg/L	1.3 +/- 2 (18)
Conductivity	µS/cm	44.4 +/- 19.5 (19)	Toluene	mg/L	ND (1)
Copper	µg/L	5.5 +/- 11.5 (19)	Total Dissolved Solids	mg/L	25 (1)
Fluoride	mg/L	ND (19)	TOC	mg/L	2.1 +/- 1.75 (19)
Iron	µg/L	193 +/- 179 (19)	Uranium	µg/L	ND (18)
Lead	µg/L	0.17 +/- 0.85 (18)	Vanadium	µg/L	ND (18)
Magnesium	mg/L	0.8 +/- 0.35 (19)	Vinyl Chloride	µg/L	ND (1)
Manganese	µg/L	31.1 +/- 42.2 (19)	Xylenes	mg/L	ND (1)
Mercury	ng/L	1.2 +/- 1.1 (19)	Zinc	µg/L	19.9 +/- 21 (19)
Molybdenum	µg/L	ND (18)	Total Coliform	CFU/100mL	100 (1)
Nickel	µg/L	0.22 +/- 1 (18)	E. Coli	CFU/100mL	3 (1)

Contaminants of concern in the raw water included aluminum, iron, manganese and coliforms as these parameters exceeded MACs or aesthetic objectives for drinking water as outlined in the GCDWQ and shown in Table 4.4 (Health Canada, 2010). The results show that the raw water quality is typically excellent, with low levels of metals, organics (TOC) and turbidity under normal operating conditions from 2006 to 2011. Total coliforms and *E. coli* are typically present in any raw surface water source. Both manganese and iron targets are aesthetic objectives and these analytes were found to measure significantly higher during the summer months, suggesting they may be elevated due to rainfall and runoff conditions or simply increased temperature. Aluminum is the most obvious concern, especially when considering that an aluminum-based coagulant is being added in the treatment process. The effect of dissolved aluminum in the BBWTP will be further examined in the next section.

Table 4.4. Contaminants of concern in BBWTP source water.

Analyte	GCDWQ MAC (µg/L)	Winter Average (µg/L)	Summer Average (µg/L)	P-value
Aluminum	100	89 +/- 27	127 +/- 58	0.164
Manganese	50	12 +/- 8	39 +/- 29	0.046
Iron	300	104 +/- 26	246 +/- 102	0.006

4.3.7 Brierly Brook Water Treatment Plant Upsets

A sudden increase in raw water contaminants, such as turbidity and colour, will cause the coagulant demand to increase, and this is reflected in the SCM measurement as a decrease in the SC. If SC decreases significantly, an alarm notifies operators to ensure adjustments to coagulant and/or chemical dosing may be done as quickly as possible. These sudden contaminant increases tend to occur after a heavy rainfall event and occasionally lead to treatment difficulties, which may culminate in an increase in

clearwell turbidity above 0.2 NTU. This situation is referred to as a "plant upset" in this thesis.

Raw water turbidity at the BBWTP is measured continuously online, therefore the exact turbidity peak and duration of raw water turbidity increases leading to plant upsets can be identified. A summary of raw water quality changes during five runoff events that led to plant upsets between January 2010 and May 2011 is shown in Table 4.5. Apparent colour measurements were taken from grab sample analysis during the upsets, and do not necessarily (or likely) represent the maximum raw water colour occurring during the runoff event.

Table 4.5. Summary of raw water turbidity and apparent colour during BBWTP upsets.

Date	Turbidity Before Event (NTU)	Maximum Apparent Colour Measured	Turbidity Peak (NTU)	Time to Peak (hrs)	Event Duration (hrs)	Turbidity After Event (NTU)
26-Jan-10	1.3	114	15	1:40	26:30	3.4
1-Jul-10	3	211	7.7	1:20	10:00	3.3
19-Sep-10	3.8	215	34.5	4:00	42:00	1.3
8-Nov-10	1.5	125	24.5	11:05	19:00	1.9
10-May-11	1.9	229	22.1	26:40	37:00	3.5

Further investigation into plant operating conditions was required to determine exactly why plant upsets could occur when raw water turbidity peaks were as low as 7.7 NTU. In many plants with similar raw water quality, it has been found that DOC has a much more prominent role than turbidity in determining coagulant demand and, consequently, treatment performance (Edzwald, 1993; Tseng *et al*., 2000, Shin *et al*., 2008). Therefore, turbidity spikes in the raw water only provide an indication that source water quality has changed and does not necessarily reflect the degree to which coagulant

demand has increased. Grab sample analysis of raw water apparent colour has shown that in upsets where raw water turbidity increases only mildly, apparent colour may spike to 200 CU and above (e.g. July 1, 2010 upset).

A summary of rainfall events which triggered each of the five profiled plant upsets is given below in Table 4.6. Typically, a storm event of at least 20 mm of rainfall after a period of relatively calm weather caused the upset conditions to occur. However, this pattern did not appear during every plant upset, nor did similar weather patterns result in plant upset conditions on other dates, demonstrating the unpredictability of these events. For example, during the November upset, no single large rainfall event occurred but fairly steady rainfall was present in the week prior to the upset, totalling 25 mm. For the January upset, the mean temperature for two weeks prior to the event was -8 °C before increasing to 5 °C on the day of the event, suggesting that runoff from the heavy rainfall event may have been compounded by snowmelt.

Table 4.6. Summary of rainfall conditions prior to plant upsets.

Date	Days Since Last Storm Event > 10 mm	Total Rainfall Since Last Storm Event > 10 mm (mm)	Total Rainfall during Event (mm)	Mean Temperature during Event (°C)	Minimum Temperature during Event (°C)
26-Jan-10	16	0	31.8	4.8	0.7
1-Jul-10	20	5.4	37.8	14.9	10.4
19-Sep-10	12	18.6	25.2	13.7	10.1
8-Nov-10	8	23.4	16.4	14.8	10.6
10-May-11	21	31.5	20.5	8.7	5

Figure 4.14 below shows the SC values vs. turbidity readings taken in the raw water, DAF effluent, and clearwell during a plant upset on January 26 and 27th, 2010. It can be seen that a sudden decrease in the SC coincided with a spike in turbidity. A decrease in SC represents an increase in coagulant demand, and since coagulant dosing is manually controlled at the BBWTP, sudden decreases in SC indicate a deficiency in coagulant dose being applied to the rapid mixer. Increased coagulant demand is typically not solely due to turbidity, and since colour measurements are not performed continuously the impact of coagulant demand due to colour vs. turbidity cannot be fully quantified. However, it is likely that raw water colour is a more important factor in coagulant demand than turbidity. Since there has been a correlation shown between turbidity and colour at the BBWTP, it is likely a spike in raw water turbidity also indicates an increase in raw water colour. Also not recorded continuously at the BBWTP is the applied coagulant dose, and therefore increases in SC due to additional coagulant are not explicitly shown.

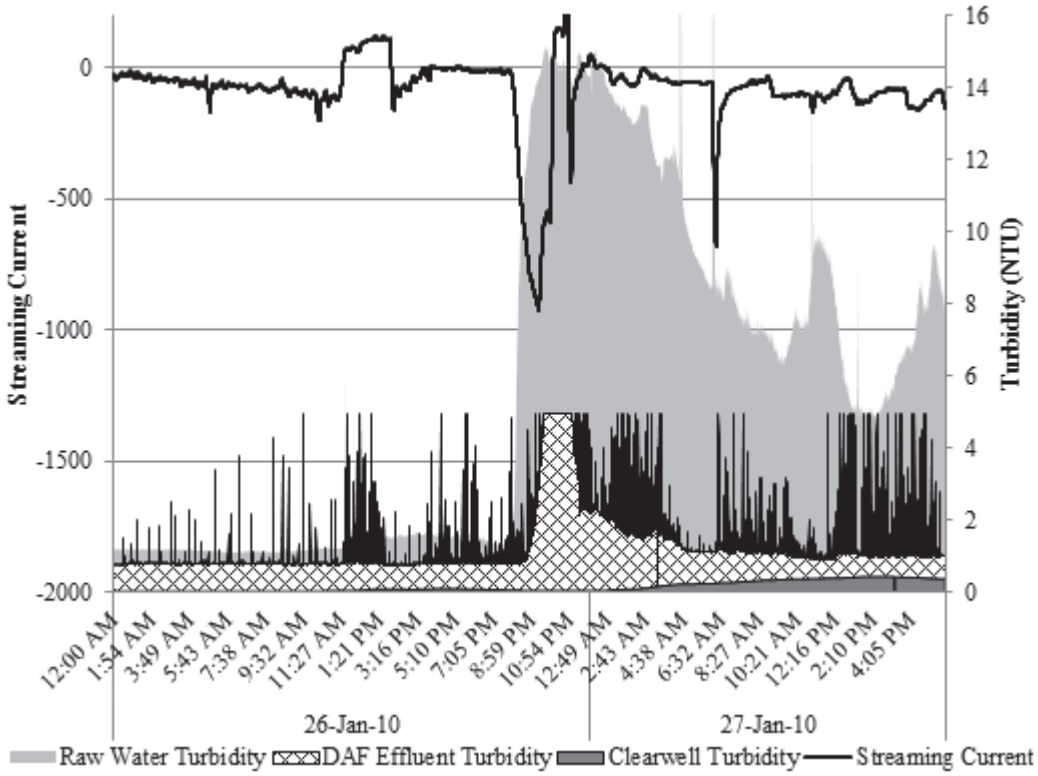

Figure 4.14. Streaming current and turbidity values at the BBWTP during plant upset, January 26 to 27, 2010.

Filter turbidities are not shown, however they can be misleading as whenever filter turbidities increase above 0.2 NTU the plant automatically diverts the filter effluent to waste. Therefore, increases of turbidity in the clearwell above 0.2 NTU may not be caused by the physical transfer of particles from the filter effluent—at steady state and only after an extended period of time would filter effluent of 0.2 NTU lead to a clearwell turbidity of 0.2 NTU. Particle size distributions taken during normal operation of the BBWTP and analyzed in the DAF and filter effluents, along with the clearwell, are shown in Figure 4.15.

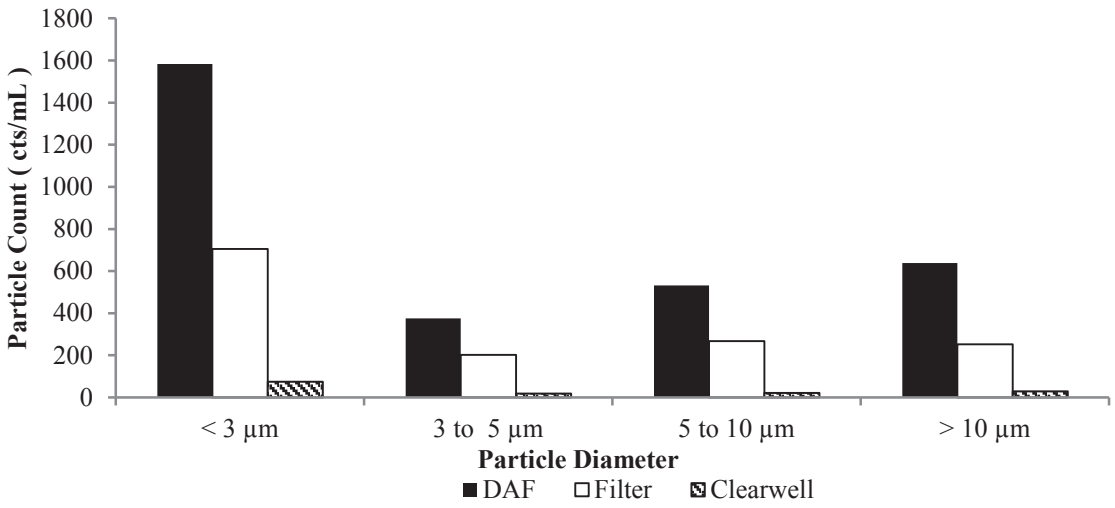

Figure 4.15. Particle counts in DAF, filter and clearwell effluent at BBWTP: June 21, 2011.

From Figure 4.15 it can be seen that the particle count, at all particle sizes, decreases from the filter effluent to the clearwell effluent. This indicates that particles are being removed somehow between the filter effluent and clearwell effluent, likely through settling in the clearwell at the BBWTP, which may act as a sedimentation tank. The clearwell at the BBWTP is approximately 1200 m^3, therefore at a normal flowrate of 250 m^3/h a retention time of 4.8 hours is being achieved. This is beneficial, not only to allow any particulate matter which has passed the filters to be removed from the water supply via settling in the clearwell, but also to provide extra chlorine contact time to enhance disinfection efficacy. However, if particle settling does occur in the clearwell, it is unclear how clearwell turbidity exceeds 0.2 NTU at any point when the maximum filter effluent turbidity of water routed to the clearwell is 0.2 NTU. Therefore, particles must be added to the water after passing through the filters, and the only possible source of these particles is the precipitation of dissolved components in the treated water itself. Because aluminum is being added in the plant and is sensitive to pH with regards to its

solubility, the pH profile through the treatment process (measured at the rapid mixer and clearwell) during the January 2010 plant upset is plotted in the Figure 4.16 alongside clearwell turbidity.

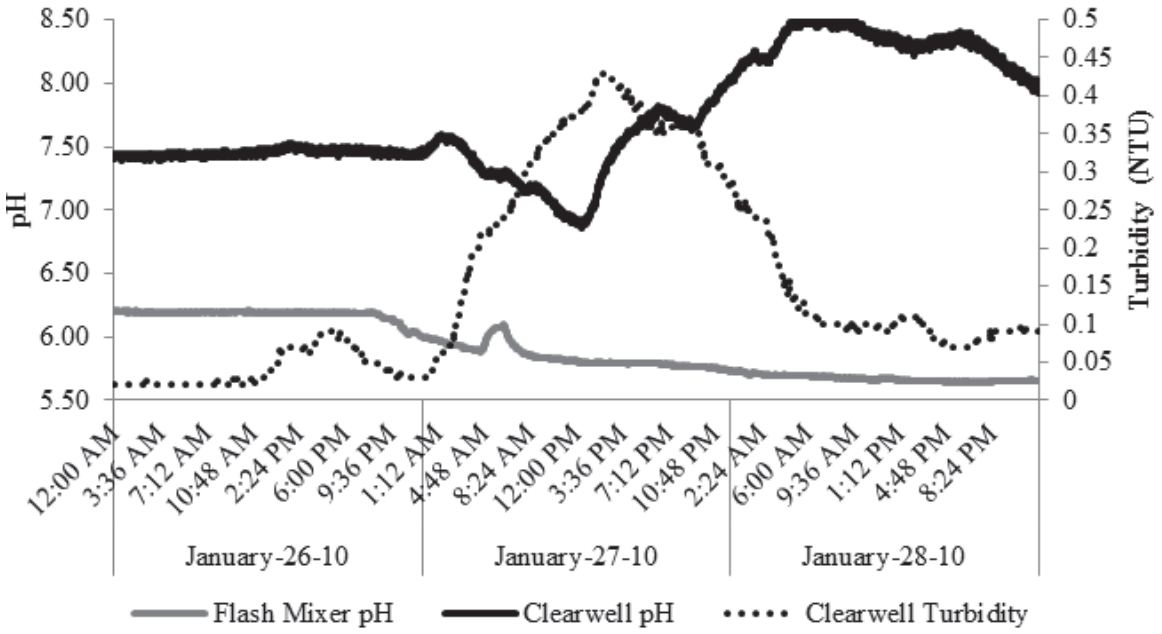

Figure 4.16. pH and clearwell turbidity profile for BBWTP upset, January 26 to 28, 2010.

A common pattern exists for each of the plant upsets, with the flash mixer pH decreasing before an increase in clearwell turbidity occurs. The turbidity, SC and pH profiles for the other plant upsets are presented in Appendix A.

Coagulation pH is controlled both by acidic PACl coagulant addition and the use of caustic soda or soda ash for buffering the pH in the flash mixer. The solubility of aluminum in medium basicity PACl with sulphate has been established by Pernitsky (2001) at an aluminum molar concentration of 5×10^{-4}, and is shown in the Figures 4.17 and 4.18. Experimental data is indicated by points and theoretical solubilities for Al^{3+},

$Al(OH)^{2+}$, $Al(OH)_4^-$, and Al_{13}^{7+} are indicated by solid lines. At 20° C, the experimental log[Al] increases from -5.9 to -3.7 when decreasing pH from 6.3 to 5.5 This roughly represents a 160-fold increase in the solubility of aluminum over just 0.8 pH units. At 5° C, experimental log[Al] values increasing from -7.1 to -4.6 when decreasing pH from ~6.6 to 5.5 representing an even greater increase in Al solubility of over 300-fold. The data clearly indicates that Al solubility is highly sensitive to pH, and confirms that a decrease in the flash mixer pH at the BBWTP would result in higher dissolved aluminum residuals which could then be precipitated with added hydroxide ions in the clearwell.

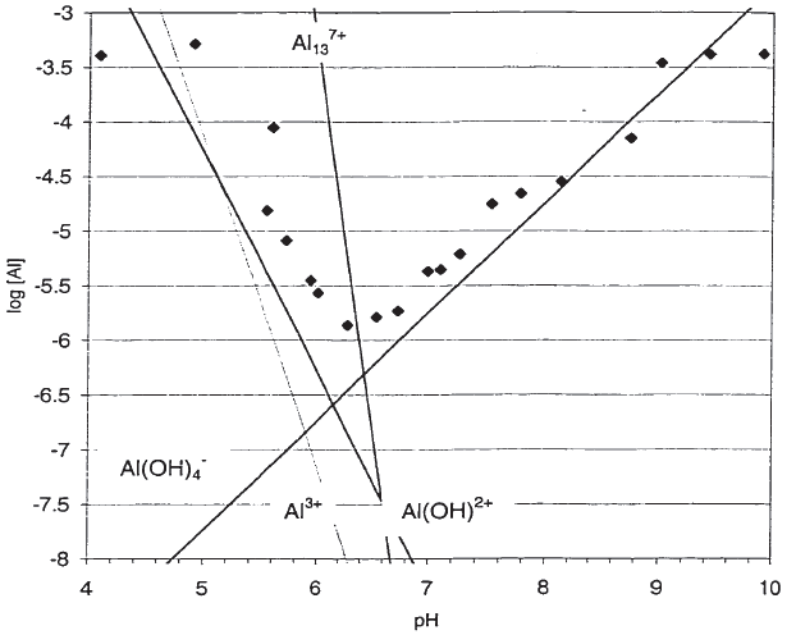

Figure 4.17. Solubility of aluminum in medium basicity PACl with sulphate at 20° C (Pernitsky, 2001).

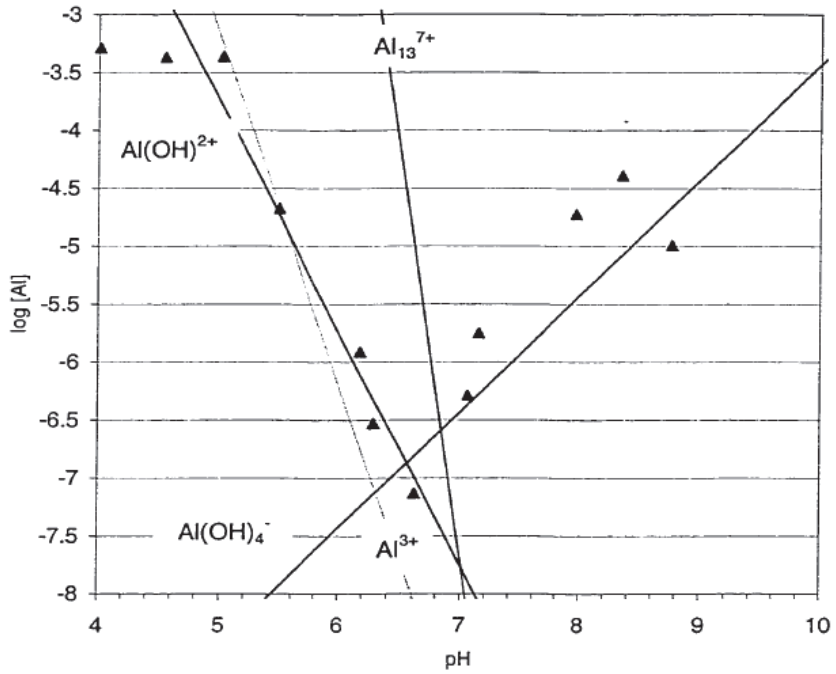

Figure 4.18. Solubility of aluminum in medium basicity PACl with sulphate at 5° C (Pernitsky, 2001).

4.4 Conclusions

An extensive review of the technical operations of the BBWTP was conducted, including analysis of source water quality, unit operations within the treatment train and plant performance during periods of deteriorated source water quality.

Raw water pH remained constant between 6.4 and 6.7 during the study period, from January 2010 to May 2011. Average turbidity varied between 1.5 in January and 4.6 in September, with average apparent colour lowest in February (15 CU) and highest in September (122 CU).

The first treatment unit within the treatment train at the BBWTP consists of a series of mechanical mixers, which induce tapered velocity gradients to allow floc formation and growth. Polyaluminum chloride is added in the flash mixer along with either sodium hydroxide or soda ash, which are used for pH control. DAF is used for clarification before water passes through dual-media anthracite-sand rapid filters, is chlorinated, and sent to the clearwell. From the clearwell it is pumped to the distribution system or utilized for filter backwashes.

Examination of plant upsets between January 2010 and May 2011 at the BBWTP revealed a pattern; once raw water turbidity and apparent colour increased, the subsequent increase in coagulant addition caused the coagulation pH to decline to less than 6.0. Despite automatic redirection of filter effluent to waste when turbidity rose above 0.2 NTU, these events caused the clearwell turbidity to increase to as high as 0.7 NTU. A hypothesis was developed that lowered coagulation pH led to high concentrations of dissolved aluminum during the initial stages of the plant upsets passing through the treatment train and into the clearwell where pH was increased, allowing the

formation of aluminum hydroxide precipitates. Bench-scale testing to further investigate this hypothesis is conducted in the following chapter.

Further investigation into the SC where optimal treatment occurs would be enhanced if the coagulant dose was recorded continuously using the SCADA system, which at the time of this study was not among the measured parameters.

Chapter 5. Impact of Chemical Factors on DAF Optimization

This study was done in order to evaluate the effect of manipulating key chemical factors on dissolved air flotation (DAF) clarification efficacy at the bench-scale in order to determine potential routes to achieve optimization of DAF clarification in a full scale water treatment plant (WTP). The application of pH control via two alternative alkalinity sources was also examined.

5.1 Introduction

Research has shown pretreatment coagulation-flocculation processes to be extremely important in achieving optimum DAF clarification performance. Various factors affecting the chemistry in these processes have been examined at the bench-scale, including raw water quality, coagulant type and dose and coagulation pH (Yan *et al.*, 2008; Tseng *et al.*, 2000; Bunker *et al.*, 1995).

Rapid changes in raw water quality have led to process disruptions and plant upsets in a full-scale WTP, as discussed in Chapter 4, and therefore a comparison of the treatment of baseline raw water and synthetic challenge water source has been done. Coagulation pH and coagulant dose were investigated, as these factors have been found in previous studies to be extremely important in determining coagulation-flocculation performance (Duan & Gregory, 2003; Pernitsky, 2001; Bunker *et al.*, 1995; Edzwald, 1993). A comparison of two polyaluminum chloride (PACl) coagulants was also conducted to examine the effect of coagulant basicity, which may alter the active coagulant species in rapid mixing and thereby affect the mechanism of coagulation (Pernitsky, 2001).

Identifying differences in optimum DAF pretreatment chemistry as determined by DAF performance using baseline and challenge water typical for Atlantic Canada has not been previously studied. These experiments were conducted to provide a better understanding of some of the factors affecting DAF performance which may be used to implement more suitable treatment practices for DAF WTPs in Atlantic Canada.

5.2 Materials and Methods

5.2.1 Source Water

A total of 240 L of raw water samples were collected from the Brierly Brook Water Treatment Plant (BBWTP) in Antigonish, Nova Scotia from November 12th to December 8th, 2011 and stored at 4 °C prior to bench-scale experiments. This water was intended for use as baseline source water with characteristics commonly found in surface waters in Nova Scotia. On April 26th, 2012, 120 L of raw water was collected from the BBWTP during a process disruption which led to mild plant upset. This water was intended for use as challenge water, representing the conditions experienced following a heavy rainfall and runoff event. However, the actual peak turbidity and colour were not outside the normal range for BBWTP source water. Therefore, artificial turbidity and organic matter were added to the water, and the resulting combination is referred to as synthetic challenge water in this thesis. 5 mg/L of humic acid (Alfa Aesar) and 20 mg/L of kaolin clay (Fisher Scientific) were used to simulate natural organic matter (NOM) and eroded soil particles typical of those found in surface water in Nova Scotia. The samples were blended and analysis of both source waters was done, with the results presented in Table 5.1.

Table 5.1. Bench-scale DAF study source water quality characterization.

Analyte	Unit	Baseline Raw Water	Challenge Synthetic Water
pH		6.25 +/- 0.2	6.6 +/- 0.2
Alkalinity	mg/L as $CaCO_3$	< 5	< 5
Turbidity	NTU	8 +/- 0.3	15 +/- 1.2
Particle Count	cts/mL	35,000 +/- 5600	340,000 +/- 42,000
True Colour	TCU	40 +/- 1	103 +/- 5
UV_{254}	cm^{-1}	0.236 +/- 0.001	0.363 +/- 0.001
TOC	mg/L	5.9 +/- 0.1	8.1 +/- 0.3
DOC	mg/L	5.7 +/- 0.1	6.2 +/- 0.2
SUVA		4.1	4.5
Aluminum	µg/L	116 +/- 3	99 +/- 7
Zeta Potential	mV	-23.5 +/- 2.7	-30.1 +/- 2.3

5.2.2 Experimental Design

A 2-level factorial design was used in order to compare the effect of pH and coagulant basicity at optimum coagulant concentration. Jar tests were run at coagulant concentrations ranging from 10 to 95 mg/L, and the data obtained at all doses was used to select an optimum dose. The optimum coagulant doses were defined as those that produced low turbidity and UV_{254} while higher doses produced only marginal improvements, or impaired treatment performance. Only the data generated by jars with optimum coagulant dose was utilized for factorial analysis.

Two polyaluminum chloride (PACl) coagulants with added sulphate were compared: a 50 % basicity PACl was selected as the “low basicity” (LB) PACl (SternPAC 50, Kemira) and a 70+ % basicity PACl was used as the “high basicity” (HB) PACl (DelPAC 2020, Delta Chemicals).

A pH of 6.0 was chosen as the low coagulation pH and the pH of minimum aluminum solubility for each coagulant was used as the high value. This pH of minimum aluminum solubility varied between 6.3 when using the LB PACl and 6.9 when using the

HB PACl (Pernitsky, 2001). The factorial design parameters with low and high levels are shown in Table 5.2.

Table 5.2. Factorial design for comparison of chemical parameters.

Parameter	Low (-)	High (+)
Coagulant Basicity	50 %	70+ %
Coagulation pH	6.0	$pH_{minimum\ solubility}$ (6.3 to 6.9)

For each jar test, 1.15 L of the raw water was poured into each jar and rapid mixed at 220 rpm, corresponding to a G-value of 600 s^{-1}. The coagulant was added directly (neat) into the jar after rapid mix was initiated. The addition of 10 g/L soda ash (Na_2CO_3) solution to increase the pH to the appropriate level was done immediately after coagulant addition. The quantity of soda ash added to each jar was predetermined by gradually adding soda ash while monitoring pH in a preliminary trial, which did not produce samples for analysis. Rapid mixing was then operated for 20 s before the flocculation stage was initiated.

Two-stage flocculation was operated with 5 minutes of slow mixing at 50 rpm (60 s^{-1}) followed by 5 minutes at 32 rpm (30 s^{-1}) in order to simulate tapered flocculation. After a total mixing time of 10 minutes and 20 s, mixing was stopped and DAF clarification was initiated.

Five minutes after DAF clarification was initiated, approximately 50 mL of sample was drawn from the sample ports as waste (to ensure flocs or previous sample residue in the ports did not affect results) and 500 mL of the remaining sample was

extracted for analysis. The clarified water samples were analyzed for turbidity, particle count, UV_{254}, dissolved organic carbon (DOC), true colour and dissolved aluminum.

5.2.3 Analytical Methods

Raw and clarified water characteristics such as alkalinity, pH, turbidity, UV_{254}, particle count, TOC, DOC, true colour and dissolved aluminum were determined using equipment and following procedures consistent with those outlined in Chapter 3. Specific UV absorbance is measured according to Equation 5.1.

$$SUVA = \frac{TOC}{UV_{254}} \text{ x } 100 \qquad \text{Equation 5.1}$$

where SUVA = specific UV absorbance
TOC = total organic carbon (mg/L)
UV_{254} = UV absorbance at 254 nm

Zeta potential (ZP) measurements were conducted on 10 mL samples collected immediately following the rapid mix stage during jar testing and analyzed using the Zetasizer Nano ZS (Malvern). Samples of the rapid mixed water (175 mL) were also collected for streaming current (SC) and charge demand analysis, measured using a streaming current meter with auto-titrator (ECAT2100, Chemtrac). For charge demand titrations, polydiallyldimethylammonium chloride (polyDADMAC), a cationic polymer, was used (Nalco).

5.3 Alkalinity Source Selection

Maintaining pH control by chemical addition is of great consequence in drinking WTPs, as coagulation pH is extremely important in achieving an effective coagulation-flocculation process. For treatment systems drawing from source water with low pH and alkalinity, the addition of acidic coagulants can cause pH to decrease to a point where the coagulation-flocculation process is impaired, reducing the overall treatment efficacy and potentially leading to a plant upset. Therefore, boosting the raw water alkalinity prior to coagulation or increasing pH immediately afterwards is common practice.

From the literature review, it is apparent that two sources of alkalinity often utilized in WTPs are derived from either caustic or carbonate sources (Jensen, 2003; Droste, 1997). The difference between caustic and carbonate alkalinity has been previously addressed in Chapter 2. In order to identify the effect of using each type of alkalinity, baseline raw water taken from the BBWTP was buffered using caustic soda (NaOH) or soda ash and titrated using a 1 mol/L sulphuric acid (H_2SO_4) solution to produce two pH profiles, shown below in Figure 5.1. This titration was done to observe total alkalinity as well as buffering intensity at varying pH levels with each alkalinity source. It can be seen from the figure that the diprotic nature of carbonic acid (carbonate alkalinity) results in two inflection points occurring along the soda ash titration line. From pH 5.9 to 6.8 there is a mild slope on the soda ash line, which indicates a high degree of buffer intensity at this pH. For caustic alkalinity, the monoprotic nature results in only one inflection point, and buffer intensity is high only at the upper and lower range of the pH scale. The buffer intensity at pH 5.9 to 6.8 is very low. Therefore, the addition of an acid or base to a system buffered mainly by caustic alkalinity will result in a

relatively large shift in pH as compared to a system buffered with carbonate alkalinity. For this reason, soda ash was chosen to provide alkalinity for the bench-scale trials to allow for more accurate pH control at a wide range of coagulant concentrations.

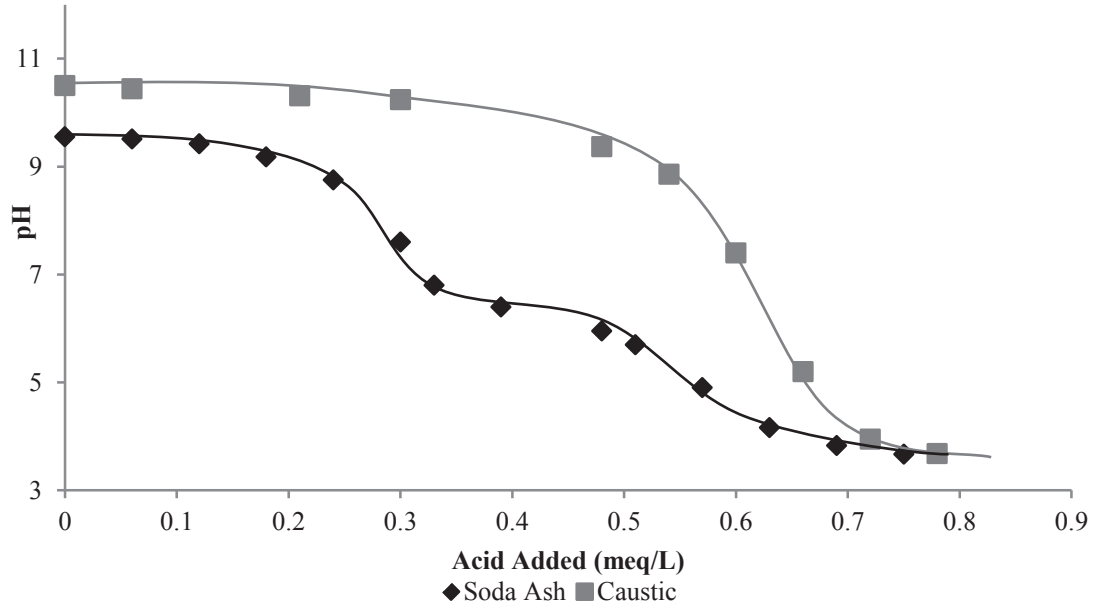

Figure 5.1. Titration of raw water buffered with soda ash and caustic by strong acid.

5.4 Bench-Scale Baseline Raw Water DAF Experiments

The results of analyses performed on treated baseline raw water samples produced in bench-scale DAF testing are divided into Sections 5.4.1 and 5.4.2, discussing the effects of coagulation pH and coagulant basicity, respectively, on treatment performance. The two parameters used in identifying optimum coagulant dose for factorial analysis were turbidity and UV_{254}, therefore the results for these analytes are shown in this section. Full results for particle count, DOC and true colour are presented in Appendix B.

5.4.1 Effect of Coagulation pH on DAF Performance

Coagulation pH has been described as the most important parameter in coagulation-flocculation processes, as it affects the surface charge of colloids, charge of NOM functional groups, charge of the dissolved coagulant species, surface charge of floc particles as well as the coagulant solubility (Pernitsky, 2001). Therefore a shift in coagulation pH from the pH of minimum solubility (6.3 to 6.9, depending on PACl basicity) to pH 6.0 was examined to determine possible impacts on overall treatment performance.

5.4.1.1 Turbidity

Clarified baseline water turbidity from low and high pH levels at all coagulant doses is shown in Figure 5.2. Bench-scale DAF treatment of the baseline raw water at optimum coagulant dose resulted in improved turbidity removals at high pH, with clarified water turbidity 1.0 NTU at the low pH level and 0.6 NTU at high pH ($p=0.027$). Optimum coagulant concentration was found to be 15 to 20 mg/L at the low pH condition and 25 to 30 mg/L at high pH. It has been previously reported that the greatest

particulate matter removals occur under conditions of sweep flocculation (Duan & Gregory, 2003), which appeared to be the dominant mechanism of coagulation at the high pH level based on the higher turbidity removal and higher optimum coagulant dose. At low pH, coagulation followed the charge neutralization/destabilization "four zones of coagulation" as proposed by Duan & Gregory (2003). A coagulant dose of 25 mg/L, above optimum at the low pH condition, appeared to result in restabilization and impaired flocculation, leading to higher turbidity in the clarified samples. At high pH, DAF performance did not deteriorate at higher coagulant doses, however turbidity removals did not improve beyond the optimum dose, again suggesting sweep flocculation as the dominant mechanism.

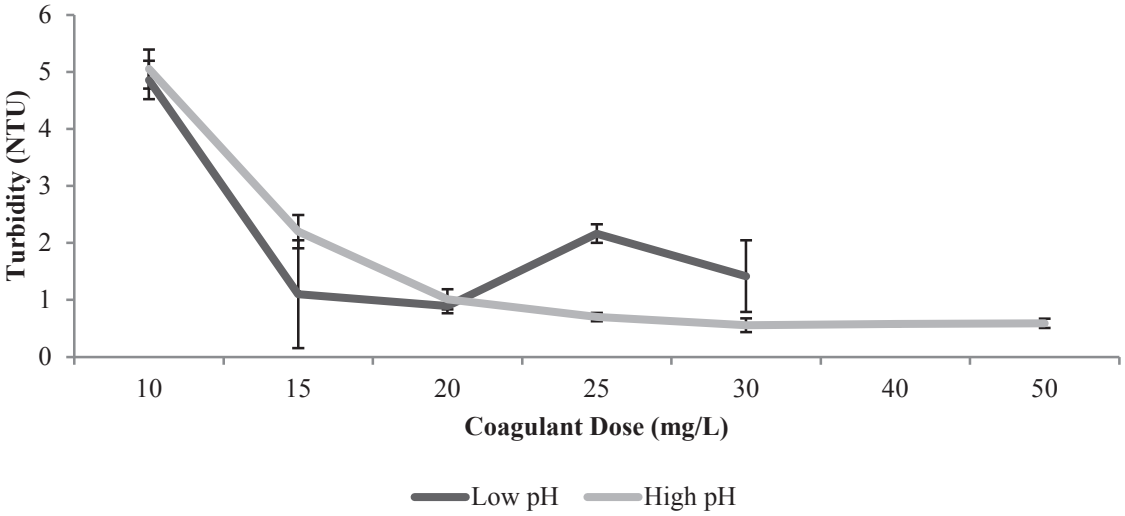

Figure 5.2. Effect of pH on clarified water turbidity during baseline raw water trials.

The patterns shown by turbidity removal at low and high pH are also seen in particle count results, which are presented in Appendix B.

5.4.1.2 UV_{254}

Clarified baseline water UV_{254} from low and high pH levels at all coagulant doses is shown in Figure 5.3. Optimum removal of UV_{254} at low and high coagulation pH occurred at coagulant doses of 25 and 30 mg/L, respectively. As with turbidity removal, a higher coagulant dose was required to maximize UV_{254} removal at the high pH setting. Optimum UV_{254} removal was slightly better at the low pH condition, measured as 0.018 cm^{-1} vs. a measurement of 0.020 cm^{-1} at the high pH condition, although this result was not statistically significant (p=0.263). At both pH levels, there is no increase in UV_{254} above the optimum coagulant dose—at higher coagulant doses performance did not suffer, but no further UV_{254} removal was achieved.

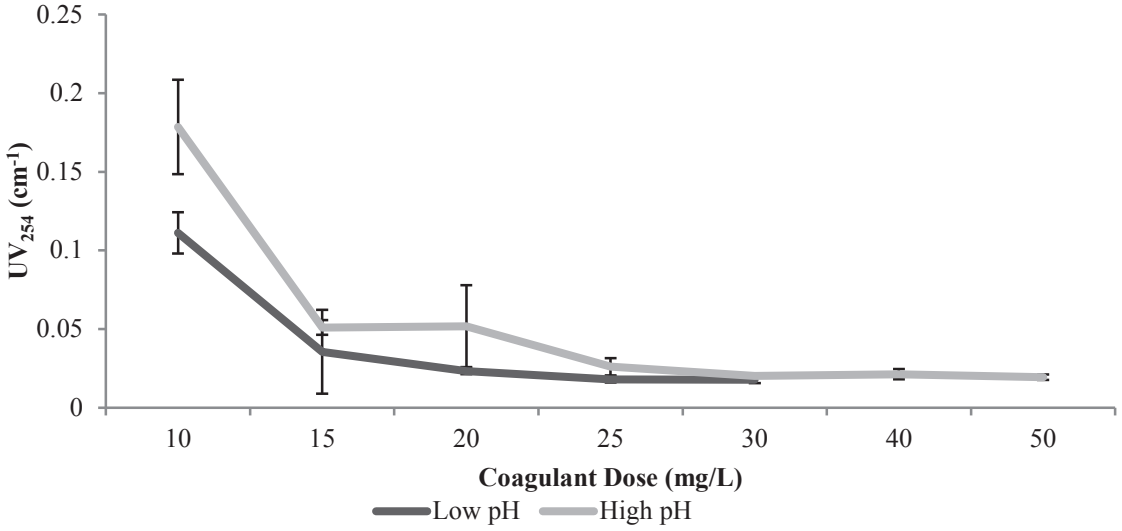

Figure 5.3. Effect of pH on clarified water UV_{254} during baseline raw water trials.

The patterns shown by UV_{254} removal at low and high pH are also seen in DOC and true colour removal results, which are presented in Appendix B.

5.4.1.3 Effect of Coagulation pH on DAF Performance at Optimum Coagulant Dose

A summary graph presenting the percent removals for turbidity, particle count, UV_{254}, DOC and true colour is presented in Figure 5.4. Turbidity removal was found to improve by 4 %, corresponding to 0.34 NTU, with experiments conducted at high pH (the pH of minimum aluminum solubility), a significant result confirmed using ANOVA with a p-value of 0.000. Particle count showed similar improvement at high pH, with removal increasing by 4.5 % (1627 particles/mL) with a p-value of 0.033. DOC removal was significantly improved at high pH by 8.9 % (0.43 mg/L), with p-value 0.002. No statistically significant differences for NOM removal as measured by UV_{254} (p=0.263) and true colour (p=0.97) were found.

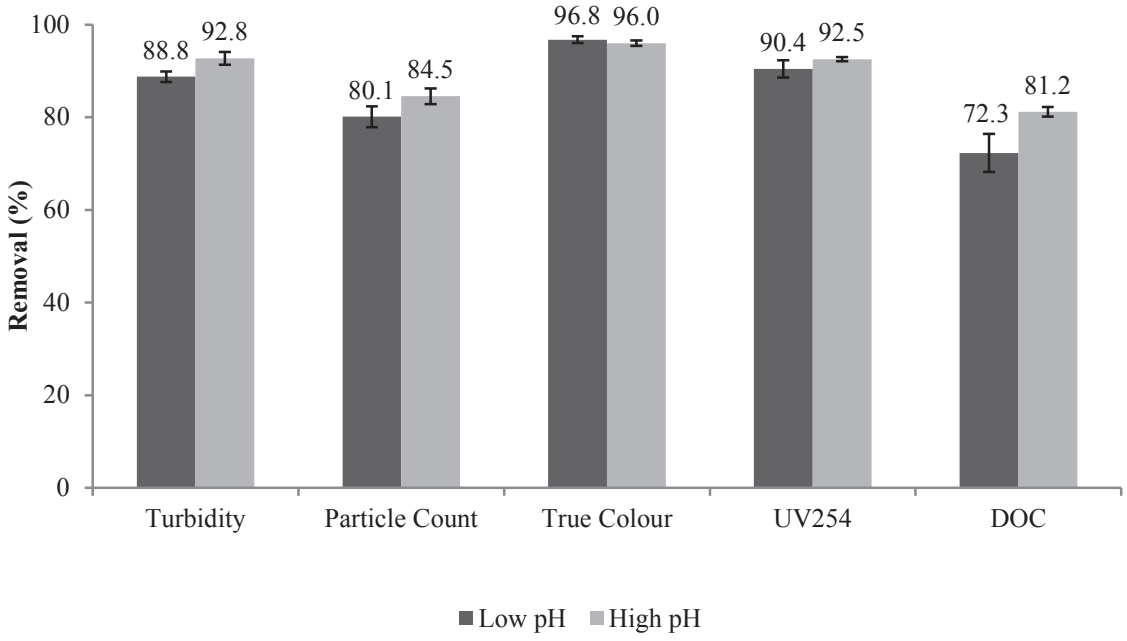

Figure 5.4. Impact of pH on optimum removal of target contaminants during baseline raw water trials.

5.4.2 Effect of Basicity on DAF Performance

5.4.2.1 Turbidity

Clarified baseline water turbidity from low and high basicity levels at all coagulant doses is shown in Figure 5.5. Turbidity removal was optimized at 15 mg/L for HB PACl and 20 mg/L for LB PACl, corresponding to 0.7 and 1.0 NTU, respectively, although no statistically significant improvement was found at higher coagulant doses ($p=0.606$). At 20 to 25 mg/L some restabilization occurred with HB PACl and a spike was seen in residual turbidity before regaining treatment performance at higher doses of 30 mg/L and above. This restabilization was found in HB PACl and not LB PACl, possibly due to the magnitude of difference between the pH of minimum solubility and pH 6.0 that both trials were run at—since HB PACl is further removed from its pH of minimum solubility at pH 6, restabilization may have occurred more readily. At very high coagulant doses of 30 mg/L and above, turbidity measurements of LB and HB PACl improved slightly above the removal attained at 15 to 20 mg/L. This may be due to the influence of sweep flocculation, as only the high pH trials were run at these high coagulant doses.

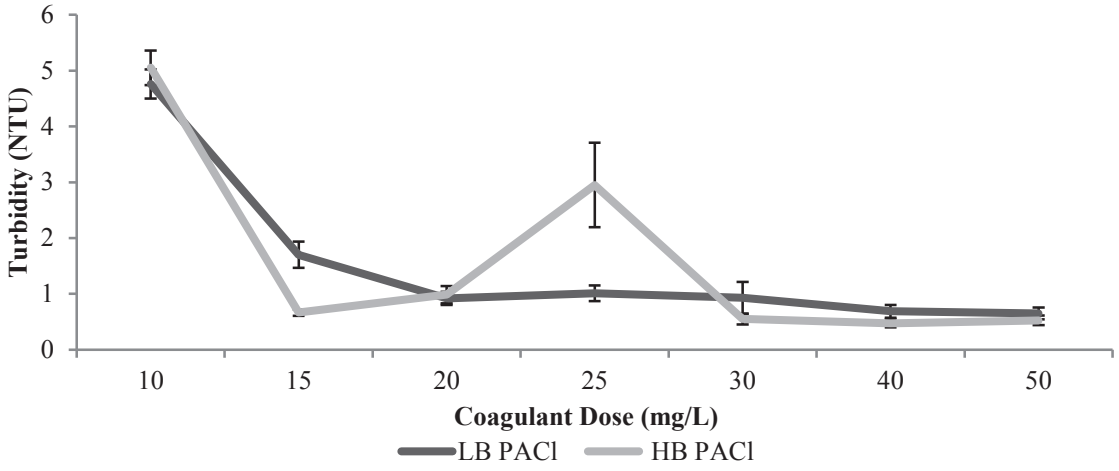

Figure 5.5. Effect of basicity on clarified water turbidity during baseline raw water trials.

The patterns shown by turbidity removal at low and high basicity are also seen in particle count results, which are presented in Appendix B.

5.4.2.2 UV_{254}

Clarified baseline water UV_{254} from low and high basicity levels at all coagulant doses is shown in Figure 5.6. Residual UV_{254} in the treated water was optimized at 25 mg/L for both LB (0.022 cm^{-1}) and HB (0.016 cm^{-1}) PACl, with no statistically significant difference found (p=0.332). As identified when examining pH effects, treatment performance does not deteriorate at high coagulant doses, but no substantial further treatment improvement occurs beyond the optimum coagulant dose.

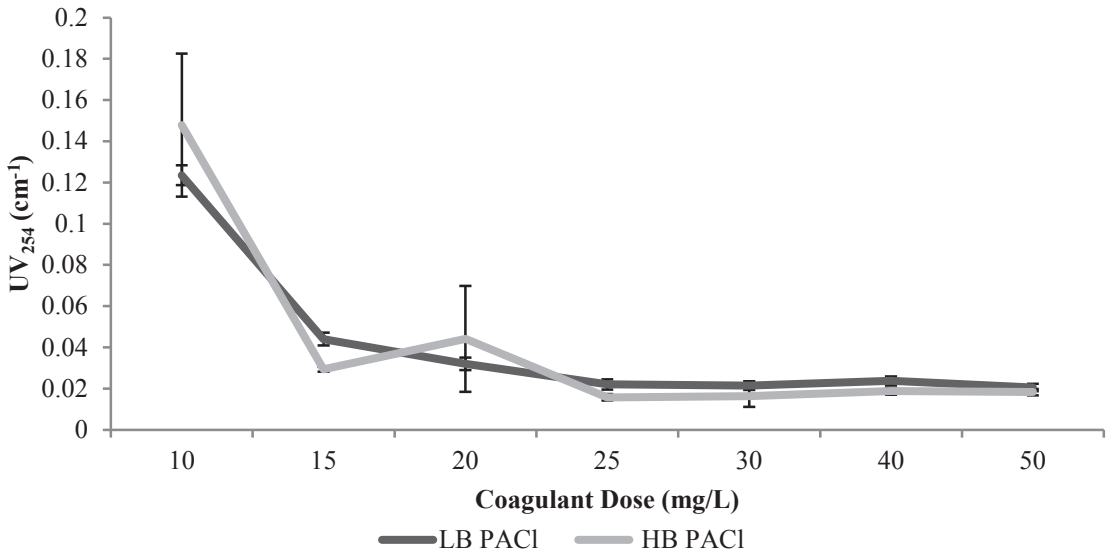

Figure 5.6. Effect of basicity on clarified water UV_{254} during baseline raw water trials.

The patterns shown by UV_{254} removal at low and high pH are also seen in DOC and true colour removal results, which are presented in Appendix B.

5.4.2.3 Effect of Basicity on DAF Performance at Optimum Coagulant Dose

A summary graph presenting the percent removals for each parameter at optimum coagulant dose is presented in Figure 5.7. On average, UV_{254} and DOC removals improved by 3.3 and 4.9 % when using HB PACl. However, no statistically significant difference in treatment performance was found when using ANOVA to compare LB and HB PACl for treating the baseline raw water. Parameters examined included turbidity ($p=0.606$), particle count ($p=0.911$), UV_{254} ($p=0.332$), DOC ($p=0.431$) and true colour ($p=0.149$).

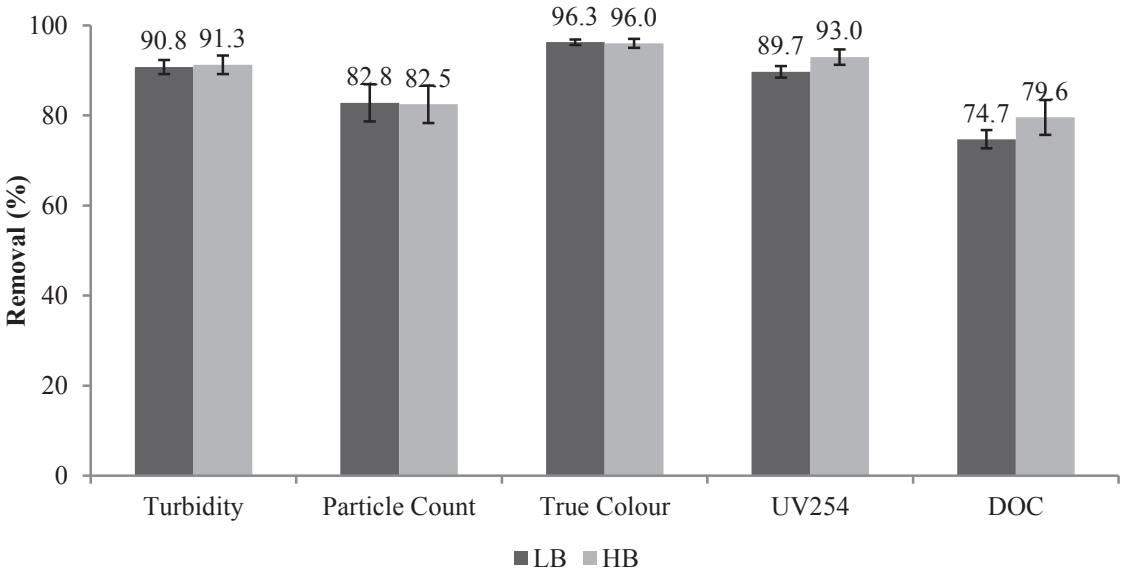

Figure 5.7. Impact of basicity on optimum removal of target contaminants during baseline raw water trials.

5.4.3 Charge Analysis

Samples were collected immediately after rapid mixing in all jar tests and analyzed for ZP. ZP measurements comparing effects of basicity and pH are presented in Figure 5.8. The ZP measurements, as discussed in Section 2.4.2.2, are an estimate of the magnitude of the surface charge of particles in the sample. As coagulant dose was increased from 10 to 50 mg/L, an increase in ZP from -25 mV (no coagulant added) to positive ZP values was seen for experiments using both LB and HB PACl at both low and high pH. At the high pH level, a higher dose of coagulant (40 to 45 mg/L) is required to achieve charge neutralization than at the low pH level (18 to 24 mg/L).

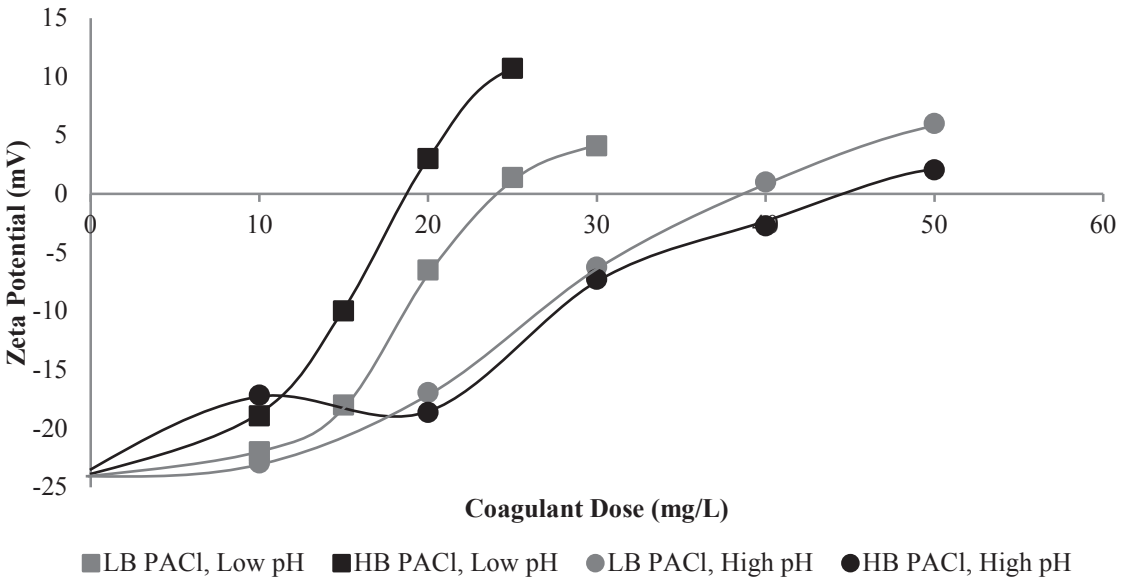

Figure 5.8. Zeta potential vs. coagulant dose after rapid mixing for raw water trials.

The SC and charge demand was also measured after rapid mixing. The results for SC at each coagulant dose comparing basicity and pH effects are shown in Figure 5.9. At equivalent coagulant doses, the SC measurements showed a similar pattern to zeta

potential measurements, with the zero point of charge (ZPC) being achieved between 15 and 20 mg/L of HB PACl and approximately 25 mg/L of LB PACl at pH 6. A strong relationship between ZP and SC was found, with Pearson correlation coefficient of 0.97 and 0.90 for low pH and high pH trials, respectively (p=0.000 for both). However, at the higher pH level, the ZPC is not reached even at the highest coagulant dose. Since SC is an indirect method of measuring surface charge, ZP is a more accurate predictor of particle behaviour during coagulation under all pH conditions. The SC value could be used to determine optimum coagulant dose, but this may not necessarily occur at the ZPC, particularly at the pH of minimum solubility where sweep flocculation is the dominant coagulation mechanism.

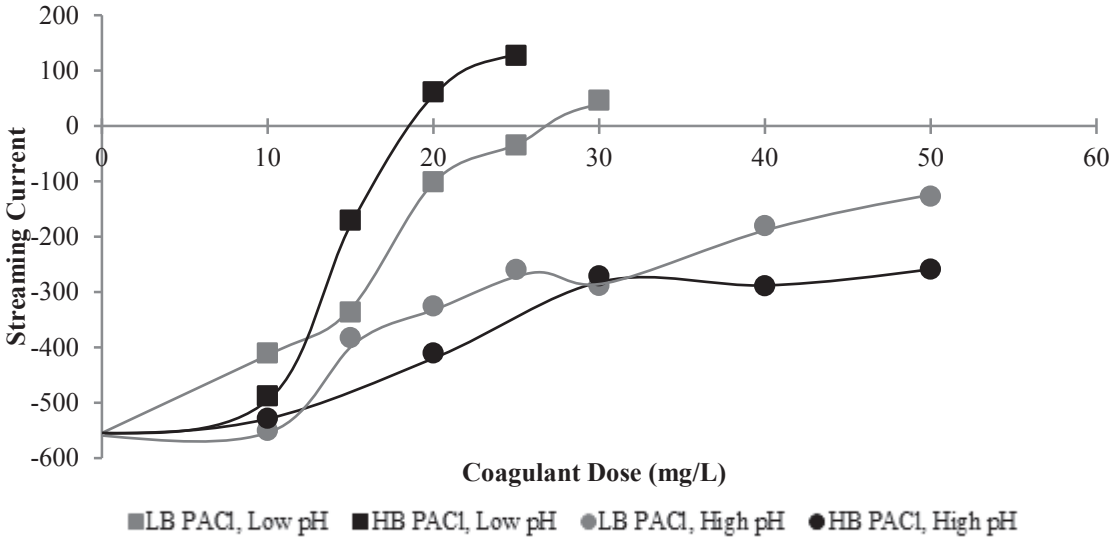

Figure 5.9. Streaming current vs. coagulant dose after rapid mixing for raw water trials.

The results for charge demand (expressed as μeq/L) at each coagulant dose comparing basicity and pH effects are shown in Figure 5.10. The charge demand also shows that at high coagulant doses in high pH trials, a small positive charge exists on the

particles. This may indicate that particle charge neutralization/destabilization is not the dominant coagulation mechanism at the high pH level. This also demonstrates the difficulty in utilizing the SCM for coagulant dosing control—it is a tool which is used in place of ZP, but the relationship between ZP and SC found in the trials was affected by other coagulation conditions, pH specifically. It is recommended that for the best utilization of the SCM, optimization of coagulation should first be achieved and the correlating coagulation conditions such as temperature, dose and pH along with SC value should be recorded. Once a strong relationship has been established, online SC can then be used to adjust coagulation back to the ideal SC value while incorporating these other factors.

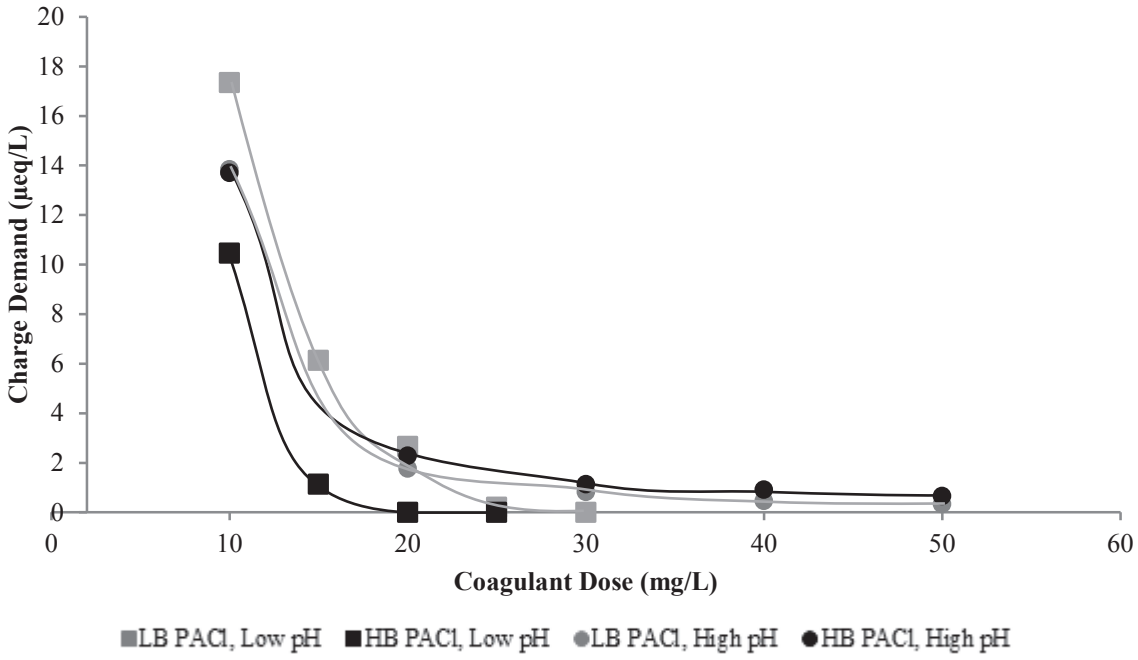

Figure 5.10. Charge demand vs. coagulant dose after rapid mixing for raw water trials.

Under rapidly changing raw water conditions in a WTP or when altered in the laboratory, the ideal SC value may change significantly. As an alternative approach, one

study has reported that the SC may be optimized at the inflection point of the curve, as most easily seen in the HB PACl curve at pH 6 shown in Figure 5.9 to occur between 10 and 20 mg/L of coagulant (Chilarescu *et al*., 1998). Bench-scale SC instruments have been unpopular with many researchers due to difficulty in data interpretation and instrument calibration (Henderson *et al*., 2008). However, SC has been successfully used in online applications in drinking water treatment as well as other industries, such as pulp and paper wastewater processing (Leiviska, 1999).

In order to compare the effect of basicity and pH and the correlation between ZP, SC and optimum treatment performance, optimum coagulant dose for turbidity and UV_{254} removal along with the ZP at that dose are presented in Table 5.3.

The optimum removals for turbidity occurred between average ZP measurements of -8.7 and -4.5 mV under all basicity and pH conditions, with coagulant doses of 15 to 20 mg/L at low pH and 30 to 35 mg/L at high pH. SC measurements were -170 to -101 at the low pH condition and -276 to -269 at the high pH condition. Charge neutralization was not required for optimum turbidity removal, but rather the surface charge was reduced enough to allow collision between the particles to overcome electrostatic repulsion and allow flocculation.

The optimum removals for UV_{254} occurred between average ZP measurements of -0.2 and 7.4 mV under all basicity and pH conditions, with coagulant doses of 25 to 30 mg/L at low pH and 40 to 50 mg/L at high pH. SC measurements were 60 to 128 at the low pH condition and -164 to -264 at the high pH condition.

Table 5.3. Zeta potential and streaming current measurements at optimum coagulant dose for turbidity and UV_{254} removal in baseline raw water trials.

Trial	Optimum Dose for Turbidity Removal	ZP (mV)	SC	Optimum Dose for UV_{254} Removal	ZP (mV)	SC
LB, Low pH	20 mg/L	-4.7 +/- 2.6	-101 +/- 8	30 mg/L	4.5 +/- 0.6	60 +/- 42
LB, High pH	30 mg/L	-8.7 +/- 1.9	-269 +/- 27	40 mg/L	7.4 +/- 9.0	-164 +/- 52
HB, Low pH	15 mg/L	-8.3 +/- 2.4	-170 +/- 14	25 mg/L	6.0 +/- 6.7	128 +/- 35
HB, High pH	35 mg/L	-4.5 +/- 2.5	-276 +/- 11	50 mg/L	-0.2 +/- 2.2	-264 +/- 16

For both turbidity and UV_{254} optimum removals, the optimum dose for LB PACl was 5 mg/L higher than that for HB PACl at the low pH condition, but 7.5 mg/L lower at high pH. This may indicate that the HB PACl is more efficient when used under conditions promoting charge neutralization/destabilization coagulation processes, since the HB PACl produces significantly more highly charged polymeric active coagulant species, specifically the tridecamer $Al_{13}(OH)_{24}^{7+}$ species (Pernitsky, 2001).

5.5 Bench-Scale Synthetic Challenge Water DAF Experiments

The results of analyses performed on treated synthetic challenge raw water samples produced in bench-scale DAF testing are divided into Sections 5.5.1 and 5.5.2, discussing the effects of coagulation pH and coagulant basicity, respectively, on treatment performance.

5.5.1 Effect of Coagulation pH on DAF Performance

5.5.1.1 Turbidity

Treated synthetic challenge water turbidity from low and high pH levels at all coagulant doses is shown in Figure 5.11. Bench-scale DAF treatment of the synthetic raw water at the optimum coagulant dose resulted in improved turbidity removals at high pH, with clarified water turbidity 0.9 NTU at the low pH level and 0.8 NTU at high pH ($p=0.009$). Optimum coagulant concentration was found to be 30 mg/L at the low pH condition and 40 mg/L at high pH. At low pH, particle restabilization occurred above a coagulant dose of 30 mg/L, leading to elevated turbidity of 5 NTU and above in the clarified water. At high pH, DAF performance did not weaken at higher coagulant doses, however turbidity removals did not improve beyond the optimum dose, suggesting sweep flocculation was the dominant mechanism of coagulation.

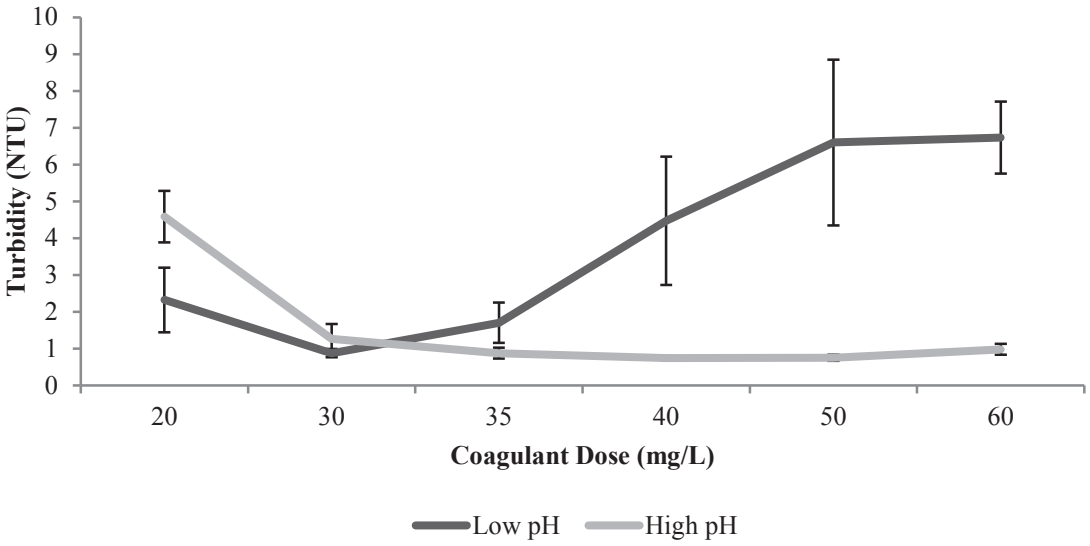

Figure 5.11. Effect of pH on clarified water turbidity during synthetic challenge raw water trials.

The patterns shown by turbidity removal at low and high pH are also seen in particle count results, which are presented in Appendix B.

5.5.1.2 UV_{254}

Treated synthetic challenge water UV_{254} from low and high pH levels at all coagulant doses is shown in Figure 5.12. Optimum removal of UV_{254} at low and high coagulation pH occurred at coagulant doses of 65 and 40 mg/L, respectively. Unlike previous results, a higher coagulant dose was required to maximize UV_{254} removal at the low pH setting. Optimum UV_{254} removal was significantly better at the low pH condition, measured as 0.010 cm^{-1} vs. a measurement of 0.025 cm^{-1} at high pH (p=0.000). At both pH levels, there was no increase in UV_{254} above the optimum coagulant dose—additional coagulant did not help nor hinder UV_{254} removal.

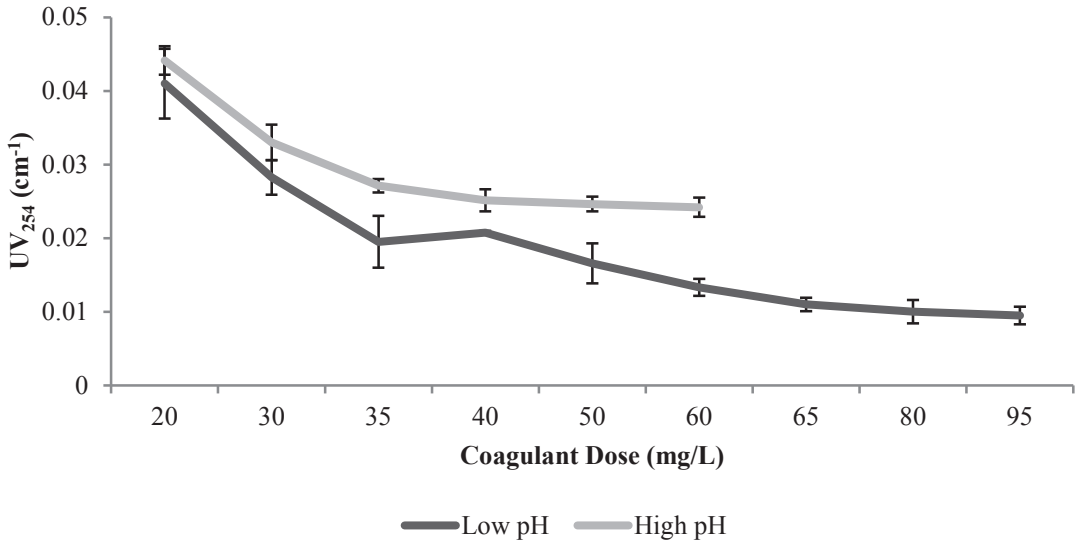

Figure 5.12. Effect of pH on clarified water UV_{254} during synthetic challenge raw water trials.

The patterns shown by UV_{254} removal at low and high pH are also seen in DOC and true colour removal results, which are presented in Appendix B.

5.5.1.3 Effect of Coagulation pH on DAF Performance at Optimum Coagulant Dose

A summary graph of the percent removals for turbidity, particle count, UV_{254}, DOC and true colour is presented in Figure 5.13. Turbidity removal was found to improve by 1.5 %, corresponding to 0.23 NTU, with experiments conducted at high pH ($p=0.009$). Particle count showed similar improvement at high pH, with removal increasing by 2.1 % (11,400 cts/mL) with a p-value of 0.006. Dissolved organic matter removal, as measured by UV_{254}, DOC and true colour, was improved at the low pH condition vs. the high pH condition: DOC removal was improved by 1.5 % (0.16 mg/L), with p-value 0.014; UV_{254} removal increased by 2.8 % (0.012 cm^{-1}) with p-value 0.000; and true colour removal improved by 2.4 % (3.25 TCU) with p-value 0.000.

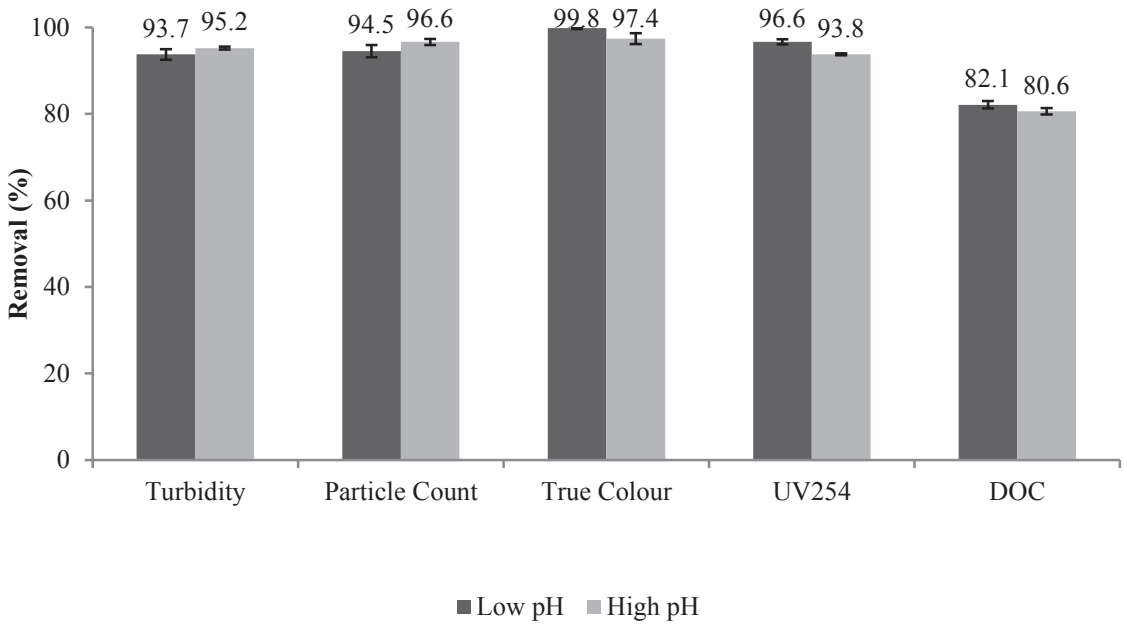

Figure 5.13. Impact of pH on optimum removal of target contaminants during synthetic challenge raw water trials.

5.5.2 Effect of Basicity on DAF Performance

5.5.2.1 Turbidity

Treated synthetic challenge water turbidity from low and high basicity levels at all coagulant doses is shown in Figure 5.14. Bench-scale DAF treatment of the synthetic raw water at the optimum coagulant dose resulted in clarified turbidity of 1.0 NTU for both HB and LB PACl. Optimum coagulant concentration was found to be 30 mg/L at the HB condition and 40 mg/L at LB. HB PACl doses from 35 to 50 mg/L resulted in elevated turbidity in the clarified water, possibly indicating charge restabilization had occurred. Although a turbidity increase did occur at 50 mg/L, LB PACl was not affected as severely above its optimum dose as the HB PACl. This may be due to the pH of minimum solubility for LB PACl being closer to pH 6.0 than for HB PACl, which allowed sweep flocculation to be more prevalent in the LB PACl trials. The large

standard deviations seen in both LB and HB trials at coagulant doses from 35 to 50 mg/L also indicate that another factor (pH) may have been highly influential in treatment performance.

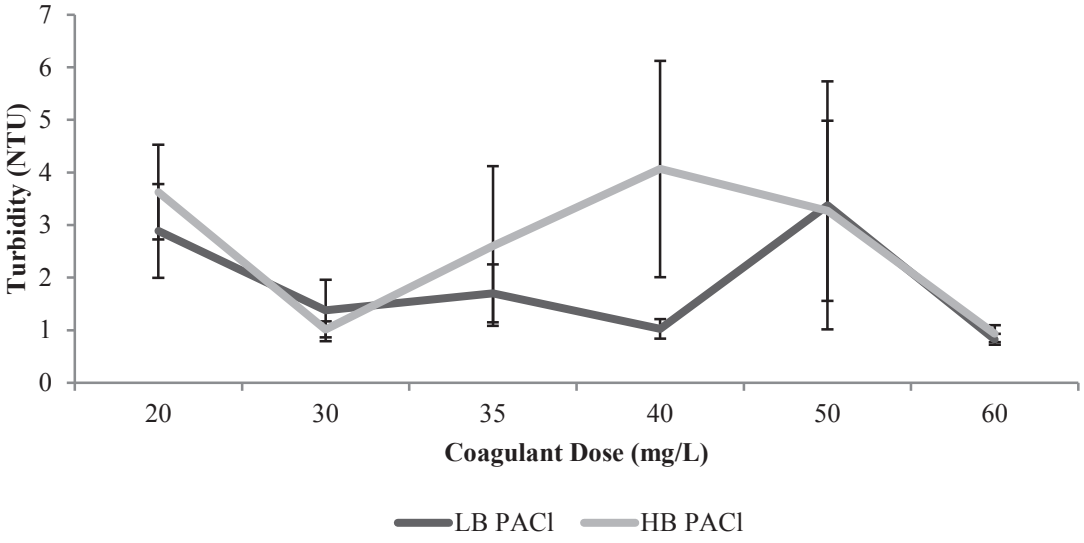

Figure 5.14. Effect of basicity on clarified water turbidity during synthetic challenge raw water trials.

In the majority of bench-scale trials, turbidity and particle count analysis showed excellent correlation. This was expected, as particulate matter in the water sample is a major factor in turbidity readings. However, when comparing LB and HB trials for synthetic challenge water, it was found that particle count showed a different trend than turbidity at coagulant doses between 35 and 50 mg/L. Treated synthetic challenge water particle counts from low and high basicity levels at all coagulant doses are shown in Figure 5.15. No restabilization phenomena appeared to occur, and optimum coagulant doses using both LB and HB PACl were found to occur at the maximum coagulant dose of 60 mg/L, with nearly identical average particle counts of 10,780 and 10,750 (cts/mL)

for LB and HB PACl, respectively. It is unclear why this discrepancy between particle count and turbidity occurred, but one possibility is that the restabilization of kaolin clay particles, which are in the colloidal range (less than 2 μm), were not counted by the Brightwell MFI, which was calibrated to measure particles of 2 microns and above. Therefore, particle count analysis would not have accurately reflected treatment performance in the sample. Particle size distribution was compared, and no difference between baseline and synthetic challenge water distribution pattern was found, ruling out the possibility of small particles aggregating into larger particles which would reduce particle count. Turbidity measurements are affected by particle shape and colour, therefore the relationship between turbidity and particle count measurements is only loosely correlated.

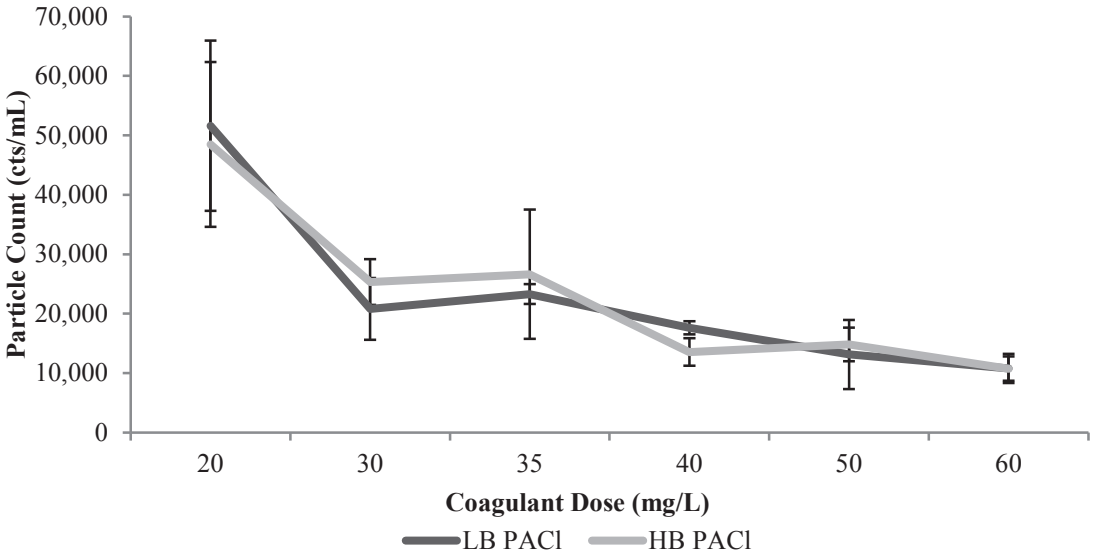

Figure 5.15. Effect of basicity on clarified water particle count during synthetic challenge raw water trials.

5.5.2.2 UV_{254}

Treated synthetic challenge water UV_{254} from low and high basicity levels at all coagulant doses is shown in Figure 5.16. UV_{254} removal was optimized at 35 mg/L for LB PACl and 40 mg/L for HB PACl, with both coagulants reducing UV_{254} to 0.020 cm^{-1} in the DAF treated synthetic challenge water. Corresponding with organics removal in the baseline raw water testing, treatment performance did not deteriorate significantly at high coagulant doses, but no further treatment improvement occurred above the optimum coagulant dose.

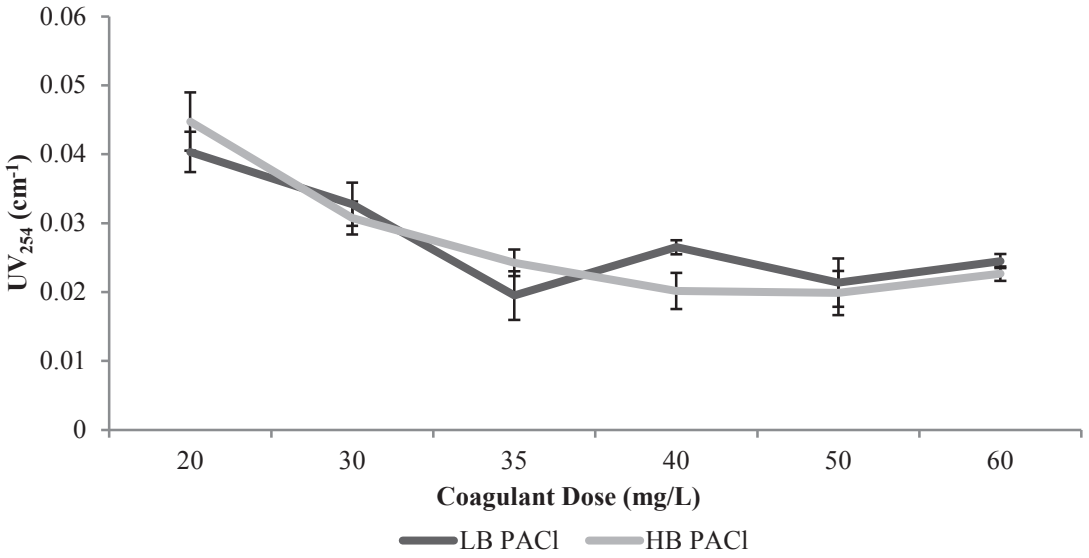

Figure 5.16. Effect of basicity on clarified water UV_{254} during synthetic challenge raw water trials.

The patterns shown by UV_{254} removal at low and high pH are also seen in DOC and true colour removal results, which are presented in Appendix B.

5.5.2.3 Effect of Basicity on DAF Performance at Optimum Coagulant Dose

A summary graph presenting the percent removals for turbidity, particle count, UV_{254}, DOC and true colour is presented in Figure 5.17. Only one parameter was affected by basicity in the synthetic water trials. UV_{254} removal was improved by 1.4 %, corresponding to a UV_{254} absorbance of 0.003 cm^{-1} (p=0.047). No other clarified water parameters were significantly affected by utilizing LB or HB PACl coagulant, although the quantity of soda ash added during the trials (not presented in this thesis) was lower when using HB PACl.

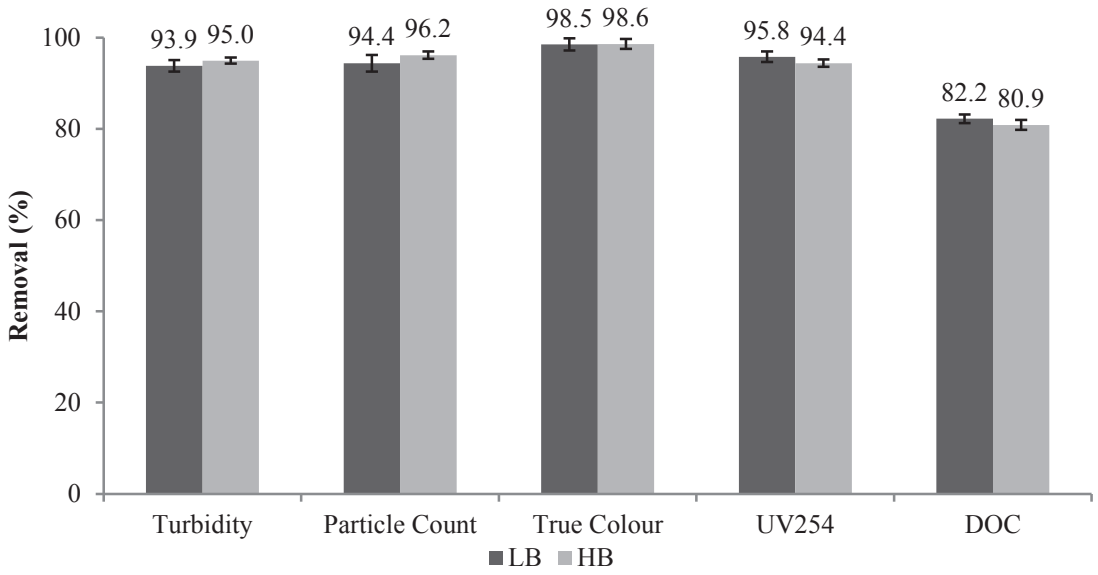

Figure 5.17. Impact of basicity on optimum removal of target contaminants during synthetic challenge raw water trials.

5.5.3 Charge Analysis

Samples were collected immediately after rapid mixing in all jar tests and analyzed for ZP. ZP measurements comparing effects of basicity and pH are presented in Figure 5.18. As seen in baseline raw water trials, at the high pH level a higher dose of

coagulant was needed to reach the point of zero charge. However, the difference in coagulant dose was less dramatic, on average only 5 to 10 mg/L greater at high pH (40 to 42 mg/L) than at low pH (33 to 35 mg/L). Both HB and LB PACl trials required similar doses at both pH levels to reach the ZPC, with HB PACl requiring 2 to 3 mg/L more on average.

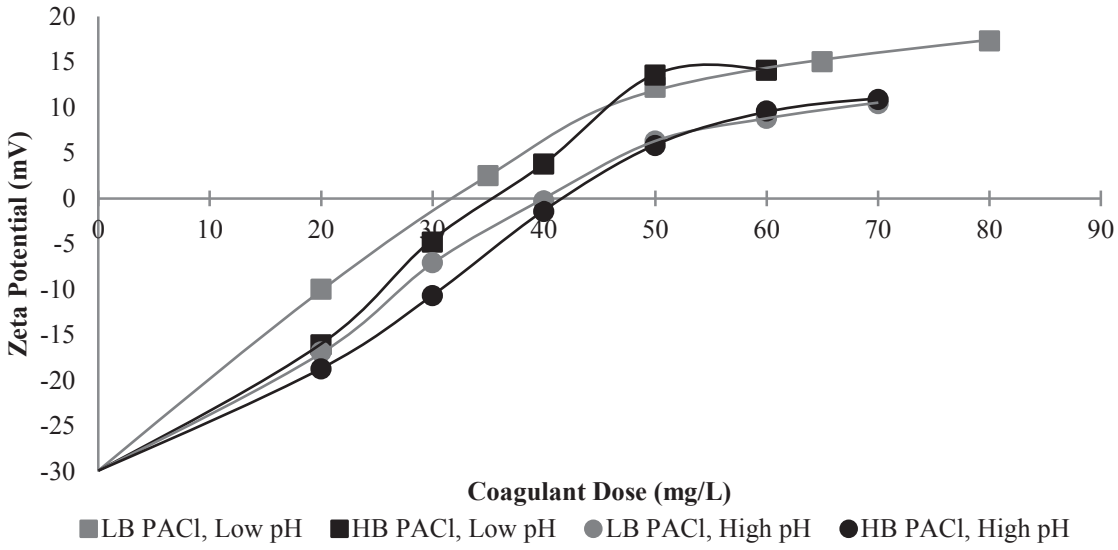

Figure 5.18. Zeta potential vs. coagulant dose after rapid mixing for synthetic water trials.

Streaming current analysis was not performed on the synthetic water trials, as it was concluded that SC results correlated well with ZP and the procedure for obtaining accurate SC data was overly time consuming and inconsistent, as noted by Henderson *et al*. (2008). Therefore, ZP was relied on to determine particle surface charge characteristics.

In order to compare the effect of basicity and pH on ZP, and the relationship between ZP and optimum treatment performance, the optimum coagulant doses for turbidity and UV_{254} removal along with the ZP at that dose are presented in Table 5.4.

The optimum removals for turbidity occurred between ZP measurements of -4.6 and 5.8 mV under all basicity and pH conditions, with coagulant doses of 30 to 35 mg/L at low pH and 37.5 to 50 mg/L at high pH. The optimum turbidity removal ZP measurements represent a shift towards the ZPC for the synthetic challenge water as compared to the baseline raw water (-8.7 to -4.7 mV for baseline raw water, -4.6 to 5.8 mV for synthetic challenge water). This may be caused by the tenfold increase in particle concentration in the synthetic challenge water as compared to the baseline raw water, making particle charge neutralization more critical to effective coagulation-flocculation and DAF performance.

The optimum removals for UV_{254} occurred between ZP measurements of 13 and 18 mV at low pH and between 6.8 and 7.1 mV at high pH. The higher charge increase at the low pH condition may again be due to the pH being further from the isoelectric point, rendering a more positively charged surface on the aluminum hydroxide flocs and therefore a higher ZP measurement.

Table 5.4. Zeta potential measurements at the optimum coagulant doses for turbidity and UV_{254} removal in synthetic challenge water trials.

Trial	Optimum Dose for Turbidity Removal	ZP (mV)	Optimum Dose for UV_{254} Removal	ZP (mV)
LB, Low pH	35 mg/L	-2.3 +/- 14	68.8 mg/L	18 +/- 2.7
LB, High pH	37.5 mg/L	-4.6 +/- 3.5	50 mg/L	7.1 +/- 1.2
HB, Low pH	30 mg/L	-3.4 +/- 4.6	52.5 mg/L	13 +/- 4.2
HB, High pH	50 mg/L	5.8 +/- 0.2	57.5 mg/L	6.8 +/- 1.9

Repeating the trend found during baseline raw water trials, for both turbidity and UV_{254} optimum removals, the optimum dose for LB PACl was 5 to 16.3 mg/L higher than that for HB PACl at the low pH condition, but 7.5 to 12.5 mg/L lower at high pH. The difference in required coagulant was more drastic in the synthetic challenge water trials, possibly suggesting the greater importance of particle charge neutralization when the water source has a high particle count. Again, this may indicate that the HB PACl is more efficient when used under conditions promoting charge neutralization and destabilization coagulation processes.

5.6 Dissolved Aluminum Residuals

Dissolved aluminum measurements were taken for samples which yielded optimum removal of turbidity or UV_{254} for both the baseline raw water trials and the synthetic challenge water trials. The summarized results of all measurements are shown in Figure 5.19, comparing the effect of basicity and pH on dissolved aluminum. Higher dissolved aluminum was present in synthetic challenge water trials. For both sets of experiments, the HB/low pH condition yielded the highest dissolved aluminum at 46.4 and 57.1 μg/L for baseline and challenge water, respectively. Also, the standard deviation under these conditions is extremely high, with the highest dissolved aluminum residuals above the Guidelines for Canadian Drinking Water Quality (GCDWQ) standard of 100 μg/L in both experiments (Health Canada, 2010). This result can be attributed to the pH of minimum aluminum solubility being higher for HB PACl, and therefore the experiments run at pH 6 allowed significant higher dissolution of aluminum. LB PACl also showed higher dissolved aluminum residuals at the low pH condition for the same reason, with the high pH condition improving residuals from 10.1 to 5.9 μg/L in the baseline trials and 22.3 to 12.5 μg/L in the synthetic water trials. At the high pH condition, ANOVA showed no significant difference in dissolved aluminum residuals between LB and HB PACl in both sets of experiments ($p=0.489$).

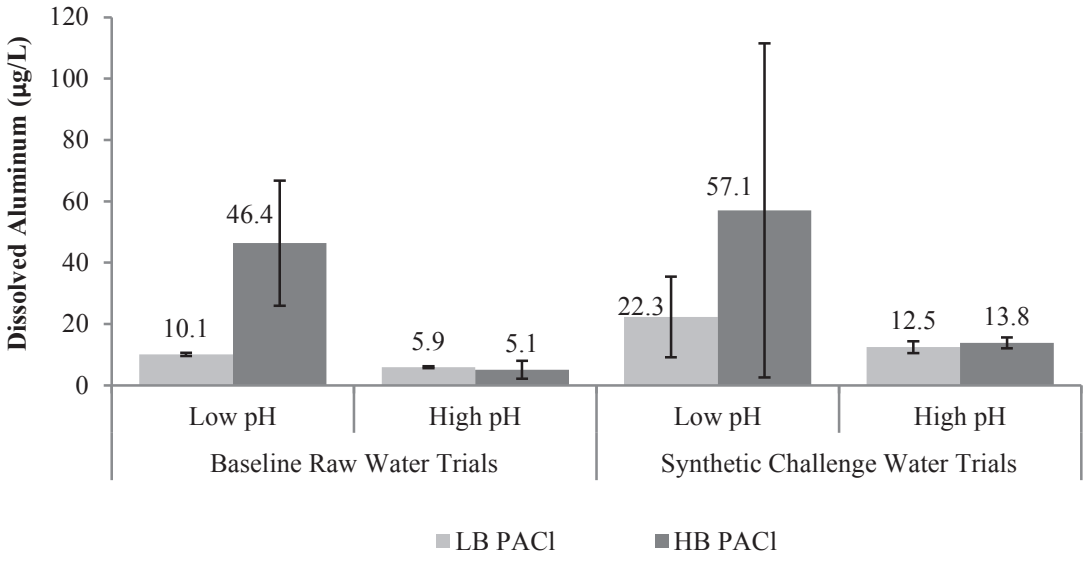

Figure 5.19. Dissolved aluminum residuals in clarified water during baseline raw water trials.

5.7 Factorial Analysis

A factorial design analysis was done on the data presented in sections 5.4, 5.5 and 5.6 using Minitab statistical software. The significant factors affecting each measured clarified water quality characteristic, as well as the estimated effect of changing each factor from the low to high setting and the p-value indicating statistical confidence in the result, are shown in Table 5.5.

Table 5.5. Results of factorial analysis showing statistically significant factors on bench-scale DAF performance, the estimated magnitude of effects and the level of confidence.

Analyte	Baseline Trials			Synthetic Challenge Trials		
	Significant Factors	Effect	P-value	Significant Factors	Effect	P-value
Turbidity	pH	-0.34	0.027	pH	-0.23	0.009
Particle Count	pH	-1637	0.033	pH	-11,400	0.006
UV_{254}	-	-	-	pH Basicity	+0.012 -0.003	0.000 0.046
DOC	-	-	-	pH	+0.16	0.014
True Colour	-	-	-	pH	+3.25	0.000
$Aluminum_{(aq)}$	pH Basicity pH*Basicity	-23.4 +17.1 -17.9	0.004 0.020 0.016	pH	-24.4	0.046

The baseline raw water trials showed that at optimum coagulant dose no factors made a significant impact on dissolved NOM removal as measured by true colour, UV_{254} or DOC, although in the synthetic challenge water these parameters were improved with high statistical significance at the low pH condition. The HB PACl was also found to improve UV_{254} removal by an average of 0.003 cm^{-1} (p=0.046). This result suggests that a high pH setting is beneficial for particle removal during all raw water conditions, but will slightly hinder NOM removal during periods of poor source water quality. Previous studies have also shown that maximum NOM removal is achieved at a lower pH level (6.0), as the increased positive surface charge on aluminum hydroxide flocs will maximize complexation with negatively charged NOM (Yan *et al.*, 2008; Wang *et al.*, 2004; Duan & Gregory, 2003).

Dissolved aluminum residuals were impacted by both pH, basicity, and the interaction between pH and basicity. At the high pH setting, which was the pH of minimum aluminum solubility for each coagulant, dissolved aluminum residuals

decreased by an average of 23.4 (p=0.004) and 24.4 μg/L (p=0.046) in baseline and synthetic challenge water trials, respectively. In the baseline trials, HB coagulant increased average dissolved aluminum residuals by 17.1 μg/L, however at the pH of minimum solubility, HB coagulant yielded aluminum residuals 17.9 μg/L below average. These results are likely due to the greater gap between the low pH setting of 6.0 and the pH of minimum solubility for LB PACl and HB PACl.

Turbidity removal was improved by 0.34 (p=0.027) and 0.23 (p=0.009) NTU at the high pH setting in baseline and challenge trials, respectively, demonstrating the improved performance of sweep flocculation as the dominant coagulation mechanism vs. charge neutralization/precipitation for particle removal. Particle count was improved by 1637 (p=0.033) and 11,400 (p=0.006) cts/mL at the high pH setting in each trial, confirming this finding.

5.8 Full-Scale DAF Performance during Challenge Conditions

On May 31st, 2012 the BBWTP experienced a process disruption caused by an increase in raw water turbidity and colour following a rainfall event. The raw water turbidity and SC during the disruption are shown in Figure 5.20. The SC declined from a normal value of +11 to a low of -135 over a period of approximately 24 hours, which indicated that the coagulant demand was not sufficiently met during the lead-up to the disruption. The turbidity increase was fairly minor other than short spikes which occurred subsequently to the SC dropping well below normal levels. This indicated that the SC was more affected by NOM levels, which may impart a higher coagulant demand without significantly affecting turbidity.

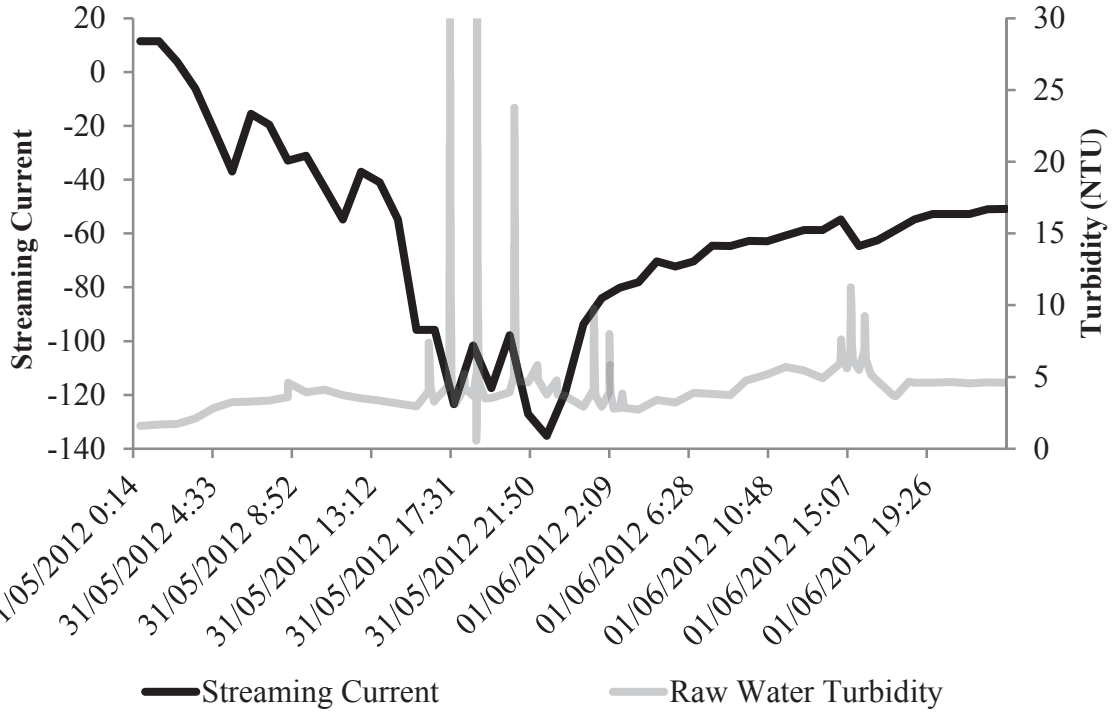

Figure 5.20. Raw water turbidity and streaming current during process disruption at BBWTP May 31 to June 1, 2012.

As SC dropped significantly during the evening of May 31, the coagulation-flocculation process was impaired as coagulant demand was not met. Since DAF performance relies on effective coagulation-flocculation pretreatment, the DAF effluent turbidity increased from the baseline level of approximately 1 NTU at 3:30 PM to at least 5 NTU at 11:00 PM, which is the maximum value recorded by the SCADA system at the BBWTP. Figure 5.21 shows the turbidity profile through the BBWTP during the process disruption including raw water, DAF effluent and filter effluent turbidities. Only 15 to 20 minutes after the DAF effluent turbidity began to increase, filter effluent turbidities increased as they were unable to compensate for the process disruption. Filter effluent turbidity surpassed 0.2 NTU approximately 90 minutes after this increase began, and filtered directly to waste for approximately 10 hours until the process was brought back under control.

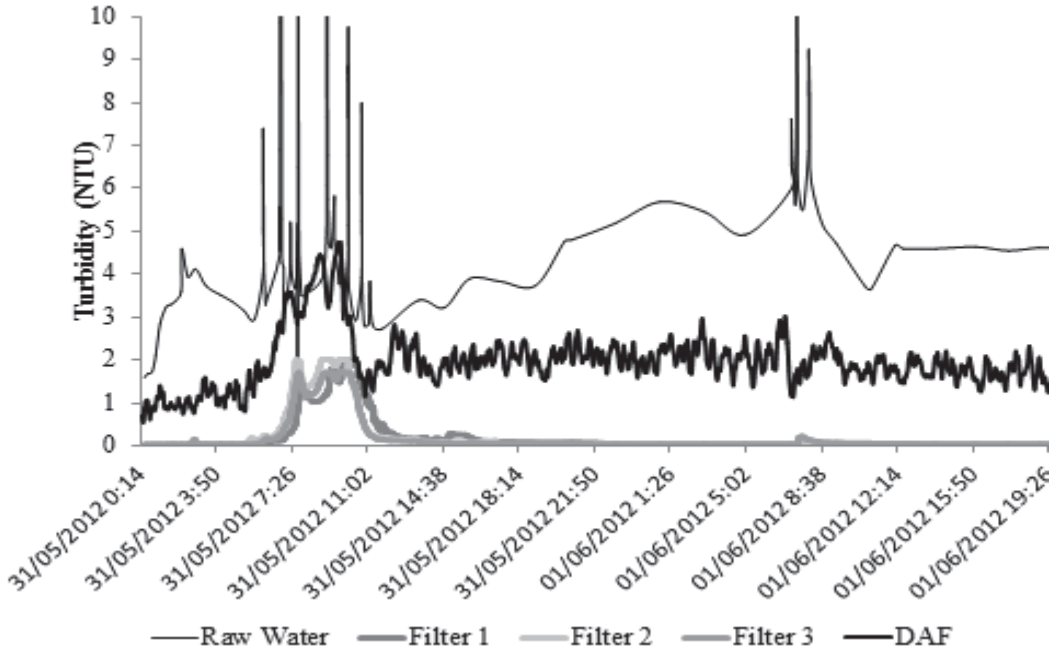

Figure 5.21. Turbidity profile in the BBWTP during process disruption, May 31 to June 1, 2012.

In Chapter 4, a hypothesis was developed that controlling the coagulation pH near the pH of minimum aluminum solubility would reduce the concentration of dissolved aluminum passing into the clearwell, which upon caustic addition would precipitate in aluminum hydroxide flocs, raising clearwell turbidity levels. In Chapter 5, bench-scale experiments showed water treated with DAF at the pH of minimum solubility had lower dissolved aluminum concentrations than that treated at pH 6.0. During the May 31, 2012 process disruption, the coagulation pH was maintained near the pH of minimum solubility, a consequence owing to low coagulant addition. The clearwell turbidity and coagulation pH are plotted in Figure 5.22. The minimum coagulation pH occurring during the process disruption was 6.2, close to the pH of minimum solubility of approximately 6.35. Clearwell turbidity peaked at 0.18 NTU at 5:30 PM during the

disruption. This coincides with the filter turbidity increasing above 0.2 NTU, at which point filtrate did not run to the clearwell. These results suggest that the clearwell turbidity spike to 0.18 NTU was due to physical turbidity transfer through the filters, and not due to excess aluminum precipitate forming in the clearwell itself.

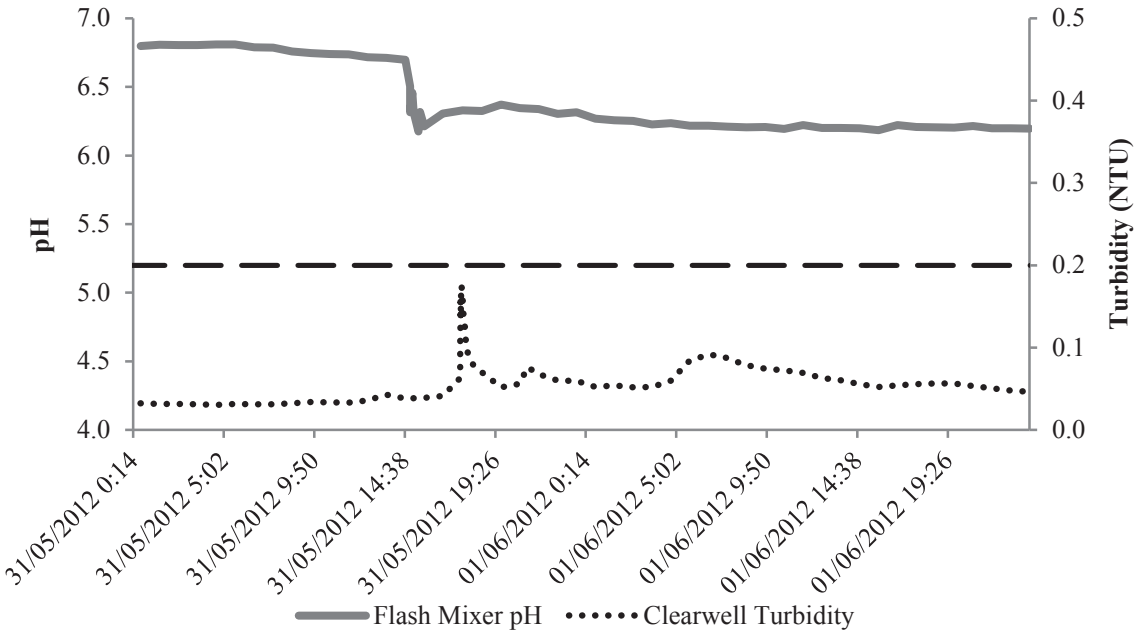

Figure 5.22. Coagulation pH and clearwell turbidity in the BBWTP during process disruption, May 31 to June 1, 2012.

5.9 Conclusions

Optimum turbidity removals were achieved at ZPs of -10 to -5 mV in the baseline raw water trials, with this value shifting to -4.6 to 5.8 mV during synthetic challenge water trials. This indicated that achieving charge neutralization was more important for particle removal when the number of particles was significantly increased. For UV_{254} removal the target ZP was found to be significantly higher, ranging from 1 to 18 mV in all experiments. This shows that the difficulty in removing NOM stems from its highly negative charge, as a highly positive aluminum hydroxide species was required for maximum complexation. The correlation between SC and ZP was strong during both the low pH and high pH trials using baseline water, but the relationship was affected by this change—SC values did not increase as quickly as ZP in the high pH trials. This was likely due to sweep flocculation playing a larger role in particle removal at high pH, making surface charge analysis of particulate matter less consistent.

The most significant factor affecting treatment performance in all experiments was the coagulation pH. In the both trials, targeting the pH of minimum aluminum solubility appeared to promote sweep flocculation which resulted in improved particle removal during DAF clarification. Analyses of full-scale results were done, combining results from BBWTP upsets presented in Chapter 4 where coagulation pH dropped to 6.0 and below with results from a BBWTP process disruption presented in Section 5.8 where coagulation pH was maintained near the pH of minimum aluminum solubility. The results show that when coagulation pH is maintained at the plant, process disruption was limited to high filtrate turbidities which can be directed to waste, as opposed to clearwell

turbidity increases when coagulation pH drops, which can negatively impact aluminum residuals in the treated water and, more importantly, disinfection efficacy.

In contrast, removal of dissolved organic matter suffered at higher pH levels, as a pH setting of 6.0 has been found to be optimum for the removal of dissolved NOM, in agreement with previous research using PACl by Yan *et al.* (2008) and Wang *et al.* (2004). This suggests that under normal operating conditions when source water is at baseline levels and turbidity removal is not problematic, a coagulation pH of 6.0 is ideal for minimizing disinfection by-product precursors. As raw water deterioration commonly occurs after rainfall events, it may be prudent to increase coagulation pH in a WTP from 6.0 to the pH of minimum aluminum solubility during such events to prevent particulate matter treatment difficulties which may lead to clearwell turbidity increases above acceptable levels.

At the higher pH, a greater coagulant dose is required to reach optimum turbidity and particle removals. This is attributed to the decreased positive charge at higher pH levels, as the isoelectric point of aluminum hydroxide is in the range of 8 to 9. As the solution pH approaches 8 to 9, the surface charge of aluminum hydroxides goes to zero, and so with increasing pH (below 8 to 9) a higher dose of cationic coagulant is required to attract these particles (Duan & Gregory, 2003).

No major differences in treatment performance were found when using LB vs. HB PACl coagulant under optimum treatment conditions (dose, pH). HB PACl did slightly improve UV_{254} removal during synthetic challenge water trials, a result that was not duplicated when analyzing DOC and true colour. In typical Atlantic Canada surface

waters with low pH and alkalinity, using HB PACl would call for a lower addition of soda ash to reach a pH of 6.0, but if the pH of minimum solubility is being targeted more soda ash is required, as the pH target increases when using HB PACl.

The results of these experiments suggest that the pH of minimum aluminum solubility should be targeted for optimum removal of particulate matter during periods of reduced source water quality.

Chapter 6: Impact of Operations on Dissolved Air Flotation

6.1 Introduction

DAF clarification relies on the solubility of air in water changing in accordance to system pressure to produce oversaturated conditions, leading to the formation of air bubbles which enable floc-bubble aggregates to form and flotation of flocs to occur. By forcing water taken from the clarifier or filter effluent (recycle water) into a pressurized vessel (saturator tank) and inducing mixing with air, the nitrogen and oxygen will dissolve in water according to their individual Henry's Law constants in order to move towards a state of equilibrium. From the saturator tank the recycle water flows towards a zone of lower pressure, and in doing so is injected through nozzles at the bottom of the DAF clarifier contact zone. After entering the clarifier a pressure drop, from approximately 500 kPa to near atmospheric pressure, initiates the formation of air bubbles (Edzwald, 2010). Oxygen and nitrogen revert back to their gaseous states in order to re-establish equilibrium concentrations.

Once micro-sized bubbles are formed they attach to flocs in the contact zone, and the combined floc-bubble aggregates float to the top of the clarifier according to the hydraulic motion in the clarifier in combination with Stokes' Law which is shown in Equation 2.3 (Section 2.3.1). Floc-bubble aggregate formation is modelled in one of two basic ways; both flocs and bubbles are treated as particles and collisions in the contact zone allow aggregation, or the whitewater approach where the rising field of bubbles is considered a bubble-water matrix which entraps flocs, analogous to a rising filter (Edzwald, 2010). DAF performance is affected by the properties of bubbles in the clarifier, such as bubble size, concentration, separation distance and attachment

efficiency in the contact zone (Edzwald, 2010; Haarhoff & Edzwald, 2001). Haarhoff & Edzwald (2004) have shown that DAF performance is maximized when bubble concentrations of 6000 ppm with a contact time of at least 1.5 mins is achieved, and that a contact time below 1 min is effective with higher bubble concentrations. Therefore, DAF treatment performance can be improved by increasing the bubble concentration with higher recycle flows or lower hydraulic loading rates (HLRs). These changes are encompassed in the recycle rate (RR), which compares the recycle flow to the total plant intake flow.

A series of experiments were carried out at the bench-scale and at full-scale at the Brierly Brook Water Treatment Plant (BBWTP) in order to explore the resulting impact of RR changes on dissolved air flotation (DAF) treatment performance under baseline raw water and challenge synthetic water conditions.

6.2 Materials and Methods

6.2.1 Source Water

Bench-scale experiments were conducted using raw water samples collected from the BBWTP on November 12th and December 8th, 2011. This water was used as a baseline source water with characteristics commonly found in surface waters in Atlantic Canada. On April 26th, 2012, raw water was collected from the BBWTP and synthetically modified to increase turbidity and organic material content of the water to represent Atlantic Canada source water during a stormwater runoff event. 5 mg/L of humic acid (Alfa Aesar) and 20 mg/L of kaolin clay (Fisher Scientific) were used to simulate dissolved natural organic matter (NOM) and eroded soil particles. An analysis of both source waters was done, with the results presented in Table 6.1.

Table 6.1. Bench-scale DAF study source water quality characterization.

Analyte	Unit	Baseline Raw Water	Challenge Synthetic Water
pH		6.25 +/- 0.2	6.6 +/- 0.2
Alkalinity	mg/L as $CaCO_3$	2.5	2
Turbidity	NTU	8 +/- 0.3	15 +/- 1.2
Particle Count	cts/mL	35,000 +/- 5600	340,000 +/- 42,000
True Colour	TCU	40 +/- 1	103 +/- 5
UV_{254}	cm^{-1}	0.236 +/- 0.001	0.363 +/- 0.001
TOC	mg/L	5.9 +/- 0.1	8.1 +/- 0.3
DOC	mg/L	5.7 +/- 0.1	6.2 +/- 0.2
SUVA		4.1	4.5
Aluminum	µg/L	116 +/- 3	99 +/- 7
Zeta Potential	mV	-23.5 +/- 2.7	-30.1 +/- 2.3

6.2.2 Experimental Design

6.2.2.1 Bench-Scale Experiments

The effect of the RR on DAF performance during baseline and challenge conditions was compared by setting the RR at 6 and 12 % during bench-scale

experiments. Between 10 and 60 mg/L of polyaluminum chloride (PACl) coagulant and soda ash (Na_2CO_3) was added during the rapid-mix stage at coagulation pH values from 6.0 to 6.9.

Recycle flow is determined by the size and number of nozzles, the nozzle type, and the pressure drop across the nozzle (which is determined mainly by saturator pressure). The flowrate through these nozzles is governed by the orifice equation which is shown in Equation 6.1.

$$Q = C_d(\frac{1}{4}\pi D^2)\sqrt{2gh} \qquad \text{Equation 6.1}$$

where Q = flowrate
C_d = coefficient of discharge
D = nozzle diameter
g = gravitational constant
h = pressure drop across nozzle

At a given saturator pressure the recycle flowrate will be therefore be constant through the nozzles. A recycle flow calibration through each nozzle of the bench-scale DAF apparatus was performed to ensure accurate recycle rates would be achieved in the bench-scale trials. The results of this calibration were presented in Chapter 3.

6.2.2.2 Full-Scale Experiments

Increasing the saturator pressure at the BBWTP by manual adjustment of the air pressure regulator would result in an increased flowrate out of the saturator tank, and a decrease in saturator pressure would lower the flowrate out. This would cause the water level of the saturator tank to increase or decrease. The water level is measured by a differential pressure transducer on the saturator tank, which is linked to a modulator valve on the saturator tank inlet. As the water level varies in the saturator tank as a result of air

pressure changes, the transducer signals the modulator valve to open or close further, restoring the set water level in the tank. As a result of this process, a new equilibrium would be established where flow into the tank equals flow out of the tank. Adjusting the saturator tank pressure in this way would be the only procedure BBWTP operators could use to control recycle flow. A simple process diagram outlining the recycle system is presented in Figure 6.1.

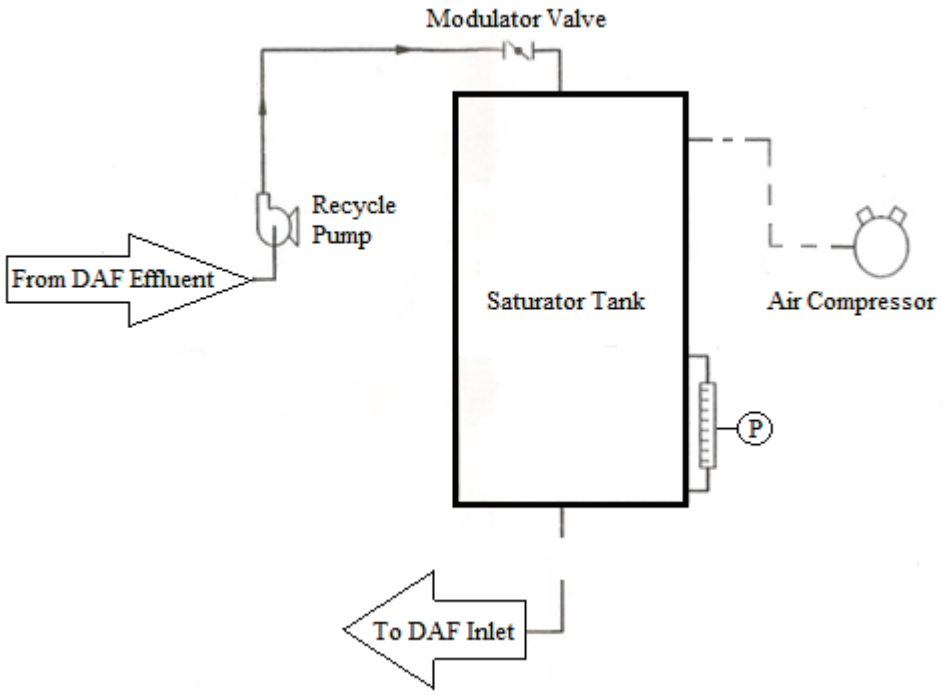

Figure 6.1. Process diagram for the BBWTP recycle system.

The relationship between saturator pressure and recycle flow at the BBWTP for the full-scale trials was established by manually adjusting the air pressure regulator and observing the resulting flowrate, as measured by the SCADA system. Based on the orifice equation, it was known that the recycle flowrate is dependent on the square root of the pressure differential. Therefore, a power regression was used to plot the trendline, and the resulting relationship is shown in Figure 6.2.

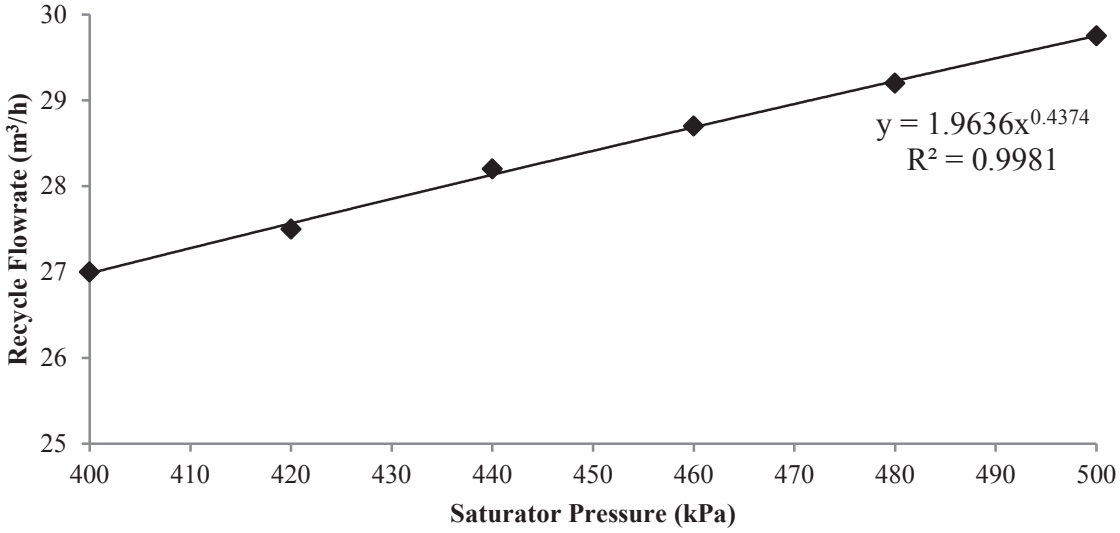

Figure 6.2. Relationship between saturator pressure and recycle flow in the BBWTP recycle system.

6.2.3 Analytical Methods

Samples taken during bench-scale trials were analyzed for turbidity, particle count, UV_{254}, true colour, dissolved aluminum and dissolved organic carbon (DOC) by the methods outlined in Chapter 3.

During the full-scale trials, grab samples were taken at 30 minute intervals during testing at four locations in the BBWTP—the DAF effluent weir and the final flocculation

basin in each of the DAF treatment trains. Photos taken of these locations can be viewed in Chapter 4. The grab samples were analyzed for turbidity, particle count, UV_{254} and dissolved aluminum. Other water quality parameters measured continuously during the full-scale trials, such as raw water and DAF effluent turbidity, rapid mix tank streaming current (SC), coagulation pH, raw water flowrate and recycle flowrate, were taken from the SCADA data logger system at the BBWTP, which is described in Section 3.1.

6.3 Bench-Scale Recycle Rate Trials

Accurate mathematical modelling of clarifier flow patterns and the effect of the air:solids ratio on sludge blanket stability is exceptionally difficult, due to both the inherent mathematical complexity of a system with water, air bubbles and solids as well as the limitations of physical modelling/tracer studies in the clarifier due to the opacity of the whitewater solution (Haarhoff, 2008). However, empirical data for saturator optimization can be obtained by modelling the clarifier as a "black box", identifying and maintaining clarifier influent water quality and comparing effluent quality while adjusting the recycle system controls. This approach was taken for testing during bench-scale experiments as well as at the BBWTP.

The results of analysis performed on treated raw baseline water and synthetic challenge raw water samples produced in bench-scale DAF testing are dividing in into Sections 6.3.1 and 6.3.2, discussing the effect of RR on DAF performance.

6.3.1 Baseline Raw Water DAF Experiments

The turbidity of the clarified baseline water using low and high RR settings at all coagulant doses is shown in Figure 6.3. The clarified water turbidity at both RR settings was excellent at the optimum coagulant dose of 40 mg/L, with slightly better removal observed at the 6 % RR at most doses. At the high RR, an optimum coagulant dose of 40 mg/L resulted in an average clarified water turbidity of 0.7 NTU. At the low RR setting, the same dose of 40 mg/L was optimum, producing a clarified water turbidity of 0.5 NTU. However, no statistically significant difference was found between the two RR settings when comparing the turbidity at each condition using paired t-tests ($p=0.457$) or at the optimum doses alone ($p=0.255$).

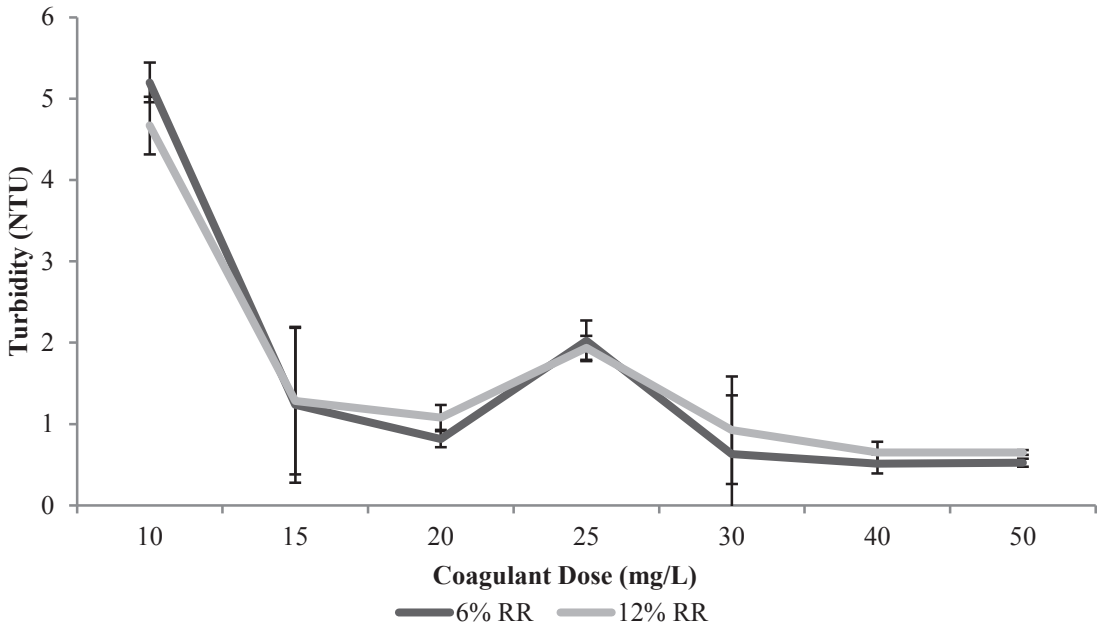

Figure 6.3. Effect of recycle rate on clarified water turbidity during baseline raw water trials.

Prior to the testing, it was expected that increasing the RR from 6 to 12 % would improve treatment via two mechanisms. Firstly, a higher concentration of bubbles in the whitewater should ensure that particles have more opportunities to become attached to bubbles and larger flocs could have a higher number of bubbles attached, lowering the aggregate density and expediting flotation to the surface. Secondly, in the bench-scale experiments the recycle water was filtered through a RO membrane before being saturated with air. Therefore, even if bubble concentrations are ignored, the 12 % RR should have effectively diluted the particle concentration in the sample to a higher degree than the 6 % RR, which delivered half the volume of recycle water with the same concentration of dissolved air.

Clarified baseline water particle counts from low and high RR trials at all coagulant doses are presented in Figure 6.4. Particle count results from the baseline water and the clarified water turbidity results showed a similar pattern, as the 6 % RR trials appeared to yield lower particle count measurements at most coagulant doses, including at the optimum dose. A minimized particle count was found at the high end of coagulant dose (50 mg/L) with an average measurement of 4167 cts/mL at a 6 % RR. At the 12 % RR, the optimum dose was determined to be 40 mg/L, with an average particle concentration of 6835 cts/mL. The particle count for low RR trials at a 40 mg/L PACl dose was 4378 cts/mL. Statistical analysis of particle count data confirmed an improvement of clarified water particle counts at the low RR over the high RR, by an average of 13,380 cts/mL when considering coagulant doses above and below the optimum dose (p=0.004) and 1840 cts/mL at the optimum coagulant dose (p=0.016).

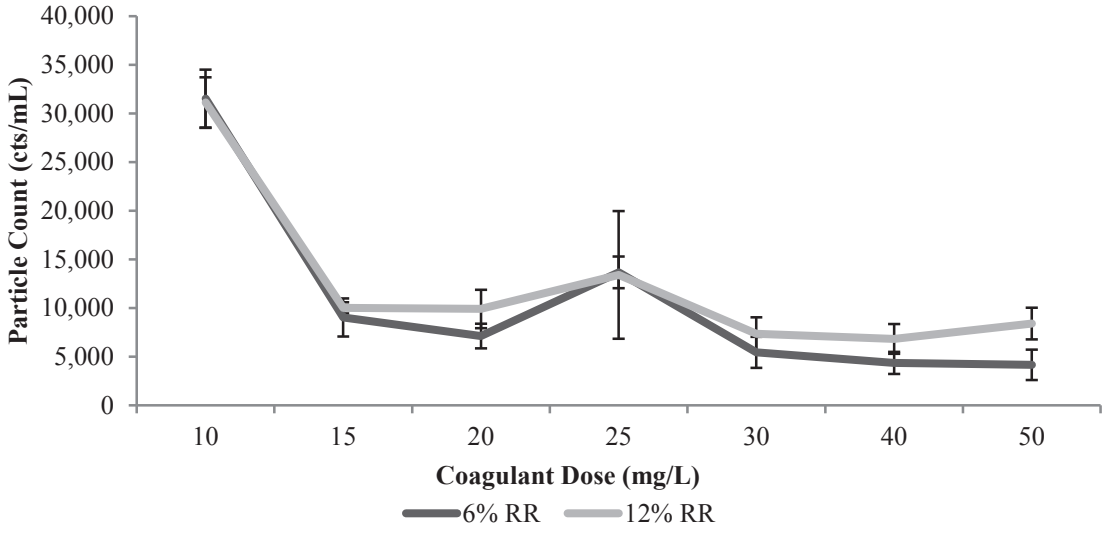

Figure 6.4. Effect of recycle rate on clarified water particle count during baseline raw water trials.

Examination of the experimental results for particle removal as quantified by turbidity and particle count measurements can be interpreted through the four zones of coagulation as described by Duan & Gregory (2003).

Zone 1: At coagulant doses up to 15 mg/L, insufficient charge neutralization occurred, particles were still negatively charged and stable; DAF performance was poor.

Zone 2: At a 20 mg/L coagulant dose, charge neutralization was achieved and the coagulation-flocculation process was successful; DAF performance was good.

Zone 3: At a 25 mg/L dose, charge reversal (from negative to positive) on the particles occurred which resulted in the restabilization of discrete particles; DAF performance was poor.

Zone 4: At coagulant doses of 30 mg/L and above, significant aluminum hydroxide precipitates were formed and sweep flocculation became the dominant coagulation mechanism; DAF performance was excellent.

Dissolved components such as UV_{254}, DOC, true colour and dissolved aluminum were not found to be affected by the RR setting in bench-scale experiments. Since DAF is a method of solid-liquid separation, and the analysis procedure for each of these components involves filtration through 0.45 micron filter paper, any difference in the clarification performance at low and high RRs would not be reflected in these measurements. A slight improvement was expected at the 12 % RR setting, as the additional dilution of air saturated RO recycle water in the sample should slightly

decrease dissolved parameter concentrations, but the results suggested that the difference due to this dilution factor was negligible.

Paired t-tests were used to compared dissolved aluminum residuals at optimum coagulant doses for turbidity and UV_{254} removal, and no significant difference was found (19.9 µg/L at low RR vs. 17.5 µg/L at high RR, p=0.417). The UV_{254} results are shown in Figure 6.5, and complete measurements of other dissolved components are displayed in Appendix B.

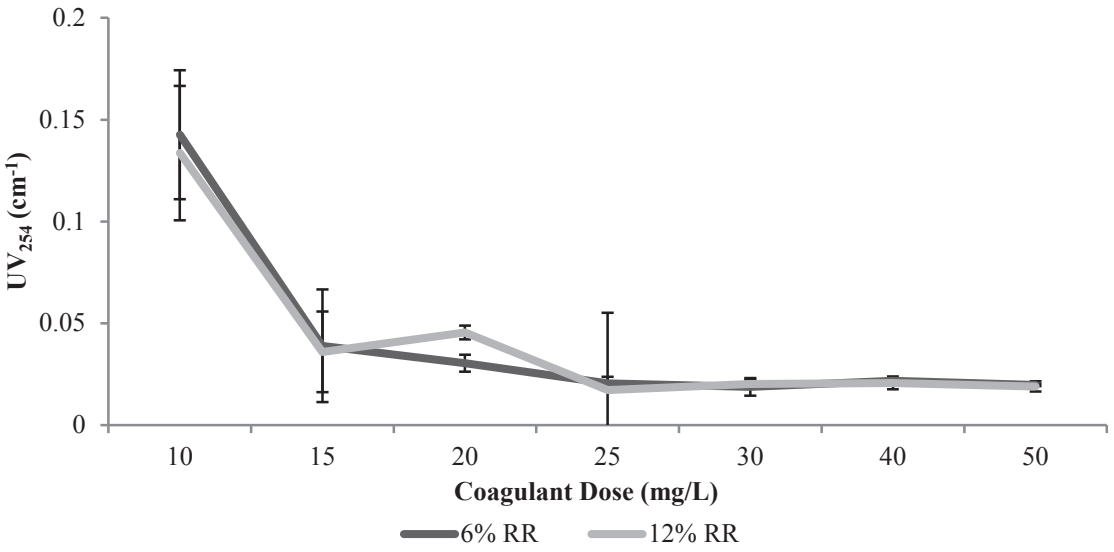

Figure 6.5. Effect of recycle rate on clarified water UV_{254} during baseline raw water trials.

A summary graph of the percent removals for turbidity, particle count, UV_{254}, DOC and true colour at optimum coagulant doses (25 to 50 mg/L) during baseline water RR experiments is presented in Figure 6.6, showing a 1.5 % increase in turbidity removal and a 4.9 % increase in particle count removal at low RR over high RR, with negligible differences in removals of other parameters observed between the two RR settings

evaluated in this study. The results suggest that at the bench-scale, the removal of particulate matter from baseline raw water is improved when using a lower RR.

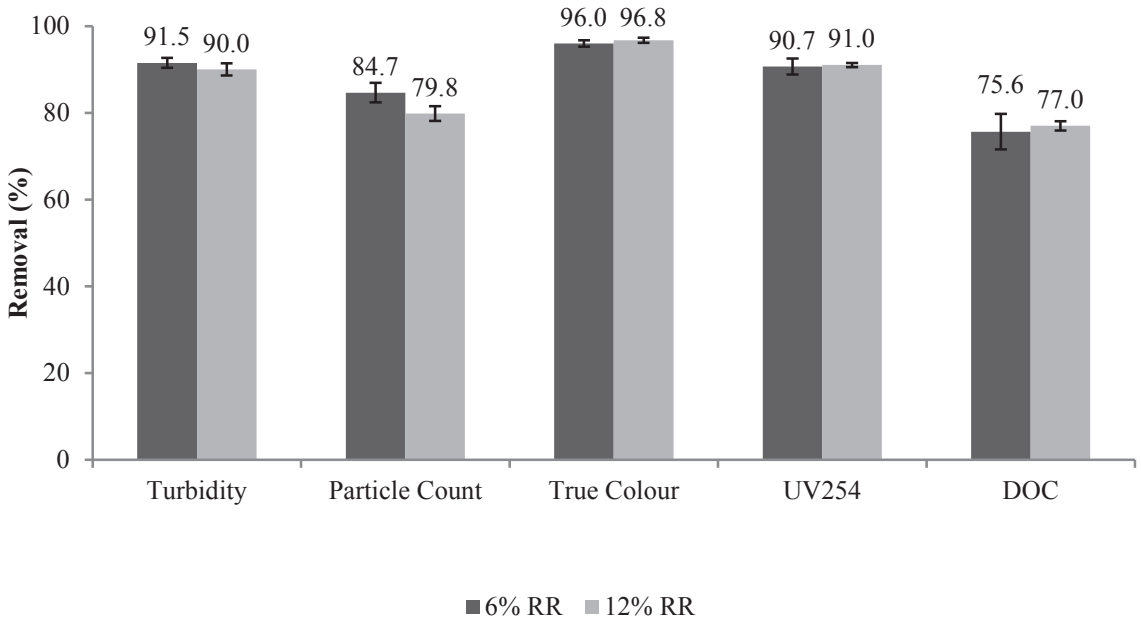

Figure 6.6. Impact of recycle rate on optimum removal of target contaminants during baseline raw water trials.

6.3.2 Synthetic Challenge Water DAF Experiments

The clarified water turbidity results comparing 6 to 12 % RR for the synthetic challenge water trials are shown in Figure 6.7. Clarified water turbidity removal in the synthetic challenge water trials was optimized at a coagulant dose of 40 mg/L at a 6 % RR (1.15 NTU) and 30 mg/L at a 12 % RR (0.9 NTU). However, standard deviations for both low and high RR trials were large, which indicated that outside factors such as coagulation pH and coagulant basicity may have caused significant variability to occur when attempting to isolate the effect of RR alone. No significant difference in optimum turbidity removal between each RR was found when using ANOVA ($p=0.205$).

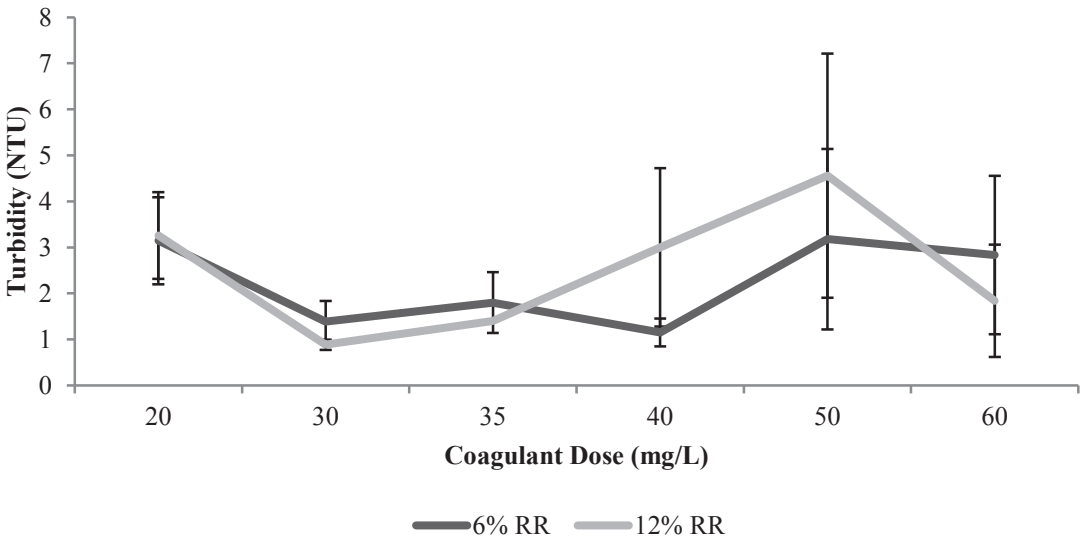

Figure 6.7. Effect of recycle rate on clarified water turbidity during synthetic challenge raw water trials.

The clarified water particle count results comparing 6 and 12 % RRs for the synthetic challenge water trials are shown in Figure 6.8. As seen when examining the effect of coagulant basicity in synthetic challenge water trials (Section 5.5.2), the particle count measurements taken from clarified water samples during both the low and high RR trials did not reflect the trends found in the turbidity analysis. These parameters showed fairly consistent trends in most trials, however the data shows that while turbidity generally increased from coagulant doses of 30 to 60 mg/L at both RR settings, the particle count continued to decline, and optimum particle count removals occurred at the upper range of coagulant dose (60 mg/L). The particle count at the optimum coagulant dose of 60 mg/L was 9188 cts/mL at the low RR and 10,750 cts/mL at the high RR setting, with no significant statistical difference found using ANOVA comparison ($p=0.411$).

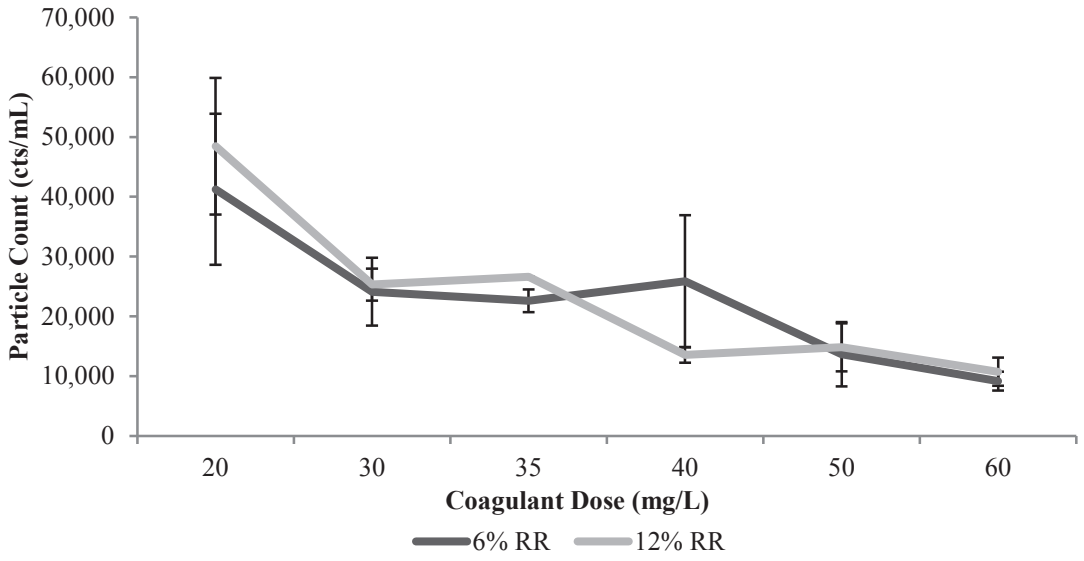

Figure 6.8. Effect of recycle rate on clarified water particle count during synthetic challenge raw water trials.

The clarified water UV_{254} results comparing 6 and 12 % RRs for the synthetic challenge water trials are shown in Figure 6.9. As with the baseline water trials, the RR was found to have no significant impact on the removal of UV_{254} or other dissolved components during the bench-scale RR trials. Only dilution from the additional recycle water used in the DAF apparatus would potentially be expected to make any difference in clarified water quality results, and statistically no difference was found between the 6 and 12 % RR trials for UV_{254} ($p=0.236$) or dissolved aluminum ($p=0.913$).

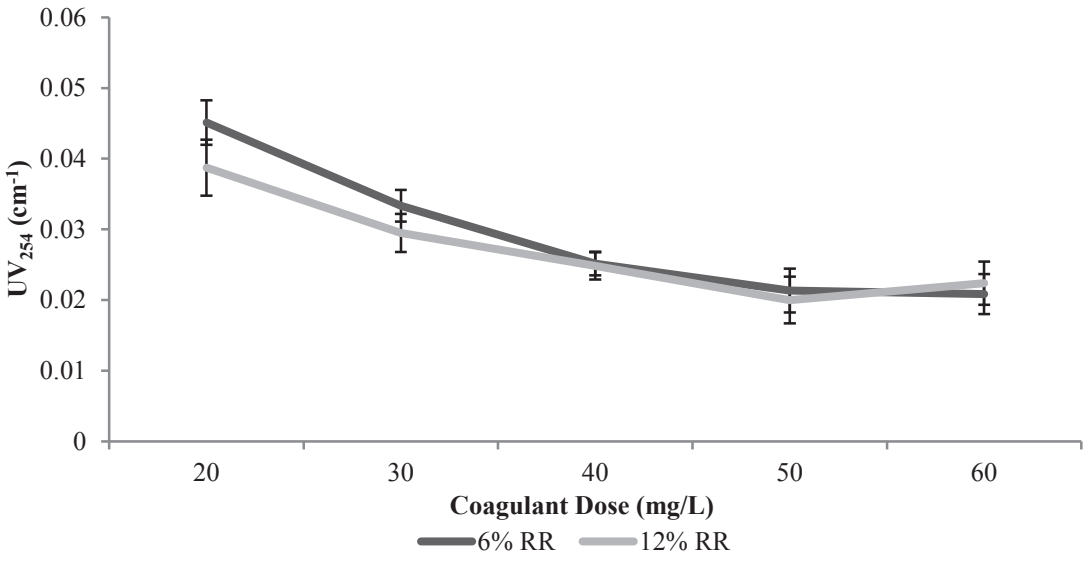

Figure 6.9. Effect of recycle rate on clarified water UV_{254} during synthetic challenge raw water trials.

The full results showing the effect of RR on other dissolved components is presented in Appendix B.

A summary graph of the percent removals for turbidity, particle count, UV_{254}, DOC and true colour at optimum coagulant doses during synthetic challenge water RR experiments is presented in Figure 6.10. The results show that at the bench-scale, the removal of particulate matter from synthetic challenge water was unaffected when the RR was changed from 12 to 6 %. This result is in contrast to the findings of baseline water experiments, which showed that the lower RR was actually more effective. It is possible that for a given source water quality and coagulant dose there exists an optimum RR which will provide maximum floc-bubble attachment and sufficient rise velocities while minimizing shear forces in the sludge blanket, which may cause flocs to be disturbed and sink back into the clarifier. It has been noted that sludge blanket thickness must not be

too great, to prevent its collapse and floc re-entry into the separation zone in the clarifier at full scale (AWWA, 2011), but shear forces acting on the sludge blanket at bench- or full-scale have not been well researched.

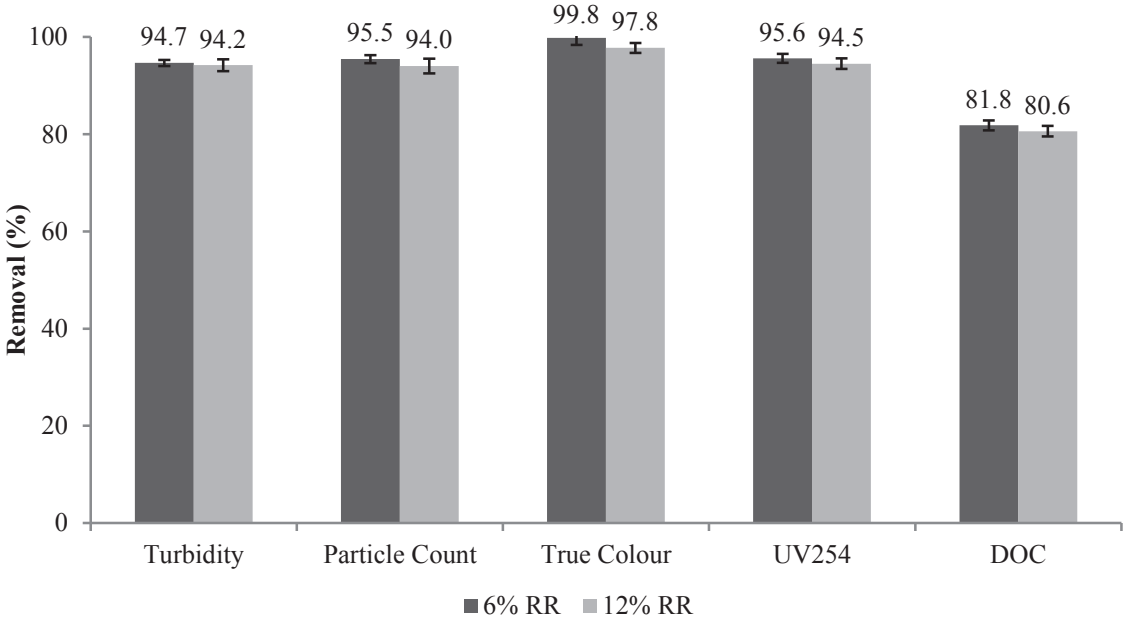

Figure 6.10. Impact of recycle rate on optimum removal of target contaminants during synthetic challenge raw water trials.

6.4 Full-Scale Recycle Rate Trials at the Brierly Brook Water Treatment Plant

It is unclear how applicable bench-scale RR trial results can be scaled up, considering the huge difference in flow patterns in a jar at the bench-scale and in a full-scale continuous flow-through DAF clarifier. Therefore, trials were conducted at the BBWTP to evaluate the effect of saturator pressure adjustment and RR on DAF treatment performance.

6.4.1 Baseline Hydraulic Loading Rate Testing

The first trial was conducted at a normal raw water flowrate of 255 m^3/h, corresponding to a hydraulic loading rate (HLR) of 6.64 m/h in each DAF clarifier. The raw water turbidity and pH remained constant throughout the trial, shown in Figure 6.11 along with the raw water flowrate.

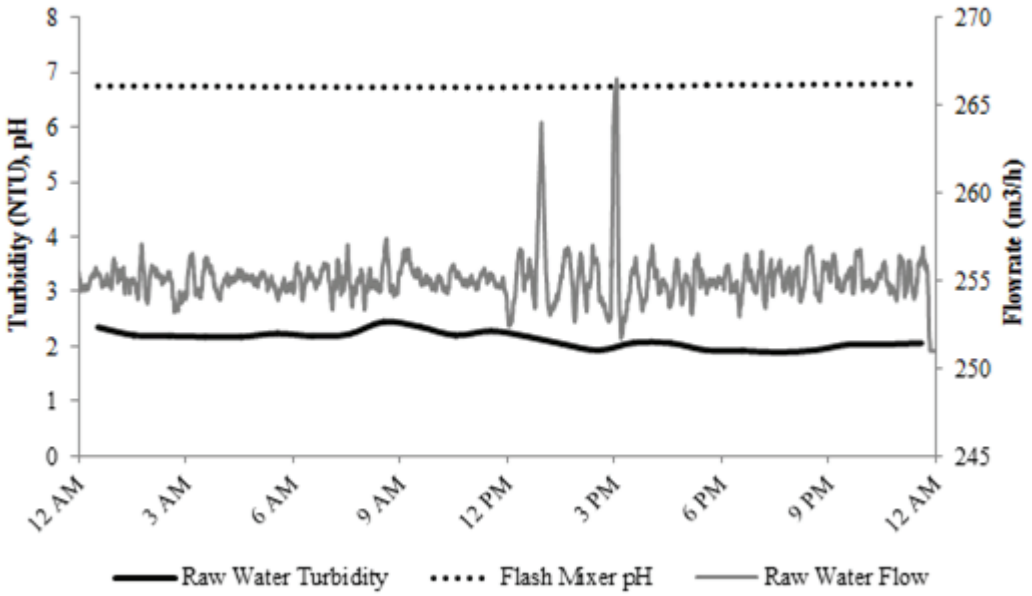

Figure 6.11. Raw water flowrate, raw water turbidity, and coagulation pH for baseline HLR testing.

Under constant raw water flow conditions, the saturator pressure was reduced from 500 kPa to 440 kPa initially for 2.5 hours and then further reduced to 400 kPa (the minimum recommended saturator pressure value found in literature as well as suggested by the plant manufacturer) for 2.5 hours. This corresponded with only a minor decrease in recycle flow, from approximately 29.7 m^3/h at the 500 kPa setting to a minimum of 27.1 m^3/h at the 400 kPa setting (11.7 % to 10.7 % RR). The most useful indicator of a process disruption due to reduced RR was assumed to be the DAF effluent turbidity, which indicated whether flocs were being effectively separated from the DAF effluent.

The decrease in recycle flow due to reductions in saturator pressure to 440 and 400 kPa during the trial can be seen in Figure 6.12. No decrease in DAF performance was found during the saturator flowrate trials, as DAF effluent turbidity remained fluctuating normally near 0.8 NTU before, during and after the experiment.

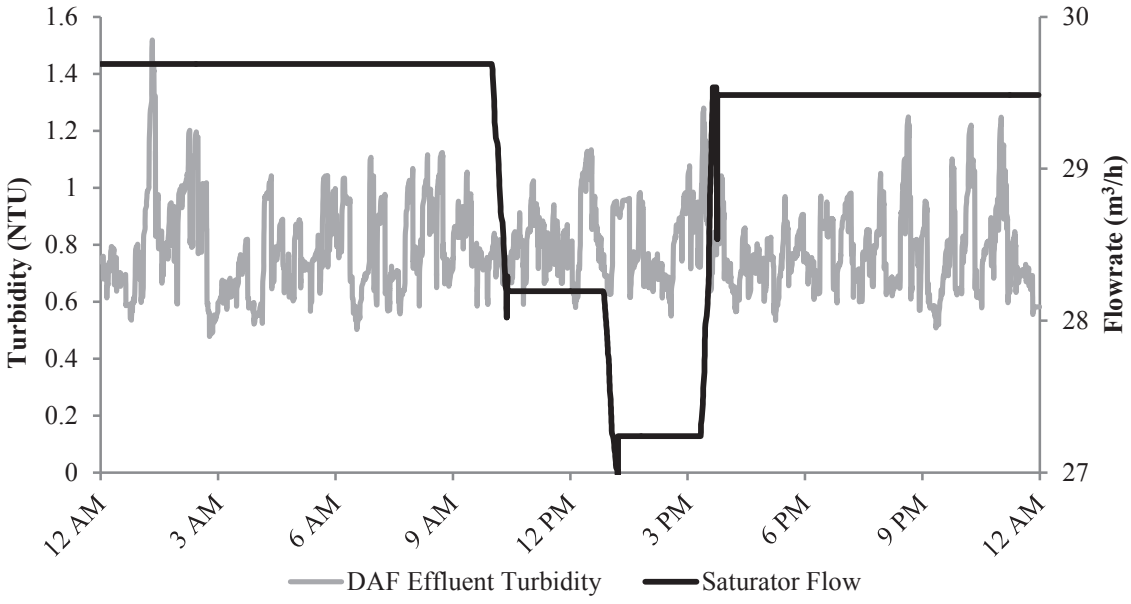

Figure 6.12. Saturator flow vs. DAF effluent turbidity for baseline HLR recycle system testing.

The average raw and DAF clarified water turbidities recorded during the trial clearly showed that the change in saturator pressure had no effect on DAF effluent turbidity at the baseline HLR, as average turbidity remained constant and the standard deviation of the values for DAF effluent turbidity were nearly identical. These results are displayed in Figure 6.13.

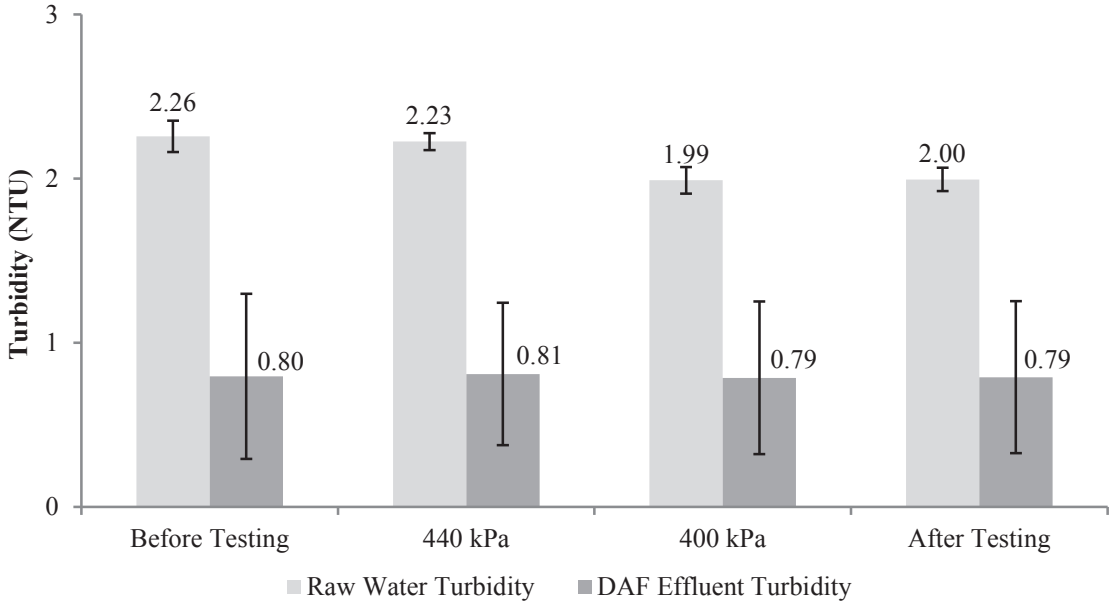

Figure 6.13. Raw and clarified water turbidities during baseline HLR recycle system testing.

As it was found that particle count and not turbidity was significantly affected by RR during bench-scale testing, samples taken during the baseline HLR trials were analyzed for this parameter and the results are shown in Figure 6.14, with particle counts of grab samples before the trial displayed as particle counts at 500 kPa.

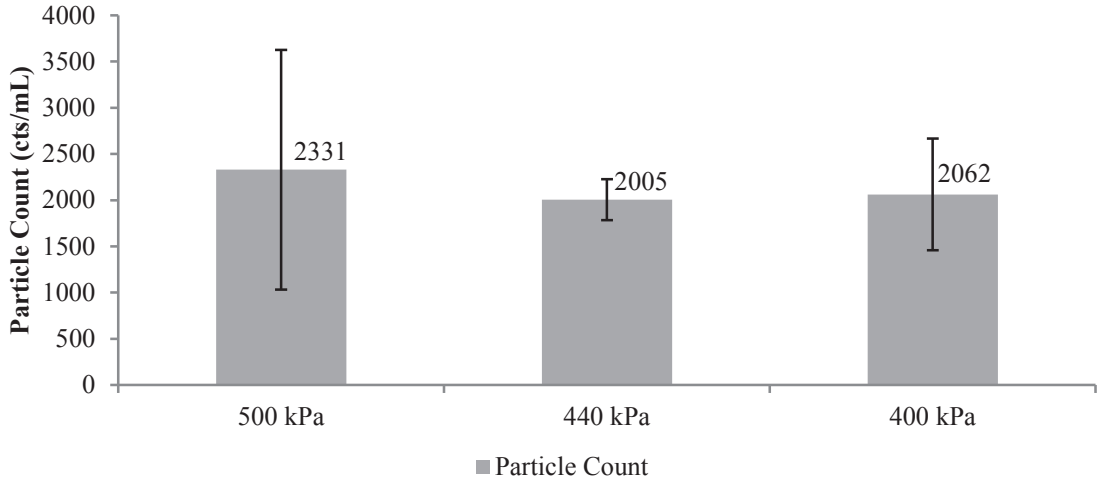

Figure 6.14. DAF effluent particle counts during baseline HLR recycle system testing.

No significant difference was found in DAF effluent grab sample particle counts before and during the trial (p=0.614). Grab sample analysis of the DAF effluent also showed no significant difference in turbidity (p=0.673), UV_{254} (p=0.518) and dissolved aluminum (p=0.474) before and during the trial. Grab samples were collected in the final flocculation basin to ensure influent water quality stability throughout the test period, and no significant difference was found in DAF influent turbidity (p=0.993), UV_{254} (p=0.536) or dissolved aluminum (p=0.809). It was also found that adjustment of the saturator flowrate to the DAF clarifier had no impact on UV_{254} removal (p=0.797) based on measurements taken at the DAF influent and effluent.

These results suggest that during normal operating conditions the saturator pressure may be reduced from 500 to 400 kPa without affecting DAF effluent turbidity. The efficacy of the DAF clarifier in the separation of floc from the clarified water was found in these trials to be unaffected by this change of 2.8 m^3/h in recycle flowrate.

However, the overall RR was only decreased from 11.7 to 10.6 %, the minimum possible allowed by the recycle system at a 255 m^3/h raw water flowrate.

6.4.2 Nominal Hydraulic Loading Rate Testing

The only way to further reduce the RR below 10.6 % was to increase the raw water flow, thereby increasing the HLR in not only the DAF clarifier but the rapid mixer and flocculation basins as well. A second trial was conducted by reducing the saturator pressure to 400 kPa and increasing the raw water flowrate to the maximum design level of 340 m^3/h. By maximizing the raw water flow at the minimum recycle flowrate, the minimum possible RR of 7.9 % was achieved. The raw water flow, saturator flow, RR and HLR for each stage of the test is shown in Table 6.2.

Table 6.2. Flow, recycle and hydraulic loading rates during full-scale nominal HLR testing.

Test Stage	Raw Flow (m^3/h)	Saturator Flow (m^3/h)	RR (%)	HLR (m/h)
1A	170	29.6	17.4	4.43
2A	228	27.1	11.9	5.94
3A	340	27.1	8.0	8.85
4A	340	29.9	8.8	8.85
5A	205	29.8	14.5	5.34

The recycle and raw water flowrates with corresponding DAF effluent turbidity are shown in Figure 6.15. DAF effluent turbidity was maintained during the reduced saturator flow at baseline raw water flowrates (Stage 2A), but it was found to increase once raw water flow was increased to the maximum (Stage 3A).

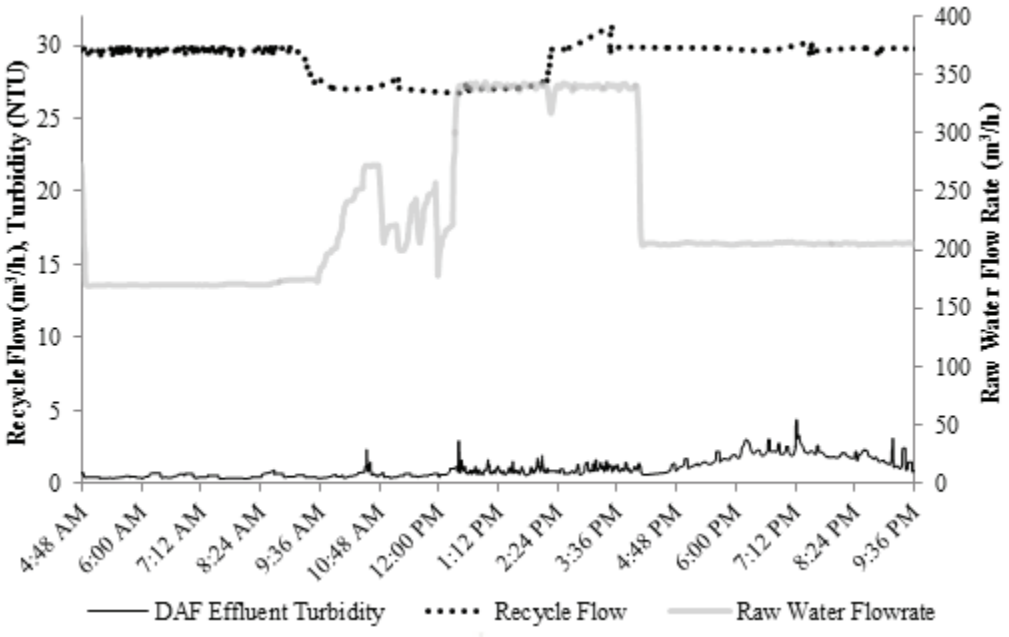

Figure 6.15. Raw water flow, recycle flow and DAF turbidity during nominal HLR testing.

Lower plant intake flowrates in the days prior to the trial followed by an increase to the maximum plant intake flowrate allowed sediment buildup in the raw water supply pipe to be scoured into the water column during the trial, substantially increasing the raw water turbidity and resulting in elevated DAF effluent turbidity.

The raw water turbidity, SC, raw water flowrate, and flash mixer pH are shown in Figure 6.16. Raw water quality must be maintained at stable levels in order to determine the effect of reducing the RR to the plant minimum. The turbidity in the raw water due to the flow increase spiked to a maximum of 17.5 NTU before returning to the baseline level of approximately 2 NTU. SC data was also recorded to determine whether an increase in coagulant demand over the course of the day was required due to the turbidity increase, as the applied coagulant dose was not adjusted during the trial.

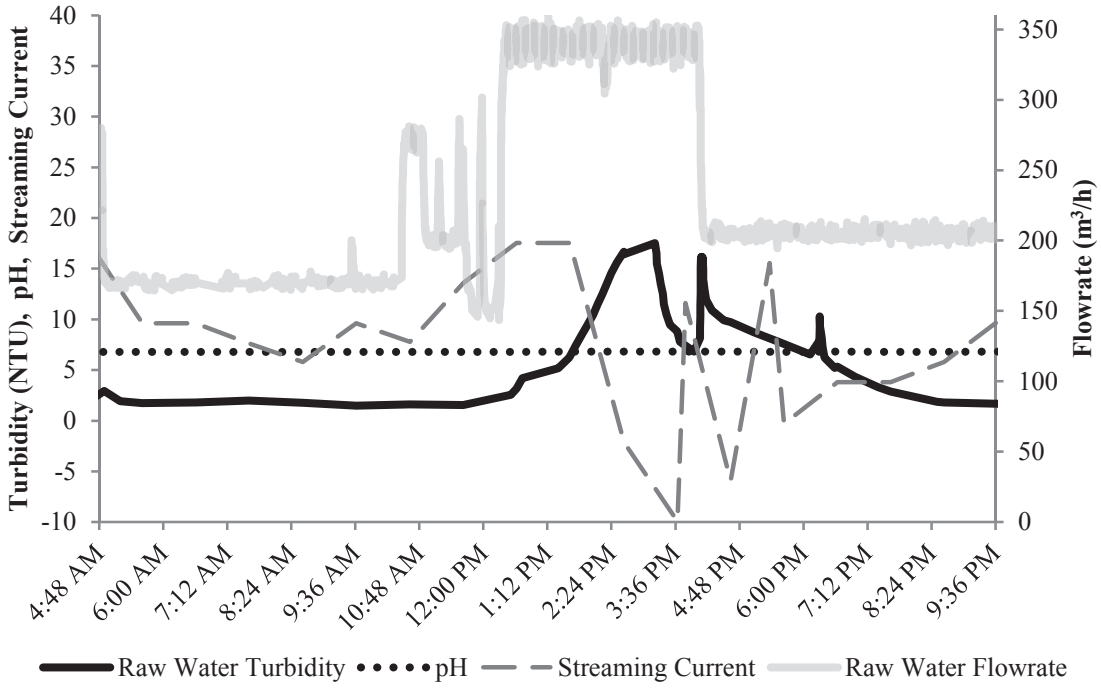

Figure 6.16. Raw water flowrate, turbidity, flash mixer pH and SC during nominal HLR testing.

A comparison of the raw water flowrate and turbidity shows that the raw water turbidity spike began shortly after the flowrate was increased from 150 m^3/h to the maximum flow of 340 m^3/h. This deterioration in raw water quality was mirrored by a decrease in SC, indicating a higher charge demand required for particle charge neutralization. However, the coagulant dose was not adjusted, as evidenced by the stable pH throughout the testing. As raw water quality was not maintained throughout the trial period, the data collected is insufficient to prove whether DAF performance was compromised by the lowered RR, increased HLR, or solely due to a decline in raw water quality.

The turbidity and raw water and DAF effluent at each stage of the test are summarized in Figure 6.17, and the trend of increasing turbidity showed results were not unaffected by the experiment order. The UV_{254} did not increase in the final flocculation basin, remaining at 0.012 cm^{-1} throughout the test (p=0.251). This indicates that the raw water quality degradation, caused by the increase to the nominal flowrate, was caused by increased particulate matter from scoured pipe sediment which increased turbidity but did not affect the concentration of dissolved organics.

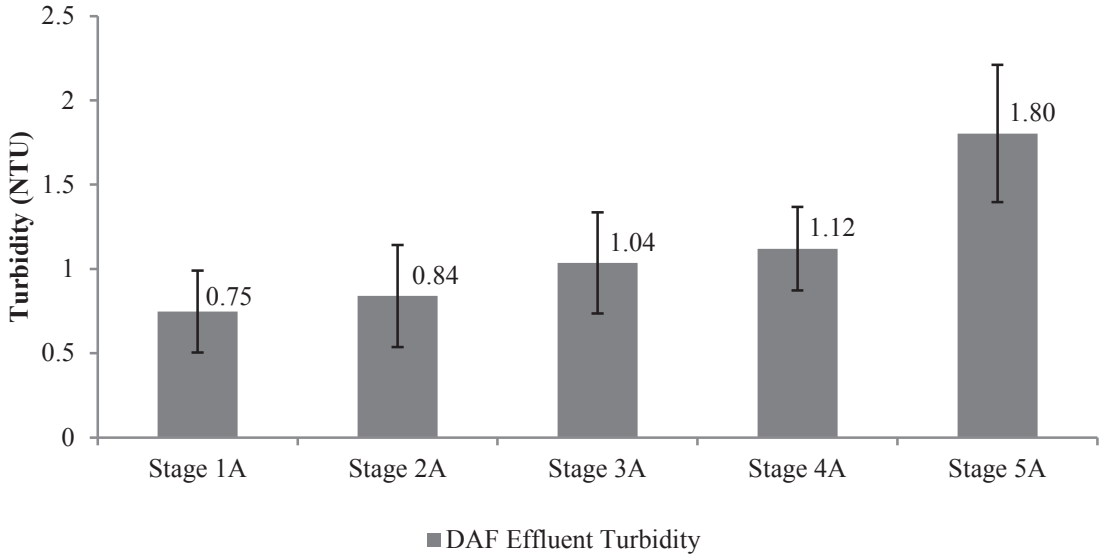

Figure 6.17. DAF effluent turbidity during each stage of nominal HLR testing.

In order to determine whether the minimum RR may be practical at the BBWTP, flushing of excess sediment from the raw water supply pipe had to be done prior to testing to ensure steady raw water quality at high raw water and low recycle flowrates.

On June 19th, 2012 a second nominal HLR test was performed at the BBWTP. 24 hours prior to the test period, the raw water flowrate was increased to the maximum (340 m^3/h) in order to mitigate the impact of the "first flush" effect which disrupted the prior

test. Raw water flow was increased to 340 m^3/h before decreasing saturator pressure from 500 kPa to 400 kPa. The raw water flow, saturator flow, RR and HLR for each stage of the testing is shown in Table 6.3.

Table 6.3. Flow, recycle and hydraulic loading rates during full-scale nominal HLR testing.

Test Stage	Raw Flow (m^3/h)	Saturator Flow (m^3/h)	RR (%)	HLR (m/h)
1B	235	29.4	12.5	6.12
2B	340	29.4	8.7	8.85
3B	340	27	7.9	8.85
4B	225	27.7	12.3	5.86

The raw water turbidity increased slightly during the trial, but did not exceed 10 NTU. The raw water flow and turbidity as well as coagulation pH are shown in Figure 6.18.

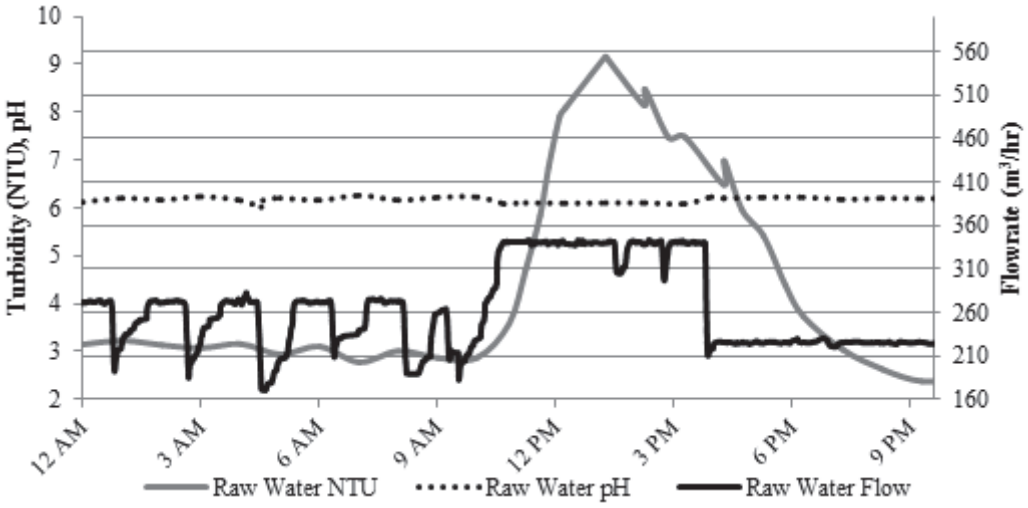

Figure 6.18. Raw water turbidity, flow and pH during nominal HLR recycle system testing.

While the primary cause for disruption of DAF efficacy during the first nominal HLR trial could not specifically be attributed to the lowered RR, if DAF performance

was unaffected at the higher HLR and turbidity load it could be stated that the lowered RR did not induce poorer DAF performance. During the second HLR trial, the raw water turbidity did increase from a baseline level of 3 NTU to a maximum of 9 NTU, but from the DAF effluent turbidity data it appeared that DAF performance was maintained. The recycle flowrate and DAF effluent turbidity during the trial are presented in Figure 6.19.

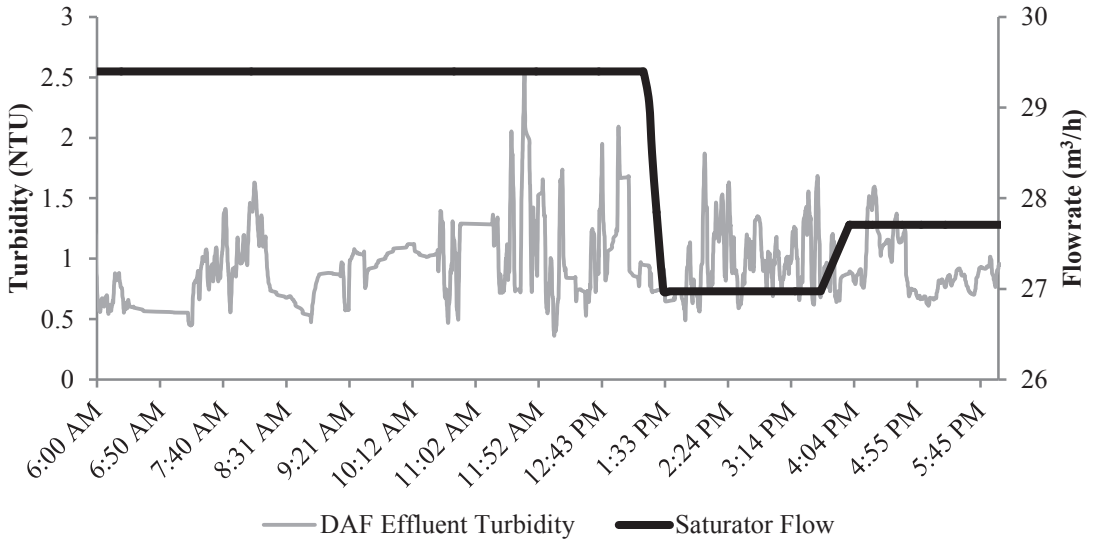

Figure 6.19. DAF effluent turbidity and recycle flow during nominal HLR recycle system testing.

To confirm that DAF effluent turbidity did not suffer as a result of lower RR, statistical analysis on the raw water and DAF effluent turbidity was done, comparing the data from before the test began (Stage 1B), the high raw water flow/high recycle flow condition (Stage 2B), the high raw water flow/low recycle flow condition (Stage 3B), and from several hours after the test ended (Stage 4B). The results are shown in Figure 6.20.

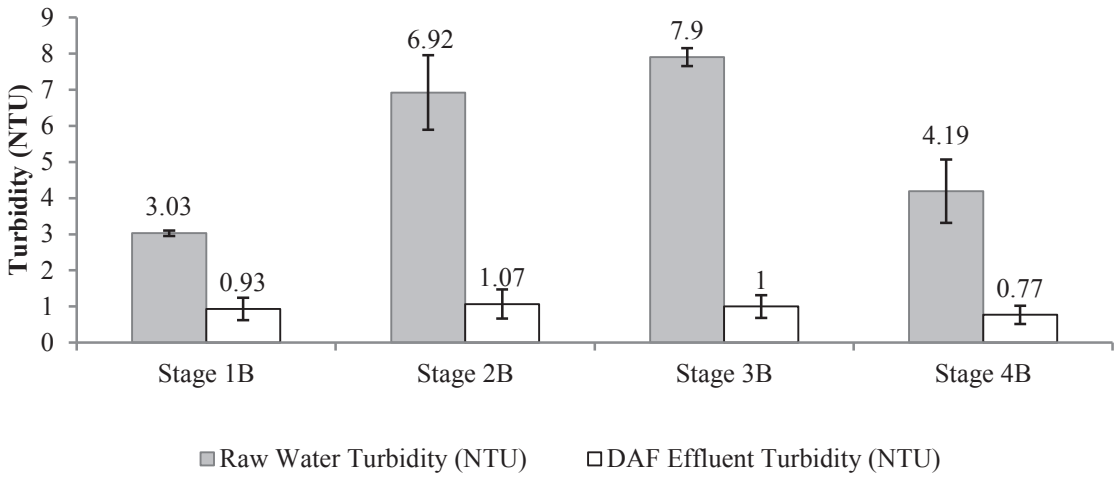

Figure 6.20. Raw water and DAF effluent turbidity during nominal HLR testing.

ANOVA tests showed that DAF effluent turbidity increased significantly between Stage 1B and 2B, or when water flowrate was increased ($p<0.01$). This increase may have been due to the high HLR, lower RR or the increased raw water turbidity. It is unlikely that during normal operation of the BBWTP the HLR would be increased to the maximum level for long enough to allow raw water turbidity to stabilize, as the maximum design flowrate is rarely employed.

Statistical analysis also showed that despite a higher average raw water turbidity, DAF performance actually improved from Stage 2B to Stage 3B when HLR was kept constant and RR was reduced from 8.7 to 7.9 % ($p=0.002$). Therefore, it was concluded that DAF effluent turbidity increased during the nominal HLR testing due to the combination of increased raw water turbidity and HLR, and that the RR decrease was not a contributing factor.

Grab samples of the DAF effluent were taken during full-scale trials and analyzed for particle count, UV_{254} and dissolved aluminum. Grab sample particle count measurements are presented in Figure 6.20.

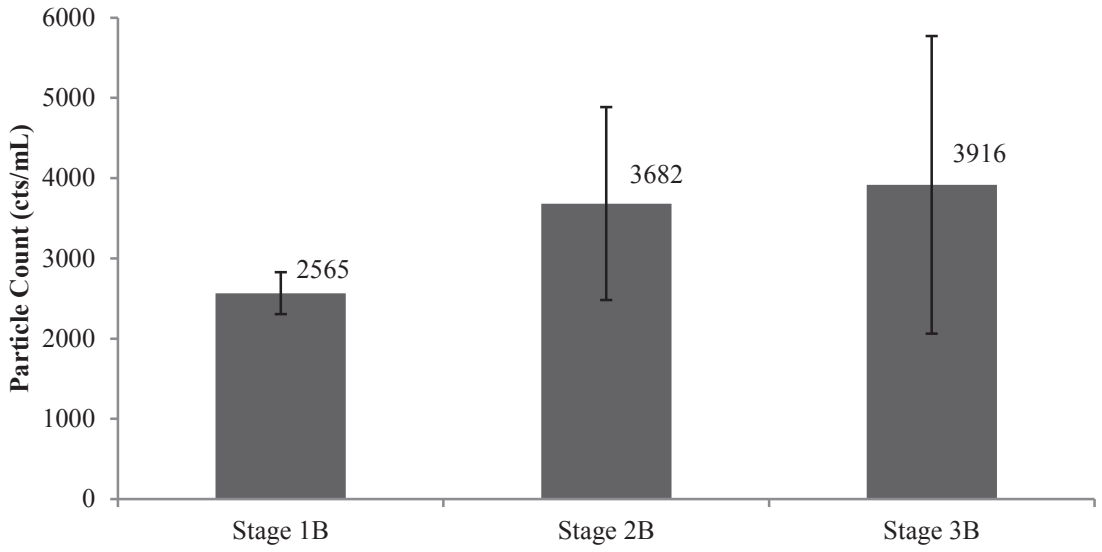

Figure 6.21. Particle counts during nominal HLR recycle system testing.

Particle counts were significantly lower in Stage 1B, before the initiation of the high raw water flowrate, however no significant difference (p=0.546) was found when comparing particle counts during the maximum flowrate/high recycle flow (Stage 2B) and the minimum RR conditions (Stage 3B).

Grab sample UV_{254} results from the nominal HLR testing are presented in Figure 6.21. UV_{254} was found to be slightly lower in Stage 1B than in Stage 2B or 3B (p=0.046), however no significant difference in UV_{254} was found between Stage 2B or 3B (p=0.059).

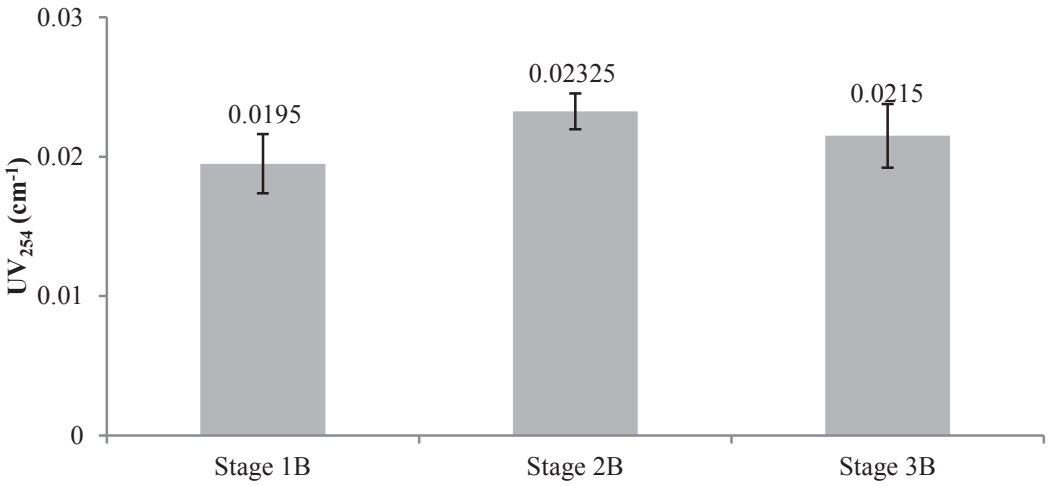

Figure 6.22. DAF effluent UV_{254} during nominal HLR recycle system testing.

The increase in UV_{254} after the raw flow was maximized indicates that the coagulant demand increased during the trial, likely due to the increase in raw water turbidity. No adjustment to coagulant addition was done during the trial. It is also possible that coagulant demand was stable, but the increased HLR negatively affected the performance of DAF pretreatment coagulation-flocculation processes. In either case, lowering the RR to 7.9 % (from Stage 2B to 3B) did not appear to negatively affect DAF performance with regards to turbidity or UV_{254} removal.

No significant difference was found in DAF effluent dissolved aluminum concentrations before or during the trial ($p=0.502$). This result was expected, as coagulation pH and temperature, which control aluminum solubility, were unchanged throughout the full-scale trials.

6.5 Conclusions

Lowering the recycle rate from 12 to 6 % in bench-scale DAF testing was found to improve particle removal by 4.9 % in baseline water trials ($p=0.016$). However, in synthetic water trials recycle rate was not found to be a significant factor in particle removal. This discrepancy may be due to the air:solids ratio achieved in the sludge blanket after clarification. During baseline trials, with a low concentration of solids, the 6 % recycle rate may have optimized this ratio. However, during synthetic challenge water trials a higher number of bubbles were required to optimize this ratio and therefore reducing the RR to 6 % did not improve treatment performance. Since the recycle water in bench-scale testing was filtered through a reverse osmosis membrane, the 12 % RR trials injecting double the amount of recycle water acted to dilute the results of all measured clarified water quality parameters. Despite this, the lower RR led to equal or improved DAF performance, which suggests that in full-scale applications where clarified or media-filtered water is used as the recycle source the improvement may be greater.

During full-scale trials, under normal operating conditions at the BBWTP with a baseline flowrate of 255 m^3/h, decreasing saturator pressure from 500 kPa to 400 kPa to reduce RR from 11.7 to 10.7 % resulted in no significant impact on DAF performance as measured by turbidity, particle count, UV_{254} and dissolved aluminum.

At the maximum plant design flowrate, increased raw water turbidity due to increased plant supply pipe water velocity led to sediment scouring which compromised raw water quality stability, making direct, unbiased comparison of low vs. high RR impossible. Statistical analysis of the data suggests that at high raw water flowrates the

DAF clarifier performance was not compromised with lowering the RR from 8.7 to 7.9 %. However, performance may decline due to increased influent turbidity levels and an increased HLR in the rapid mix and flocculation basins as well as the clarifier.

Recycle rate was the only operational factor examined at both the bench-scale and full-scale, and so optimization with respect to mixing speeds, retention times and chemical addition sequence was not investigated in the coagulation-flocculation process. 6 to 8 % RR trials performed equally to, or outperformed, 12 % RR trials on a consistent basis during both bench-scale and full-scale trials. Beside possible treatment performance improvement, reducing the RR in a DAF WTP from 12 to 6 % would be desirable, as at the very least it would reduce power requirements for saturation and pumping systems in the plant.

Chapter 7: Conclusions

7.1 Conclusions

Investigation into historical trends of raw water quality and treatment performance at a DAF WTP revealed that a series of events, often initiated by rapidly deteriorating source water quality, resulted in process disruptions and periodic increases in clearwell turbidity above the maximum allowable level. It was found that the control of coagulant and pH adjustment chemicals was inadequate during rapid source water quality degradation, leading to a low coagulation pH which possibly allowed high dissolved aluminum residuals to precipitate in the clearwell, causing turbidity increases.

Coagulation pH was evaluated in bench-scale testing of baseline and synthetic challenge water trials, and it was found that particulate matter, as quantified by turbidity and particle count measurements, was removed more effectively at the pH of minimum solubility than pH 6.0 using both a 50 % and 70+ % PACl coagulant. Dissolved aluminum concentrations in the DAF effluent samples were also found to be significantly lower in trials run at this pH level than in trials run at a pH of 6.0. In addition, no performance decline at above-optimum coagulant concentrations occurred at the pH of minimum solubility, suggesting that overdose conditions leading to treatment disruption could be avoided at this pH. However, a lower coagulant dose was needed to achieve optimum performance at pH 6.0, and NOM removal was improved in the challenge water trials at this pH.

Charge analysis parameters zeta potential and streaming current were found to have a strong correlation after rapid mixing in bench-scale treatment of baseline water, however the relationship between the two was affected by the pH. Streaming current

values yielding optimum treatment in pH 6.0 trials were well defined near the point of zero charge, but the streaming current values did not approach this point in the pH of minimum aluminum solubility trials.

In typical DAF plants, particularly those which are susceptible to rapid changes in source water quality resulting from rainfall and runoff conditions, it is beneficial to target the pH of minimum aluminum solubility to prevent plant upset conditions from arising.

The best choice for PACl coagulant basicity is closely tied with pH. When targeting a pH of 6.0, using a lower basicity coagulant reduced aluminum residuals due to its lower pH of minimum aluminum solubility.

It was found during bench-scale testing that the solid-liquid separation efficacy of DAF was either unaffected or improved by reducing the RR from 12 % to 6 %. The RR was not found to have any impact on dissolved components, such as aluminum and NOM.

At a full-scale DAF WTP under normal operating conditions, treatment performance was unaffected by a small reduction in RR of 12 to 11 %. Higher HLRs required to reduce RR to 9 % resulted in unstable raw water quality, leading to decreased DAF efficacy. However, reducing the RR from 9 to 8 % during the raw water quality upset improved DAF effluent turbidity, suggesting that DAF performance was negatively affected by the increased HLR and deteriorating raw water quality, but was improved by reducing the RR.

7.2 Recommendations

Investigation into optimizing DAF performance will become increasingly relevant in Atlantic Canada and beyond as the technology becomes increasingly popular and the global climate trends towards more frequent intense rainfall events leading to rapid changes in surface water quality.

Future work should include evaluating the impacts of several chemical and operational factors which could be manipulated to optimize the DAF process which were not examined in this study. These factors include comparison of other common coagulants such as aluminum sulphate and ferric chloride, manipulating the mixing intensity and hydraulic retention times in each stage of coagulation-flocculation, altering the chemical addition sequence, and examining the effect of alternative alkalinity sources on DAF performance. Improved characterization of particulate matter and NOM present in surface drinking water sources in Atlantic Canada after periods of rainfall and runoff should be done to better allow transferability of study conclusions to other areas.

Online monitoring practices at the Brierly Brook Water Treatment Plant should be expanded to include the dose of coagulant and buffering chemicals being applied in the plant, to accommodate future research comparing chemical additions and water quality with streaming current values and treatment performance. Streaming current may prove to be a valuable tool for optimizing treatment performance if the relationship between the streaming current value and optimum coagulant dose can be better understood.

Automatic control of coagulation pH in the plant should be considered to prevent pH from falling outside its optimum range during rapid changes in coagulant dosing. A

comparison of buffering chemicals (soda ash, lime and caustic) should also be done to determine whether treatment performance is affected at the optimum coagulation pH.

References

ACWWA (Atlantic Canada Water Works Association) (2004). Atlantic Canada Guidelines for the Supply, Treatment, Storage, Distribution, and Operation of Drinking Water Supply Systems. Available at: http://www.gov.ns.ca/nse/water/docs/WaterSystemGuidelines.pdf (Accessed July 2012).

Amirtharajah, A. & Mills, K. M. (1982). Rapid-mix design for mechanisms of alum coagulation. American Water Works Association Journal, 210-216.

APHA (American Public Health Association), AWWA (American Water Works Association) & WEF (Water Environment Federation) (2012). Standard Methods for the Examination of Water and Wastewater. Washington, DC: APHA.

AWWA (American Water Works Association) & ASCE (American Society of Civil Engineers) (1997). Water Treatment Plant Design (3rd ed.). McGraw-Hill: New York.

AWWA (2003). Water Treatment: Principles and Practices of Water Supply Operations (3rd ed.). Denver: American Water Works Association.

AWWA (2011). Operational Control of Coagulation and Filtration Processes: Manual of Water Supply Practices (3rd ed.). Denver: American Water Works Association.

Babcock, D. B. & Singer, P. C. (1979). Chlorination and coagulation of humic and fulvic acids. *Journal AWWA, 71*(3), 149-152.

Barnett, T. P., Adam, J. C. & Lettenmaier, D. P. (2005). Potential impacts of a warming climate on water availability in snow-dominated regions. *Nature*, 438:303-309.

Bates, B. C., Kundzewicz, Z. W., Wu, S. & Palutikof, J. P., Eds. (2008). *Climate Change and Water: Technical Paper of the Intergovernmental Panel on Climate Change*, IPCC Secretariat, Geneva.

Bratby, J. (2006). *Coagulation and Flocculation in Water and Wastewater Treatment*. London: IWA Publishing.

Brezonik, P. & Arnold, W. (2011). *Water Chemistry: An Introduction to the Chemistry of Natural and Engineered Aquatic Systems.* New York: Oxford University Press.

Bunker, D. Q., Edzwald, J. K., Dahlquist, J. & Gillberg, L. (1995). Pretreatment considerations for dissolved air flotation: water type, coagulants and flocculation. *Water Science and Technology, 31*(3-4), 63-71.

Charron, D. F., Thomas, M. K., Waltner-Toews, D., Aramini, J. J., Edge, T., Kent, R., Maarouf, A. & Wilson, J. (2004). Vulnerability of Waterborne Diseases to Climate Change in Canada: A Review. *Journal of Toxicology and Environmental Health*, Part A, 67:1667-1677.

Chilarescu, I. C., Berevoianu, C., Sandu, M. & Racoviteanu, G. (1998). Automatic Determination of Coagulation-Flocculation Reagents Dose. Chemical Water and Wastewater Treatment V: Proceedings of the 8th Gothenburg Symposium (pp. 71-81). Prague: Springer.

Chowdhury, S., Rodriguez, M. J. & Sadiq, R. (2011). Disinfection byproducts in Canadian provinces: Associated cancer risks and medical expenses. Journal of Hazardous Materials, 187(1-3), 574-584.

Chowdhury, Z. K., Amy, G. L. & Bales, R. C. (1991). Coagulation of Submicron Colloids in Water Treatment by Incorporation into Aluminum Hydroxide Flocs. Environmental Science and Technology, 1766-1773.

Christman, R. F., Norwood, D. L., Millington, D. S., Johnson, J. D. & Stevens, A. A. (1983). Identity and yields of major halogenated products of aquatic fulvic acid chlorination. Environmental Science and Technology, 17(10), 625-628.

Curriero, F. C., Patz, J. A., Rose, J. B. & Lele, S. (2001). The association between extreme precipitation and waterborne disease outbreaks in the United States, 1948-1994. *American Journal of Public Health*, 91:1194-1199.

Dahlquist,J. & Goransson, K. (2004). Evolution of a high rate dissolved air flotation process – from idea to full-scale application. In Hahn, H., Hoffman, E., Odegaard, H (Eds.), Chemical Water and Wastewater Treatment. IWA Publishing: Londo, 297-308.

Deryagin, B. V. & Landau, L. V. (1941). Theory of Stability of Strongly Charged Lyophobic Sols and Coalescence of Strongly Charged Particles in Solutions of Electrolytes. Acta Physicochim, 14, 633.

Droste, R. L. (1997). Theory and Practice of Water and Wastewater Treatment. New York: John Wiley and Sons, Inc.

Droppo, I. G., Leppard, G. G., Liss, S. N. & Milligan, T. G., Eds. (2005). Flocculation in Natural and Engineering Environmental Systems. Boca Raton: CRC Press.

Duan, J. & Gregory, J. (2003). Coagulation by hydrolysing metal salts. Advances in Colloid and Interface Science, Volumes 100-102, 475-502.

Edzwald, J. K. (2006). Chapter 6: Dissolved air flotation in drinking water treatment. Interface Science in Drinking Water Treatment (pp. 89-107). Oxford: Elsevier.

Edzwald, J. K. (2007). Developments of high rate dissolved air flotation for drinking water treatment. Journal of Water Supply: Research and Technology-AQUA, 399-409.

Edzwald, J. K. (2010). Dissolved air flotation and me. Water Research, 44(7), 2077-2106.

Edzwald, J. K. & Wingler, B. J. (1990). Chemical and physical aspects of dissolved air flotation for the removal of algae. Journal of Water Supply: Research and Technology - AQUA, 39(2), 24-35.

Edzwald, J. K., Tobiason, J. E., Amato, T. & Maggi, L. J. (1999). Integrating high rate dissolved air flotation technology into plant design. Journal of the American Water Works Association, 91(12), 70-84.

Edzwald, J. K., Tobiason, J. E., Parento, L. M., Kelley, M. B., Kaminski, G. S., Dunn, H. J. & Galant, P. B. (2000). Giardia and Cryptosporidium removals by clarification and filtration under challenge conditions. Journal of the American Water Works Association, 92(12), 70-84.

Gregory, D. (1998, February). Enhanced Coagulation for Treating Spring Runoff Water. Opflow, pp. 12-13.

Gregory, J. (2006). Particles in Water: Properties and Processes. London: IWA Publishing.

Haarhoff, J. (1997). Towards the maximal utilisation of air in dissolved air flotation. Dissolved Air Flotation. Chartered Institution of Water and Environmental Management International Conference, London.

Haarhoff, J. (2008). Dissolved air flotation: progress and prospects for drinking water treatment. Journal of Water Supply: Research and Technology—AQUA, 57(8), 555-567.

Haarhoff, J. & Edzwald, J. K. (2001). Modelling of floc-bubble aggregate rise rates in dissolved air flotation. Water Science and Technology, 43(8), 175-184.

Haarhoff, J. & Edzwald, J. K. (2004) Dissolved air flotation modelling: insights and shortcomings. Journal of Water Supply: Research and Technology—AQUA, 53(3), 127-150.

Han, M. & Lawler, D. F. (1992). The (relative) insignificance of G in flocculation. Journal of the American Water Works Association, 84(10), 79-91.

Han, M. Y., Park, Y. H. & Yu, T. J. (2002). Development of a new method of measuring bubble size. Water Science and Technology: Water Supply, 2(2), 77-83.

Health Canada (2010). Guidelines for Canadian Drinking Water Quality: Summary Table. Available at http://www.hc-sc.gc.ca/ewh-semt/alt_formats/hecs-sesc/pdf/pubs/water-eau/2010-sum_guide-res_recom/sum_guide-res_recom-eng.pdf (Accessed June 2012).

Henderson, R. K., Parsons, S. A. & Jefferson, B. (2008). Successful Removal of Algae through the Control of Zeta Potential. Separation Science and Technology, 43, 1653-1666.

Jensen, J. N. (2003). A Problem-Solving Approach to Aquatic Chemistry. Hoboken: John Wiley & Sons, Inc.

Kan, C., Huang, C. & Pan, J. (2002). Coagulation of high turbidity water: the effects of rapid mixing. Journal of Water Supply: Research and Technology—AQUA, 51(2), 77-85.

Leemans, R. & Kleidon, A. (2002). Regional and global assessment if the dimensions of desertification. Berlin: Dahlem University Press.

Leiviska, T. (2009). Coagulation and Size Fractionation Studies on Pulp and Paper Mill Process and Wastewater Streams. Oulu, Finland: Oulu University Press.

Leppinen, D. M. & Dalziel, S. B. (2004). Bubble size distribution in dissolved air flotation tanks. Journal of Water Supply: Research and Technology—AQUA, 53(8), 531-543.

Mosher, C. (2012). Nova Scotia Department of Environment, Water and Wastewater Branch. Personal communication, May 1, 2012.

Nova Scotia Environment (2012). Nova Scotia Treatment Standards for Municipal Drinking Water Systems. Halifax, NS, Canada.

Pernitsky, D. J. (2001). Drinking water coagulation with polyaluminum coagulants: Mechanisms and selection guidelines. Electronic Doctoral Dissertations for UMass Amherst. Paper AAI3027241.
http://scholarworks.umass.edu/dissertations/AAI3027241

Pernitsky, D. J. & Edzwald, J. K. (2003). Solubility of polyaluminum coagulants. Journal of Water Supply: Research and Technology--AQUA, 52(6), 395-406.

Schoenen, D. (2002). Role of disinfection in suppressing the spread of pathogens with drinking water: possibilities and limitations. Water Research, 36(15), 3874-3888.

Schuster, C. J., Ellis, A. G., Robertson, W. J., Charron, D. F., Aramini, J. J., Marshall, B. J. & Medeiros, D. T. (2005). Infections Disease Outbreaks Related to Drinking Water in Canada. *Canadian Journal of Public Health*, 254-258.

Shin, J. Y., Spinette, R. F. & O'Melia, C. R. (2008). Stoichiometry of coagulation revisited. Environmental Science & Technology, 42, 2582-2589.

Stevens, A. A., Slocum, C. J., Seeger, D. R. & Robeck, G. G. (1976). Chlorination of Organics in Drinking Water. Journal AWWA, 68(11), 615-620.

Stumm, W. & Morgan, J. (1995). Aquatic Chemistry (3rd ed.). Hoboken: John Wiley & Sons, Inc.

Teixeira, M. B. & Rosa, M. J. (2006). Comparing dissolved air flotation and conventional sedimentation to remove cyanobacterial cells of Microcystis aeruginosa Part I: the key operating conditions. Separation and Purification Technology, 52, 84-94.

Tseng, T., Segal, B. D. & Edwards, M. (2000). Increasing alkalinity to reduce turbidity. Journal AWWA, 92(6), 44-54.

Underwood, J., Ogden, J., Kerekes, J. & Vaughan, H. (1987). Acidification of Nova Scotia Lakes. Water, Air and Soil Pollution, 32, 77-88.

USEPA. (2012, March 6). Basic Information about Pathogens and Indicators in Drinking Water. Retrieved May 9, 2012, from United States Environmental Protection Agency: Drinking Water. http://water.epa.gov/drink/contaminants/basicinformation/pathogens.cfm

Valade, M. T., Edzwald, J. K., Tobiason, J. E., Dahlquist, J., Hedberg, T. & Amato, T. (1996). Particle removal by flotation and filtration: pretreatment effects. Journal of the American Water Works Association, 88(12), 35-47.

Valade, M. T., Becker, W. B. & Edzwald, J. K. (2009). Treatment selection guidelines for particle and NOM removal. Journal of Water Supply: Research and Technology - Aqua, 58(6), 424-432.

Van Benschoten , J. E. & Edzwald, J. K. (1990a). Chemical aspects of coagulation using aluminum salts--I. Hydrolytic reactions of alum and polyaluminum chloride. Water Research, 1519-1526.

Van Benschoten, J. E. & Edzwald, J. K. (1990b). Chemical aspects of coagulation using aluminum salts--II. Coagulation of fulvic acid using alum and polyaluminum chloride. Water Research, 1527-1535.

Verway, E. J. & Overbeek, J. T. (1948). Theory of the Stability of Lyophobic Colloids. Amsterdam: Elsevier.

Wang, D., Sun, W., Xu, Y., Tang, H. & Gregory, J. (2004). Speciation stability of inorganic polymer flocculant-PACl. Colloids and Surfaces A: Physicochemical and Engineering Aspects, 243, 1-10.

Yan, M., Wang, D., Ni, J., Qu, J., Chow, C. & Liu, H. (2008). Mechanism of natural organic matter removal by polyaluminum chloride: Effect of coagulant particle size and hydrolysis kinetics. Water Research(42), 3361-3370.

Ye, C., Wang, D., Shi, B., Yu, J., Qu, J., Edwards, M. & Tang, H. (2007). Alkalinity effect of coagulation with polyaluminum chlorides: Role of electrostatic patch. Colloids and Surfaces A: Physicochemical and Engineering Aspects, 294, 163-173.

Appendix A: Turbidity and pH Profiles during BBWTP Upsets

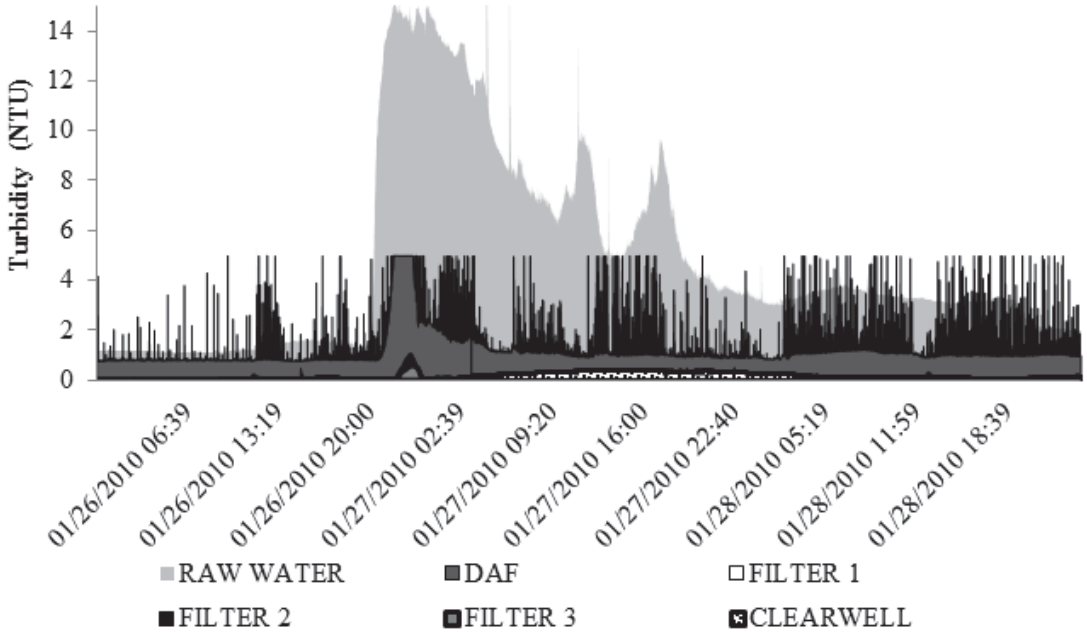

Figure A1. Raw water, DAF effluent, clearwell and filter effluent turbidities during plant upset at the BBWTP: January 26th to 28th, 2010.

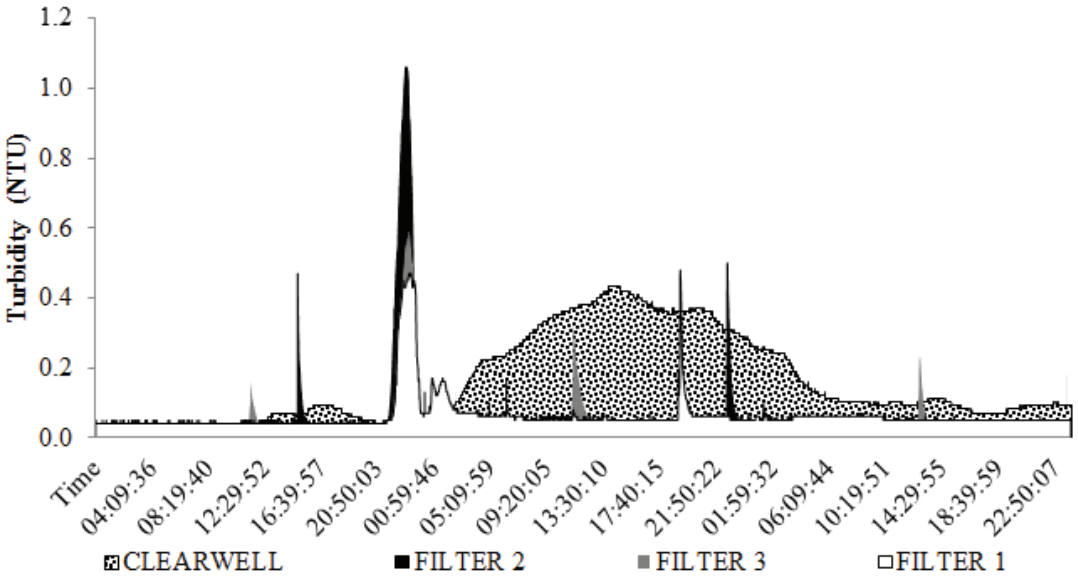

Figure A2. Clearwell and filter effluent turbidities at the BBWTP during plant upset: January 26th to 28th, 2010.

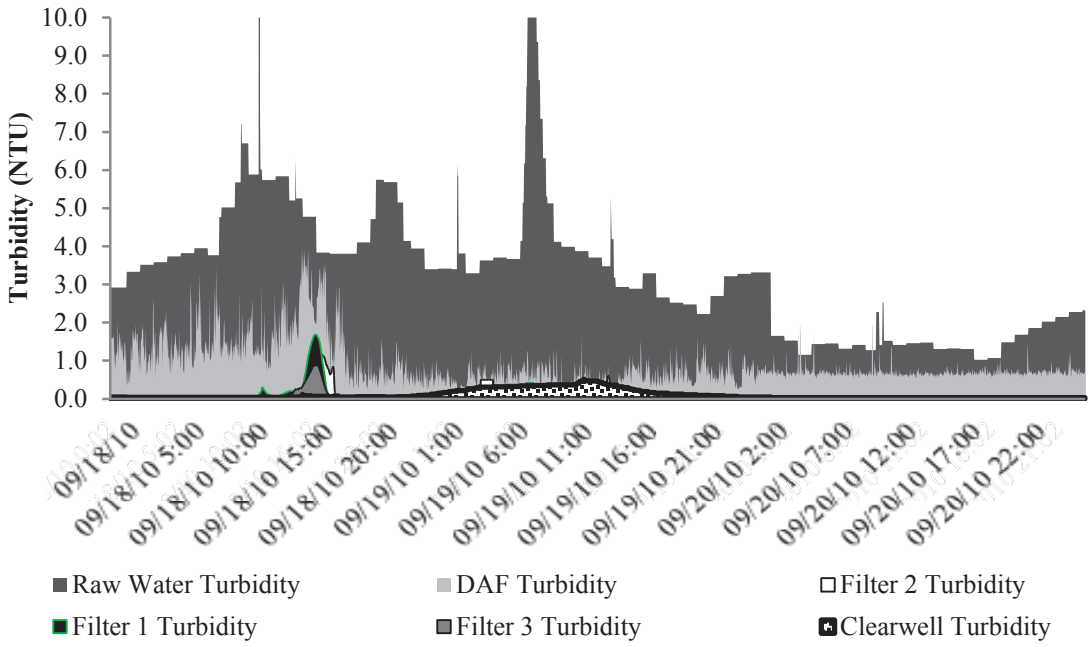

Figure A3. Raw water, DAF effluent, clearwell and filter effluent turbidities during plant upset at the BBWTP: September 18th to 20th, 2010.

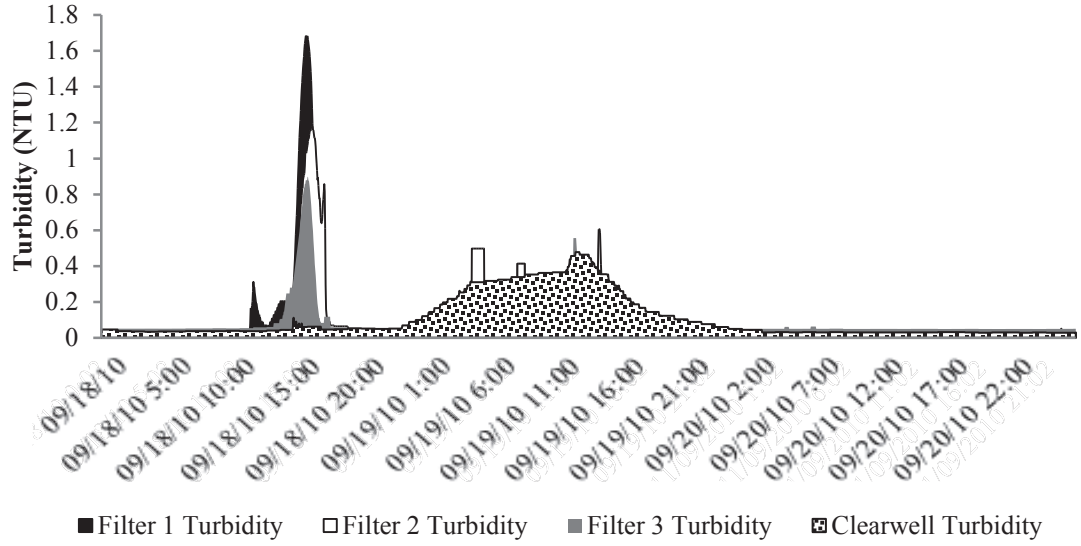

Figure A4. Clearwell and filter effluent turbidities at the BBWTP during plant upset: September 18th to 20th, 2010.

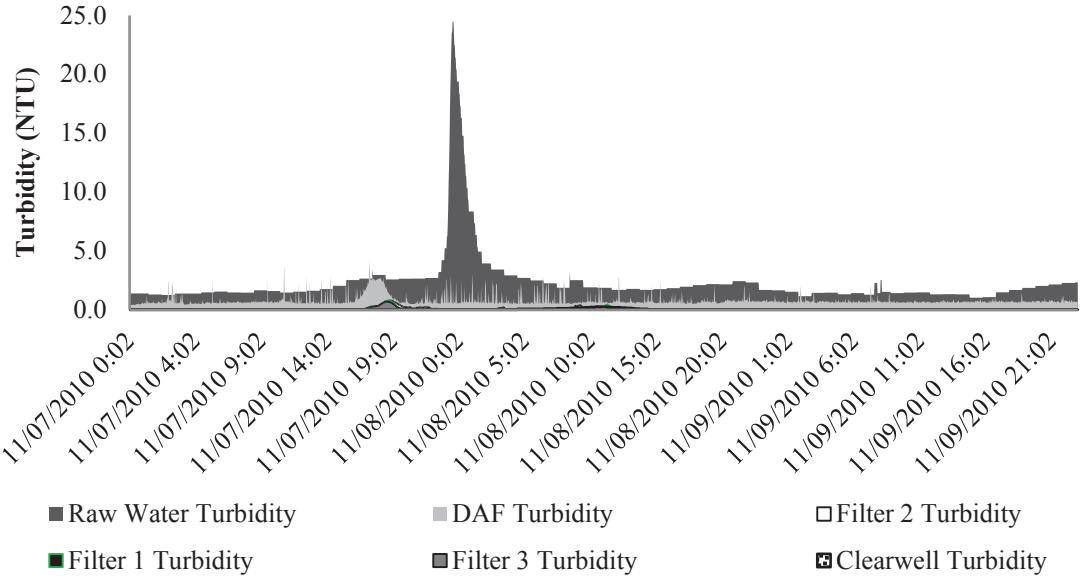

Figure A5. Raw water, DAF effluent, clearwell and filter turbidities at the BBWTP during plant upset: November 7th to 9th, 2010.

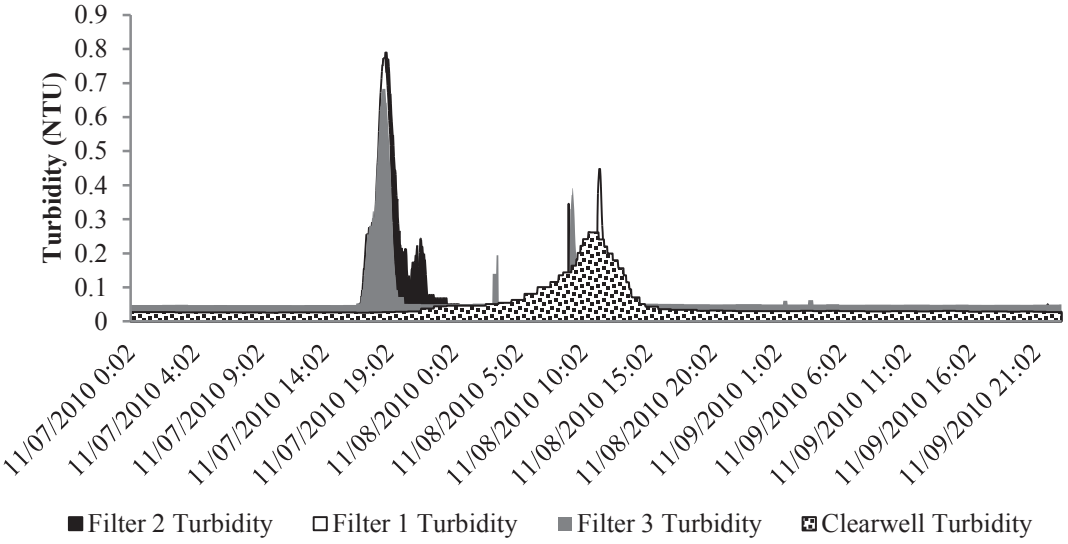

Figure A6. Clearwell and filter turbidities at the BBWTP during plant upset: November 7th to 9th, 2010.

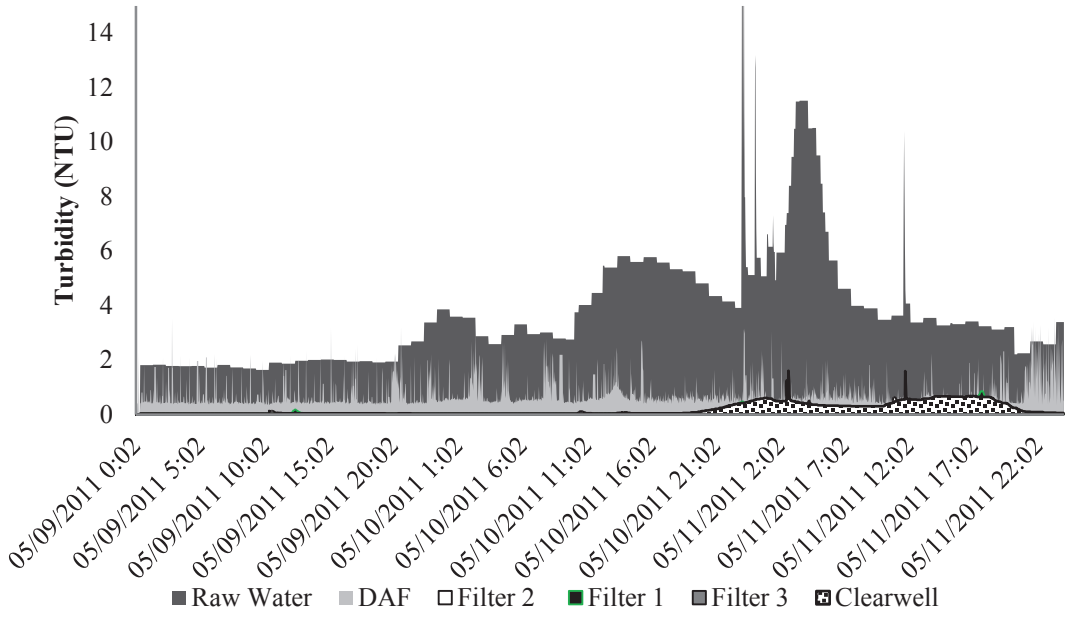

Figure A7. Raw water, DAF effluent, clearwell and filter effluent turbidity values at the BBWTP during plant upset: May 9th to 11th, 2011.

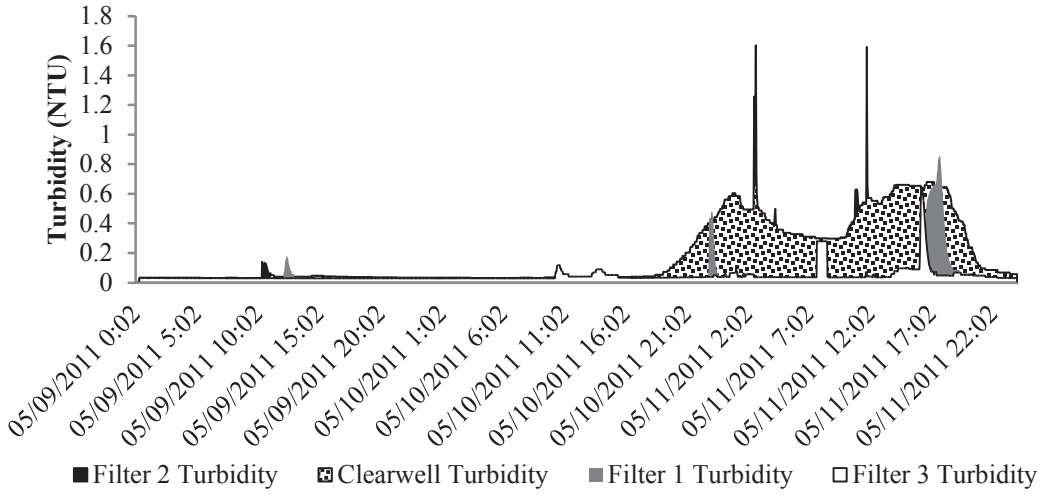

Figure A8. Clearwell and filter effluent turbidity values at the BBWTP during plant upset: May 9th to 11th, 2011.

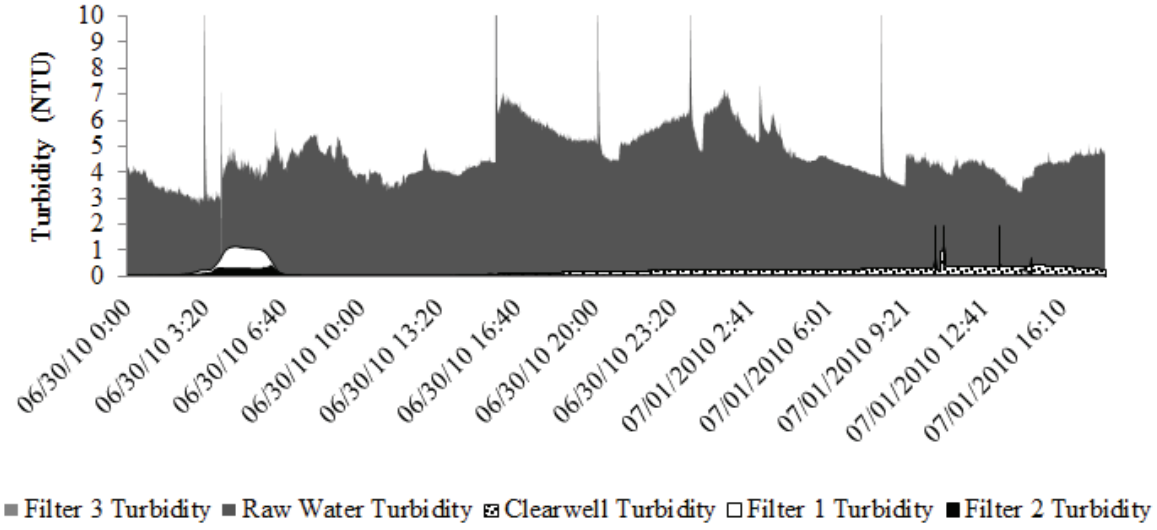

Figure A9. Raw water, clearwell and filter effluent turbidity values at the BBWTP during plant upset: June 30th to July 1st, 2010.

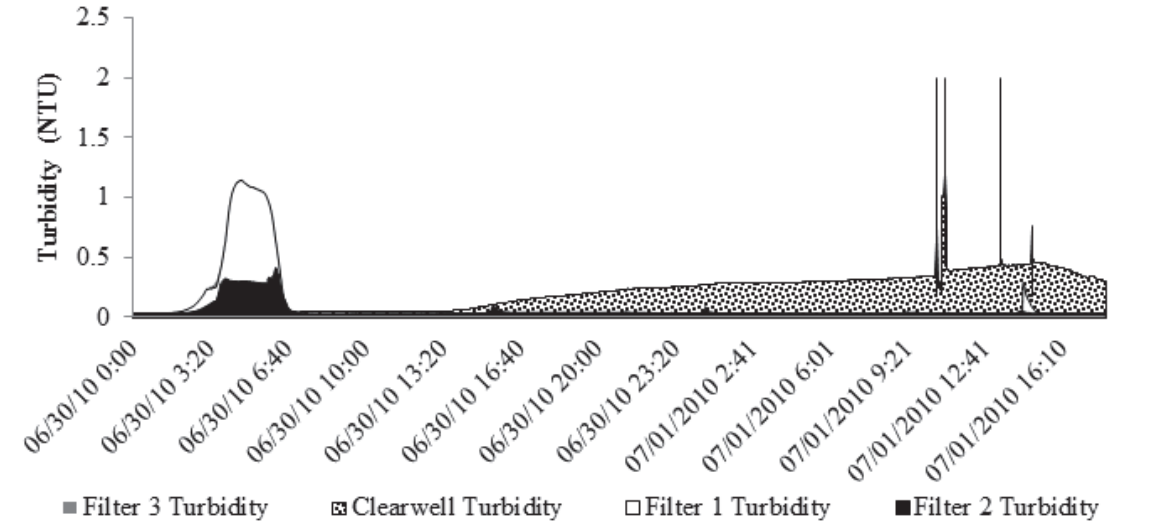

Figure A10. Clearwell and filter effluent turbidity values at the BBWTP during plant upset: June 30th to July 1st, 2010.

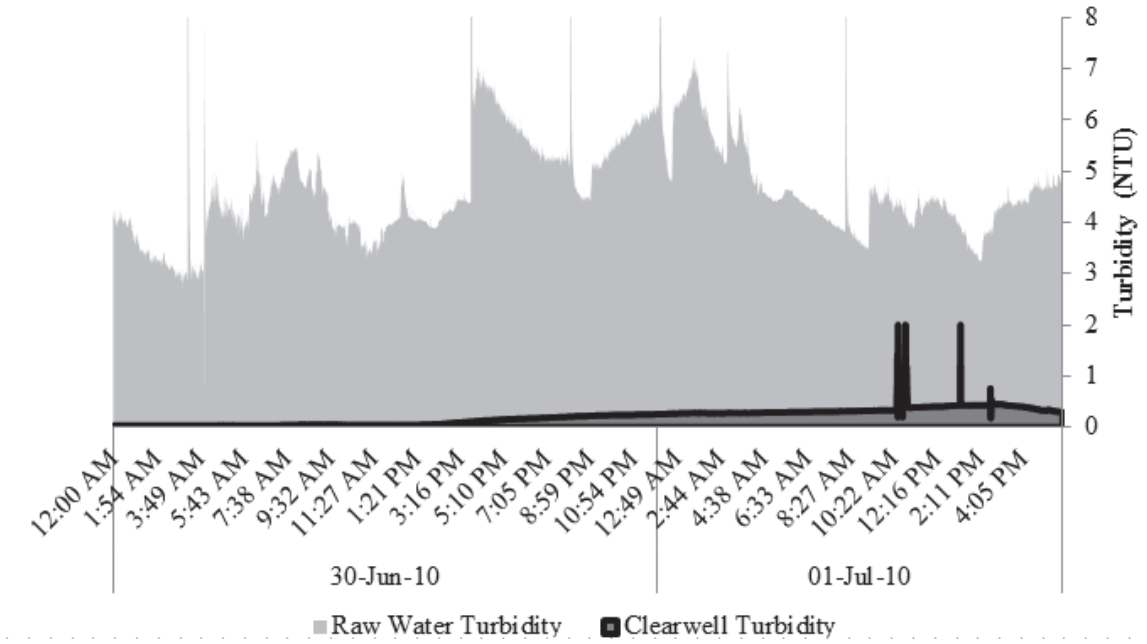

Figure A11. SC and turbidity values during BBWTP plant upset: June 30-July 1, 2010.

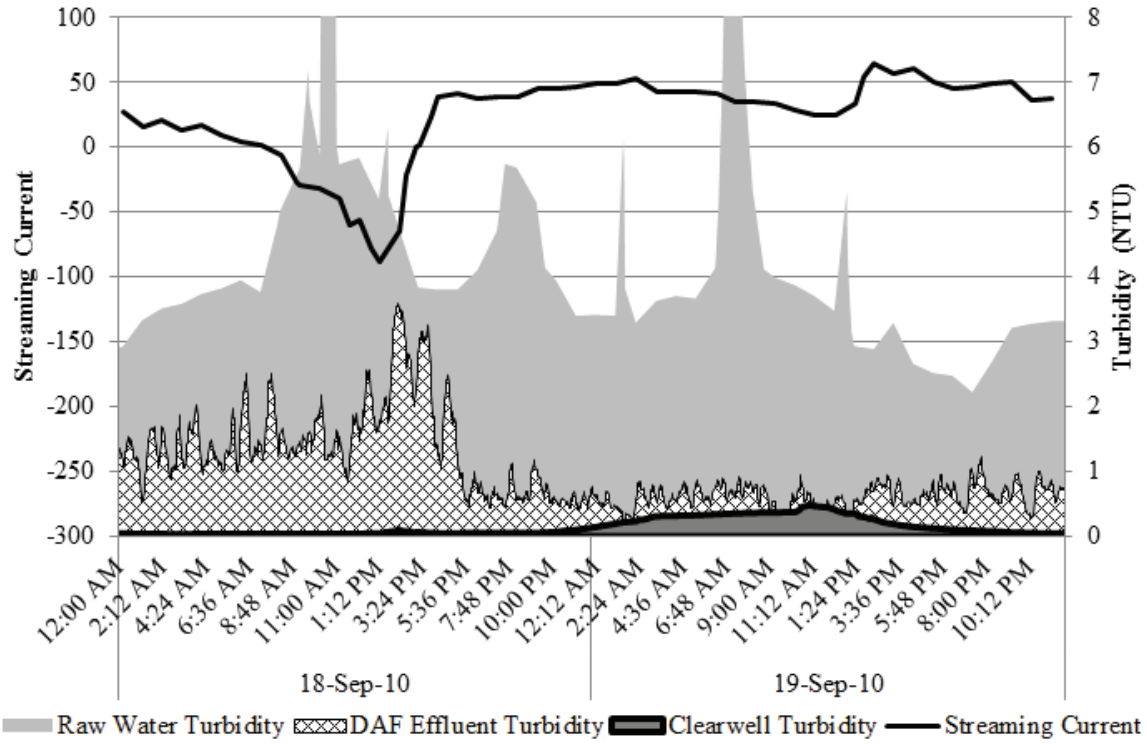

Figure A12. SC and turbidity values at the BBWTP during plant upset: September 18-19, 2010.

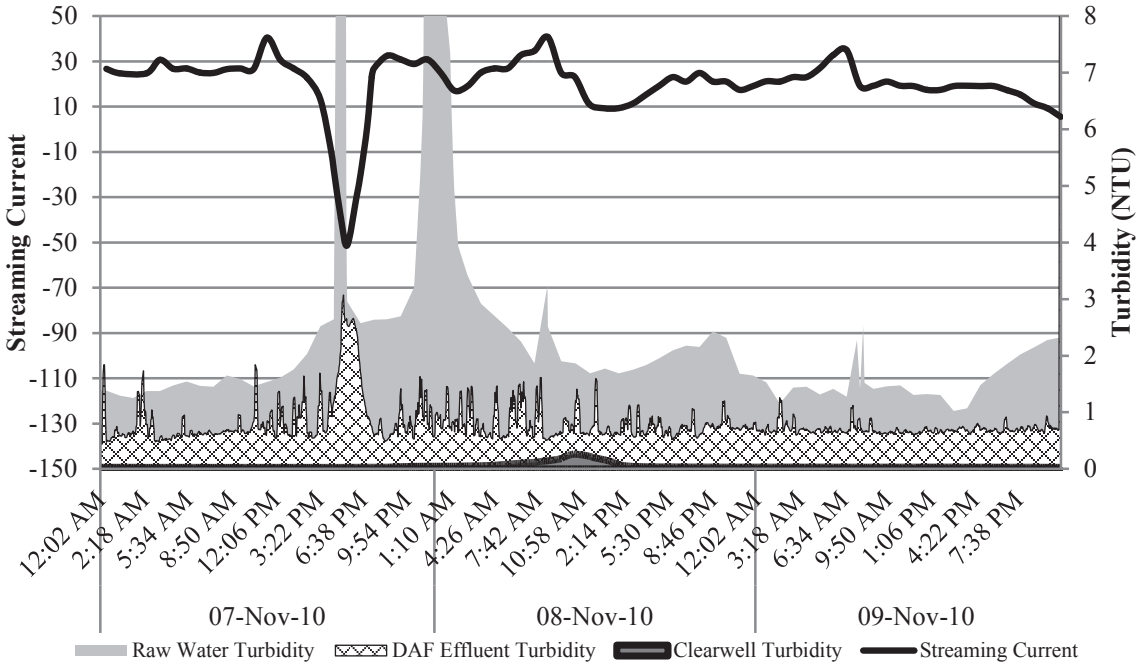

Figure A13. SC and turbidity at the BBWTP during plant upset: November 7-9, 2010.

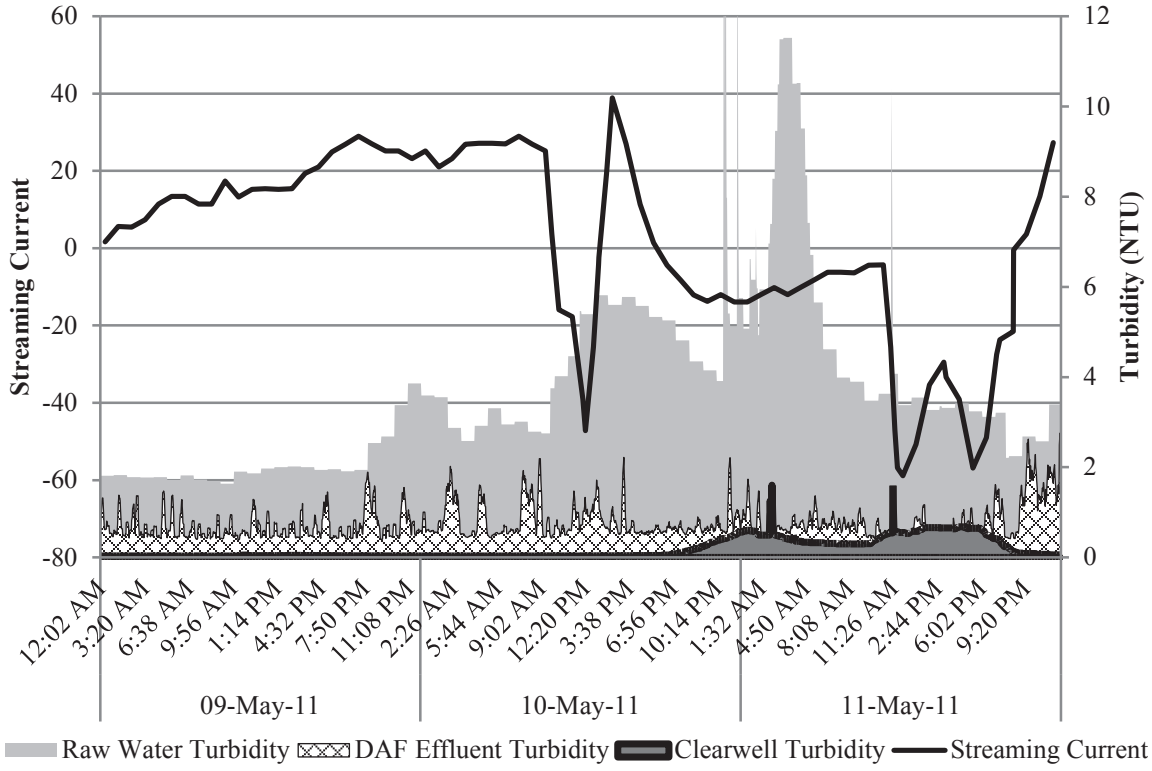

Figure A14. SC and turbidity values at the BBWTP during plant upset: May 9-11, 2011.

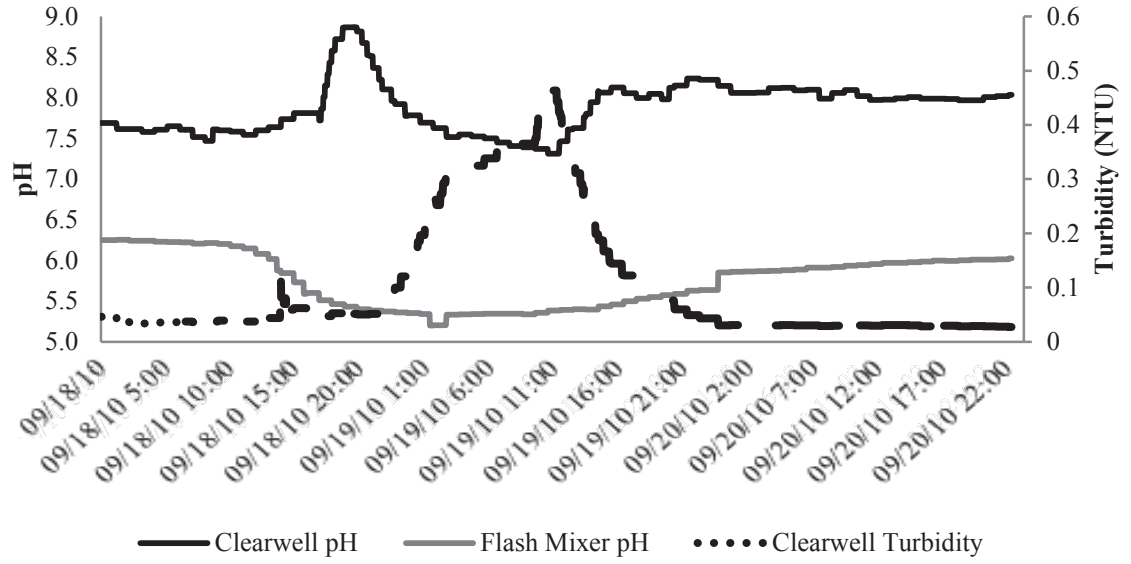

Figure A15. pH and clearwell turbidity profile for September 18-20, 2010 BBWTP upset.

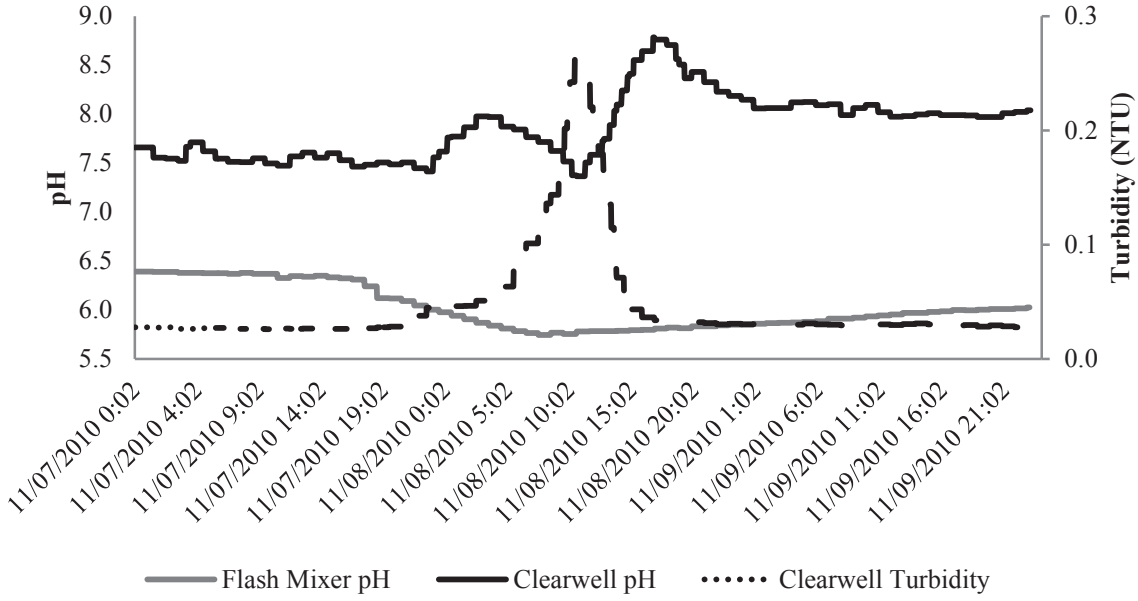

Figure A16. pH and clearwell turbidity profile for November 8th, 2011 BBWTP upset.

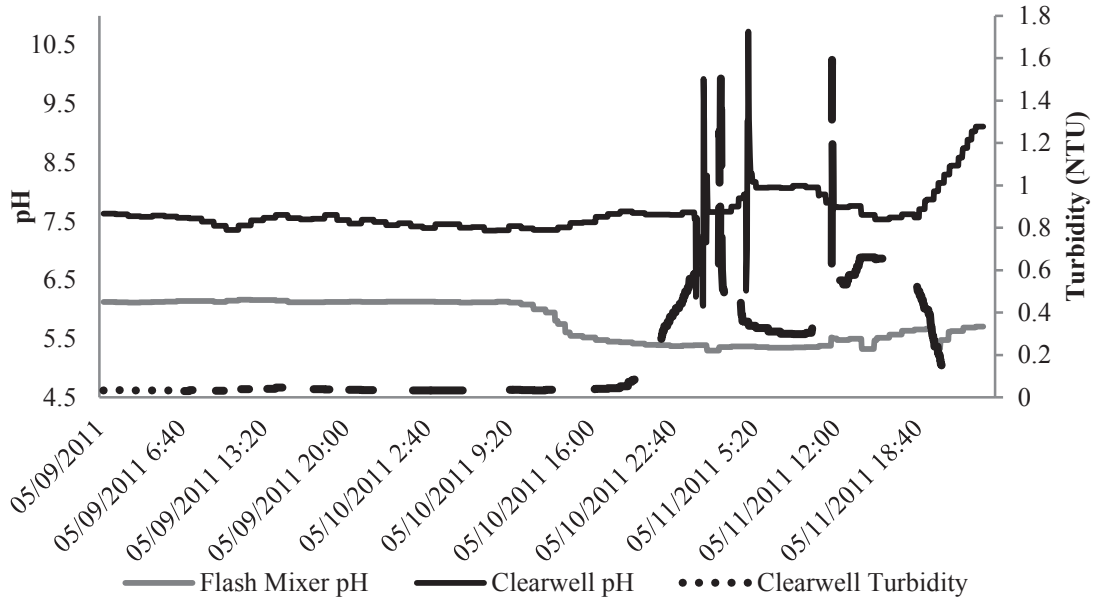

Figure A17. pH and clearwell turbidity Profile for May 11, 2011 BBWTP upset.

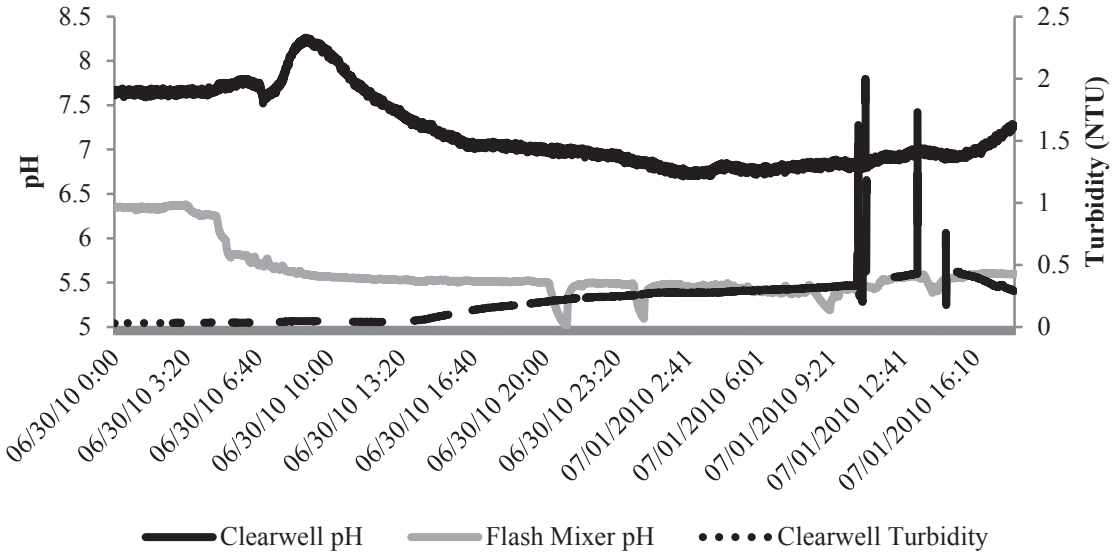

Figure A18. pH and Turbidity Profile for June 30, 2010 BBWTP upset.

Appendix B: Bench Scale DAF Testing Results

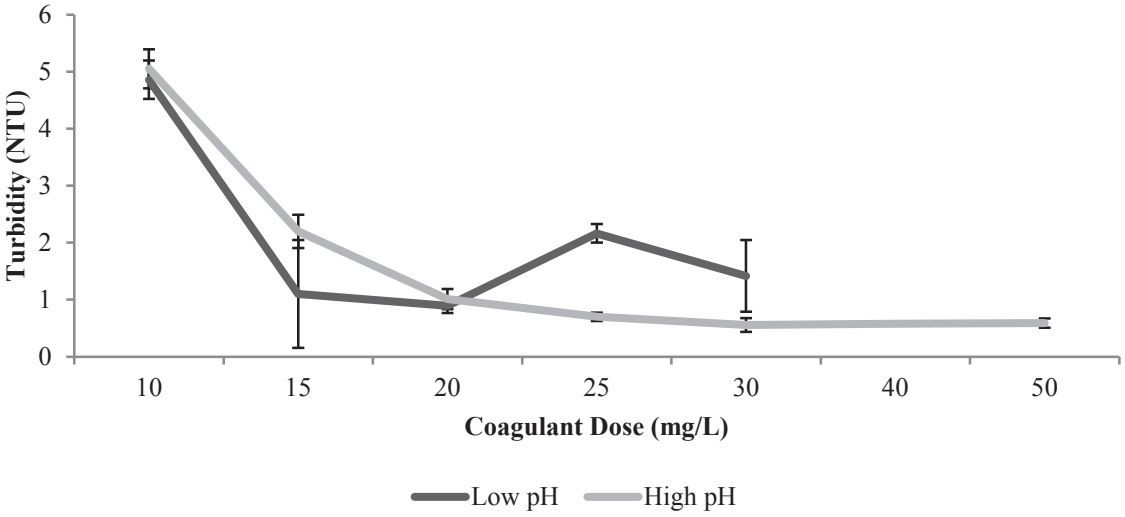

Figure B1. Effect of pH on clarified water turbidity during baseline raw water trials.

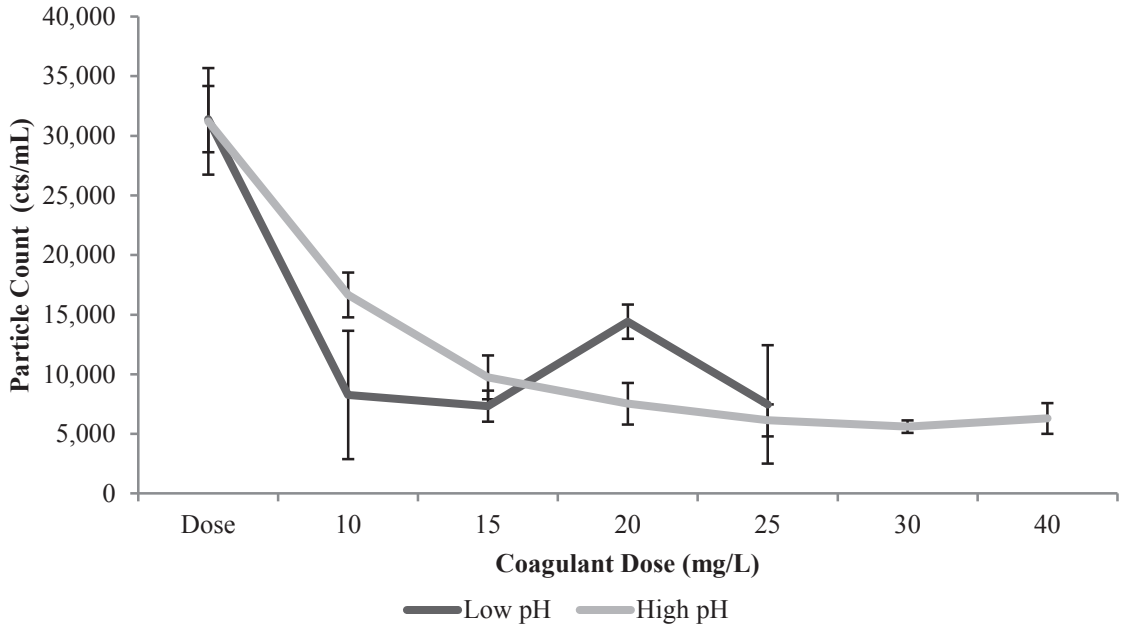

Figure B2. Effect of pH on clarified water particle count during baseline raw water trials.

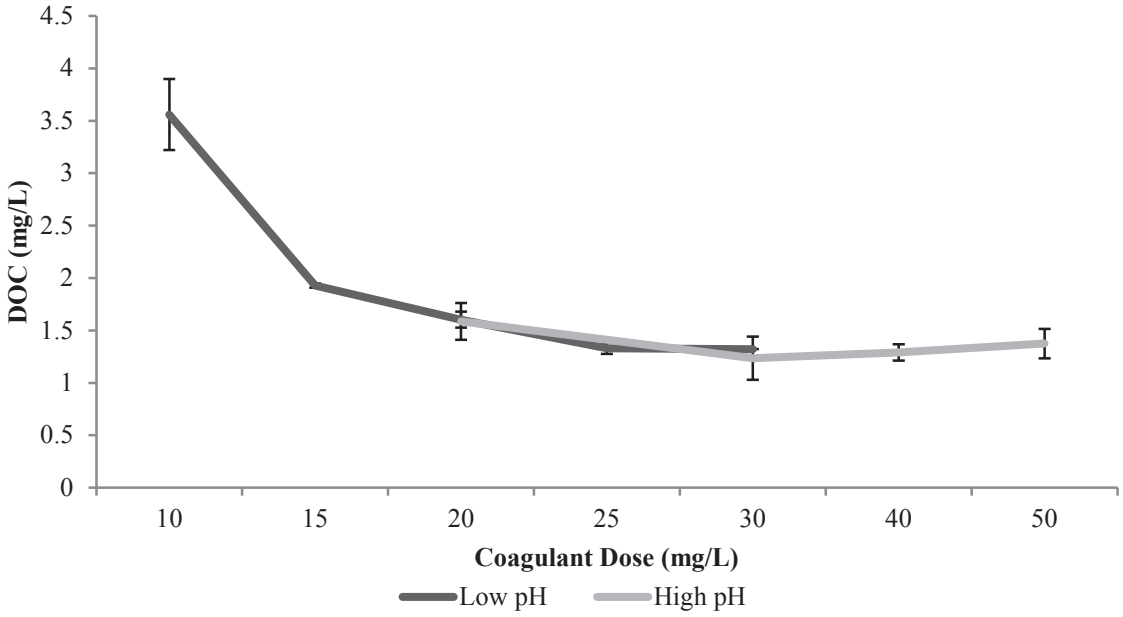

Figure B3. Effect of pH on clarified water DOC during baseline raw water trials.

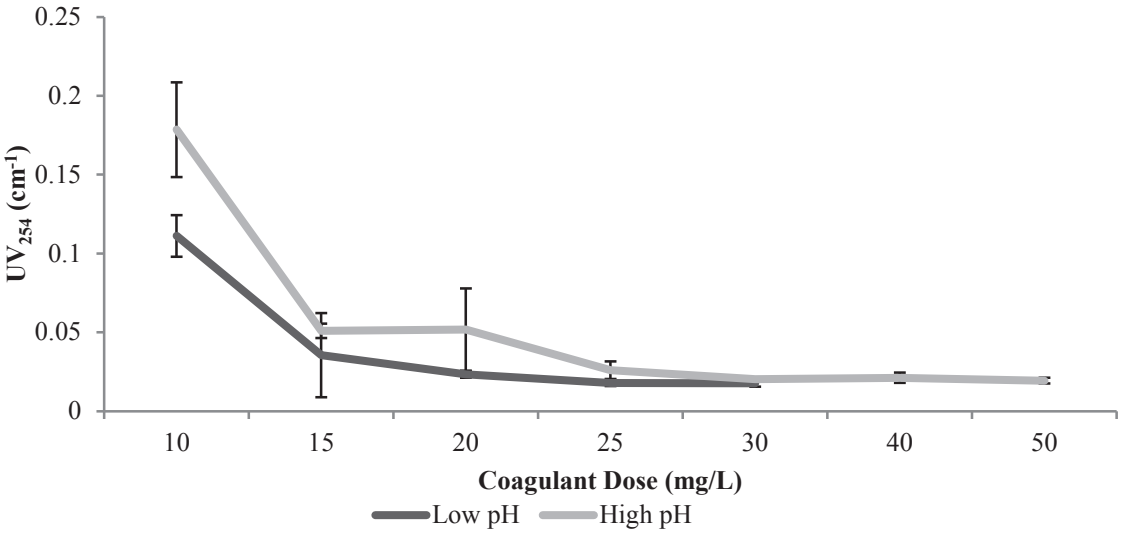

Figure B4. Effect of pH on clarified water UV_{254} during baseline raw water trials.

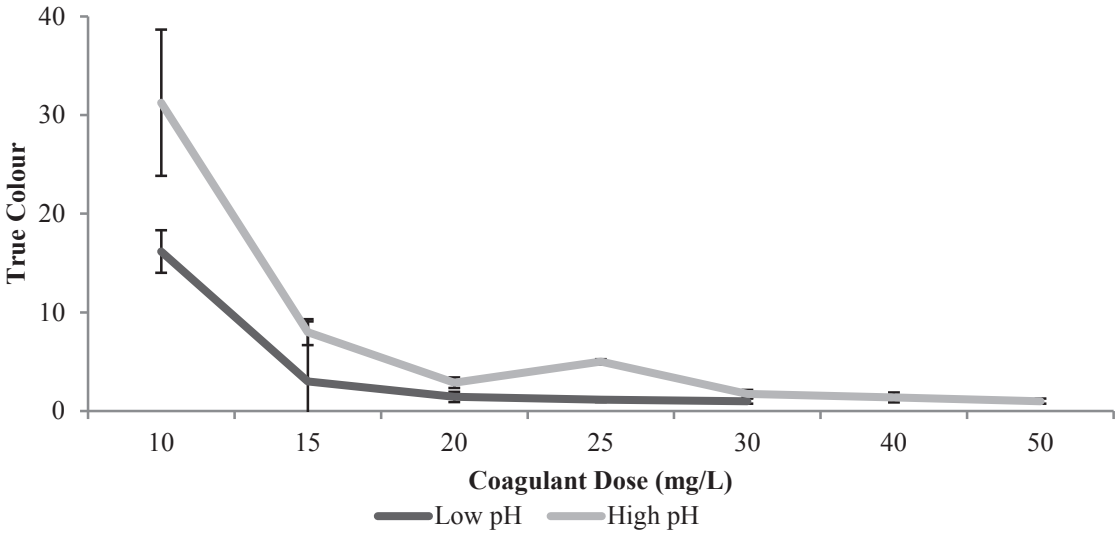

Figure B5. Effect of pH on clarified water true colour during baseline raw water trials.

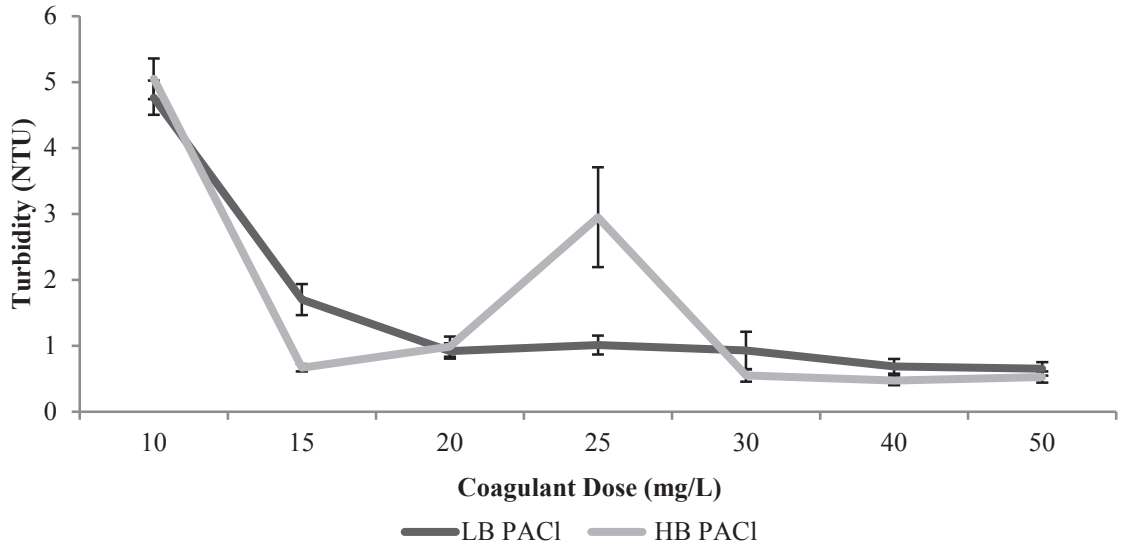

Figure B6. Effect of basicity on clarified water turbidity during baseline raw water trials.

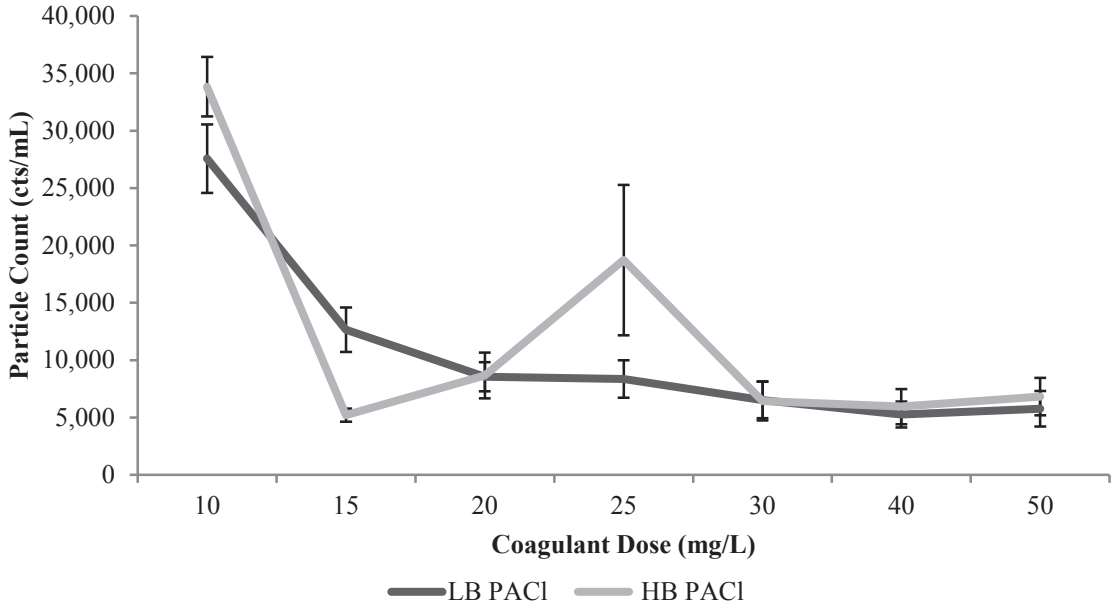

Figure B7. Effect of basicity on clarified water particle count during baseline raw water trials.

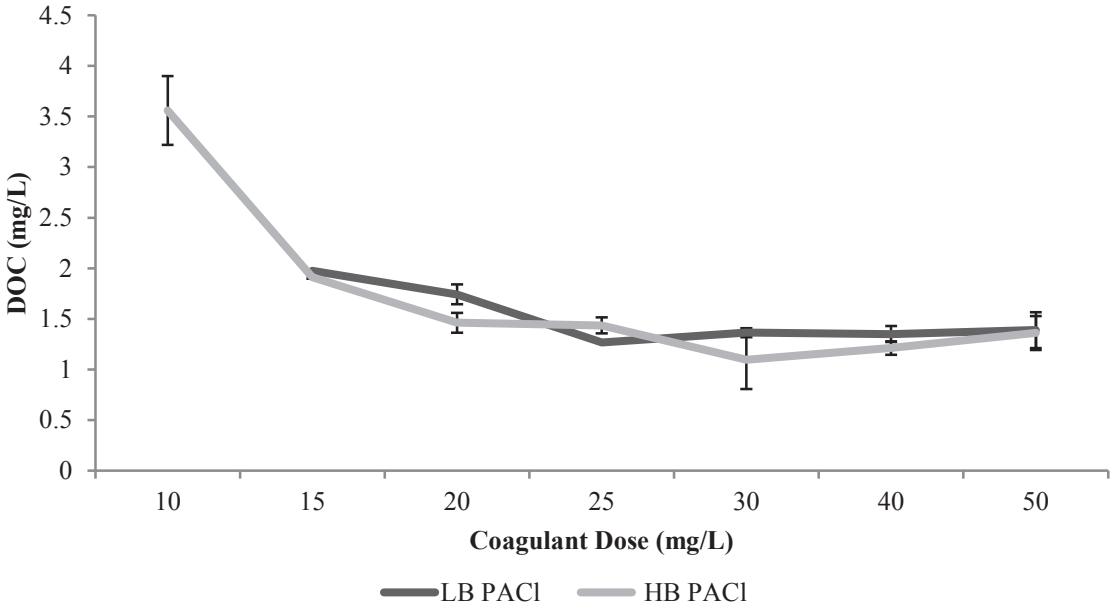

Figure B8. Effect of basicity on clarified water DOC during baseline raw water trials.

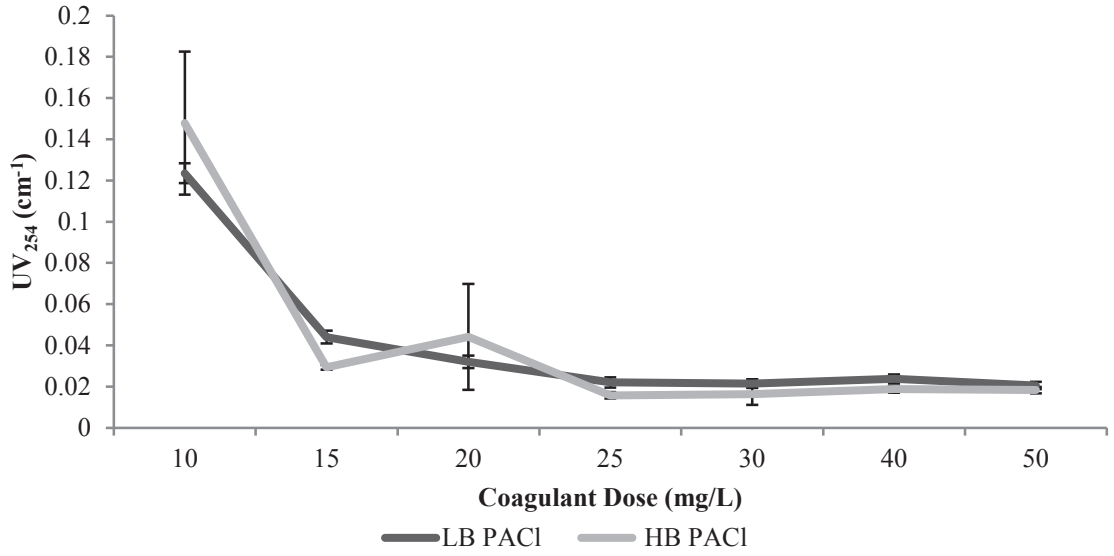

Figure B9. Effect of basicity on clarified water UV_{254} during baseline raw water trials.

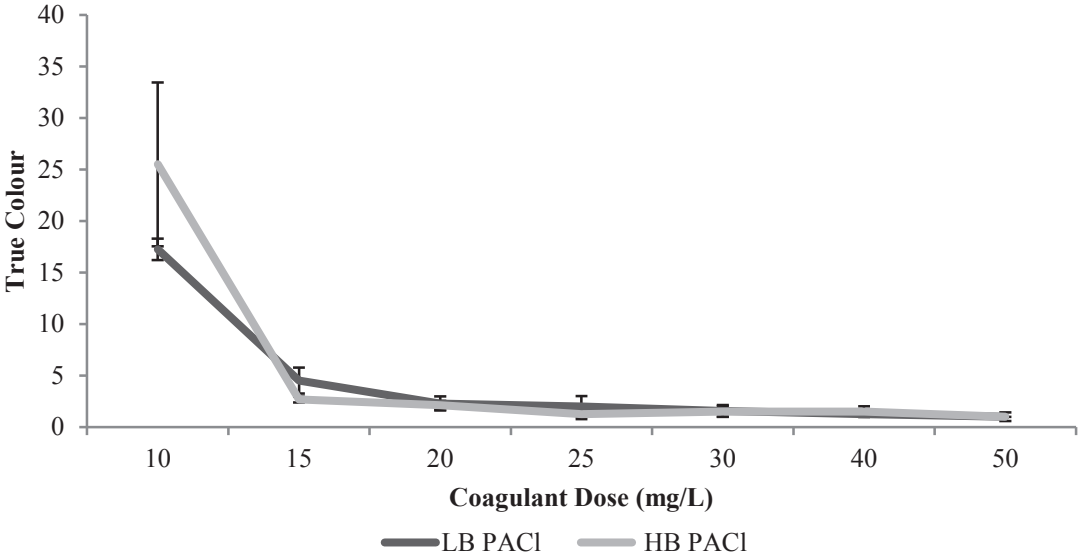

Figure B10. Effect of basicity on clarified water true colour during baseline raw water trials.

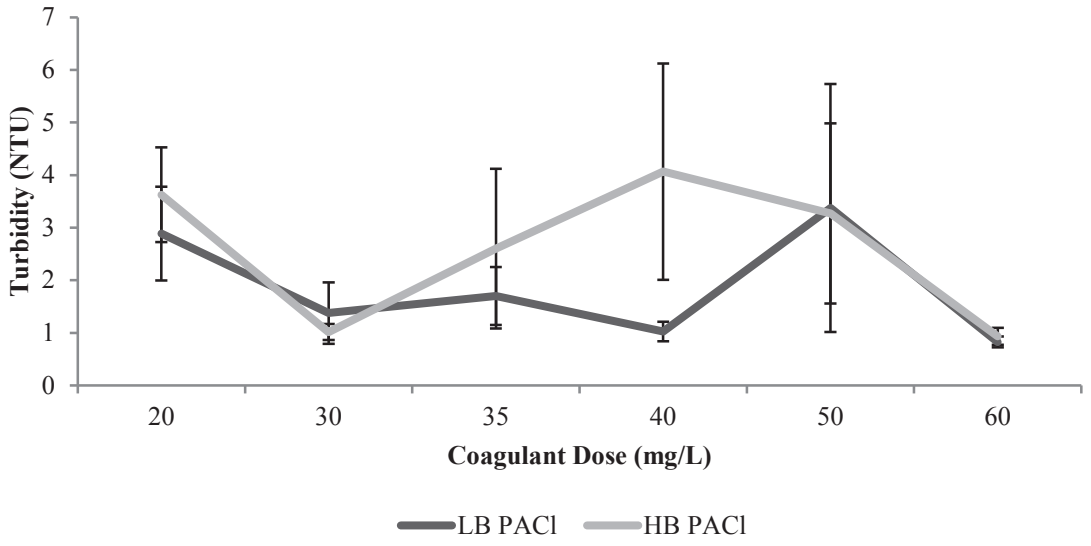

Figure B11. Effect of basicity on clarified water turbidity during synthetic challenge raw water trials.

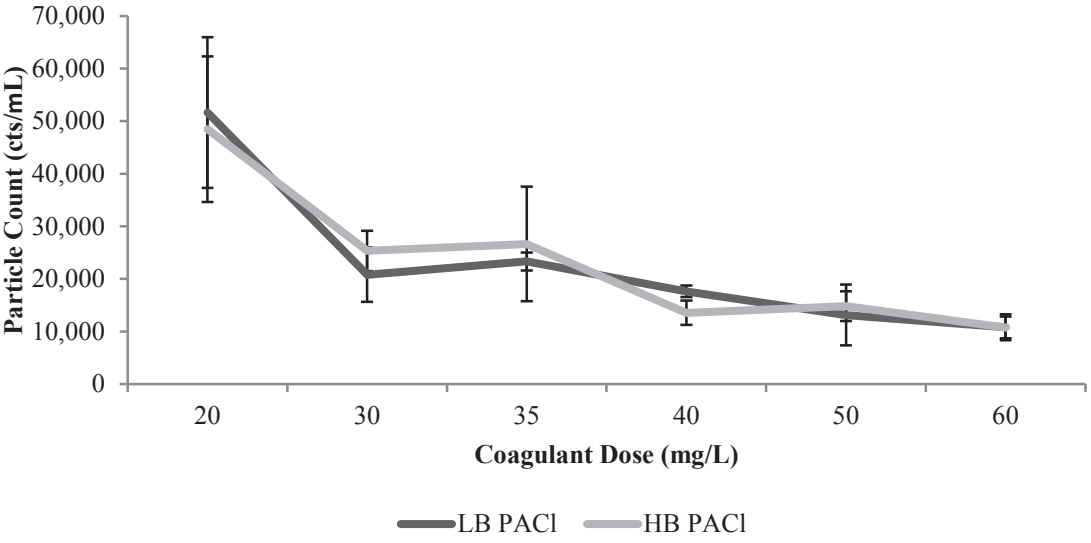

Figure B12. Effect of basicity of clarified water particle count during synthetic challenge raw water trials.

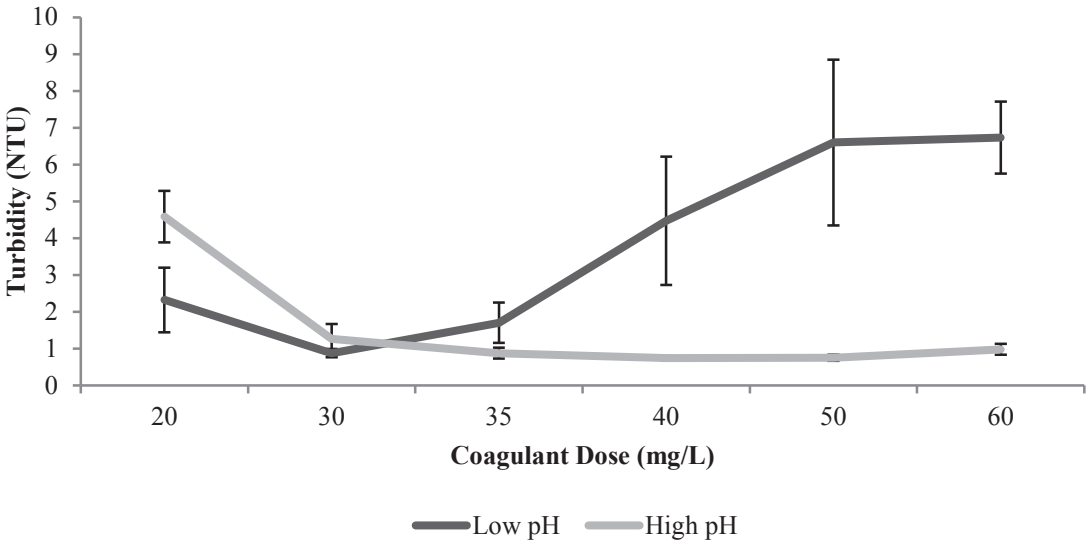

Figure B13. Effect of pH on clarified water turbidity during synthetic challenge raw water trials.

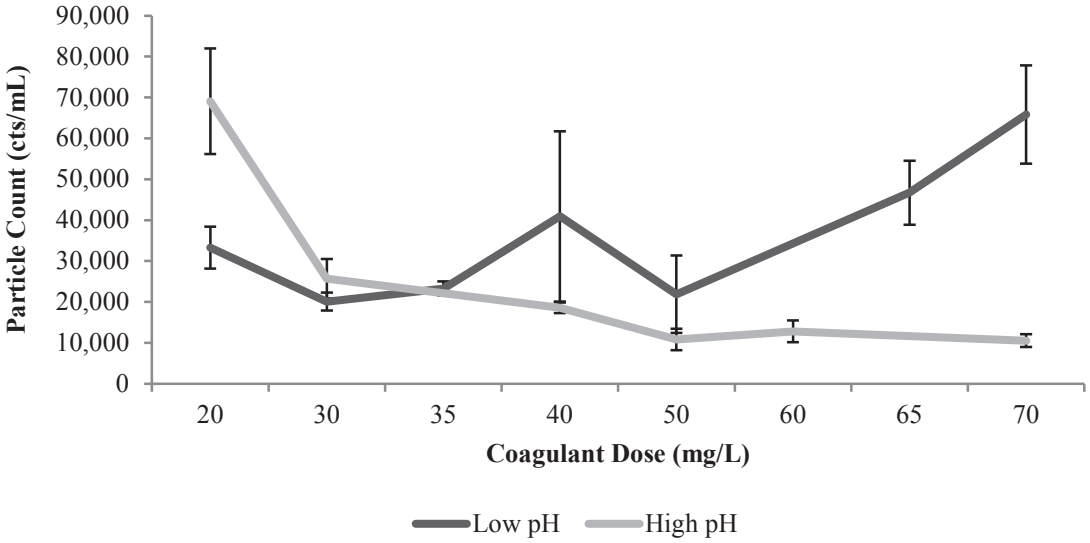

Figure B14. Effect of pH on clarified water particle count during synthetic challenge raw water trials.

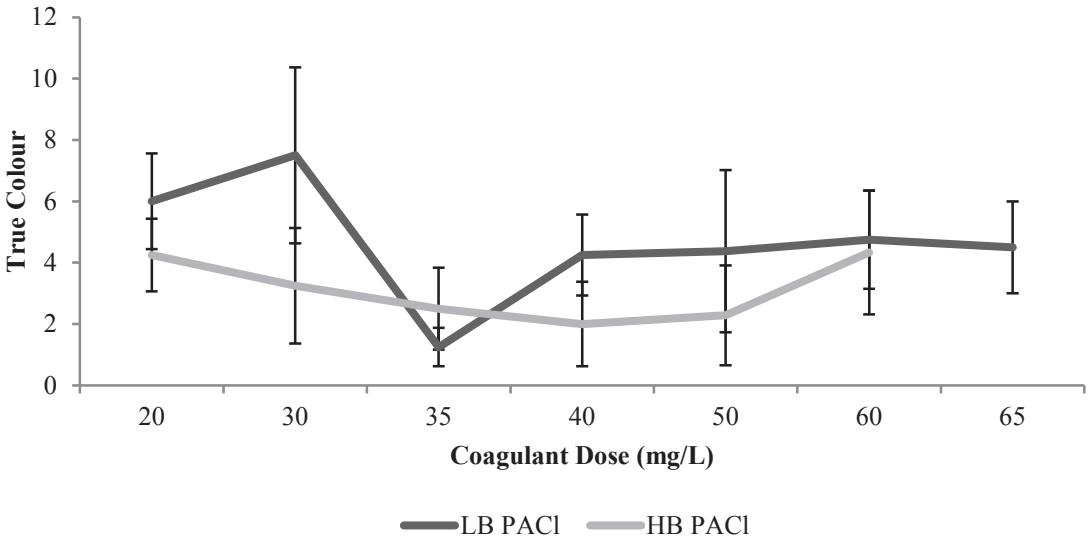

Figure B15. Effect of basicity on clarified water true colour during synthetic challenge raw water trials.

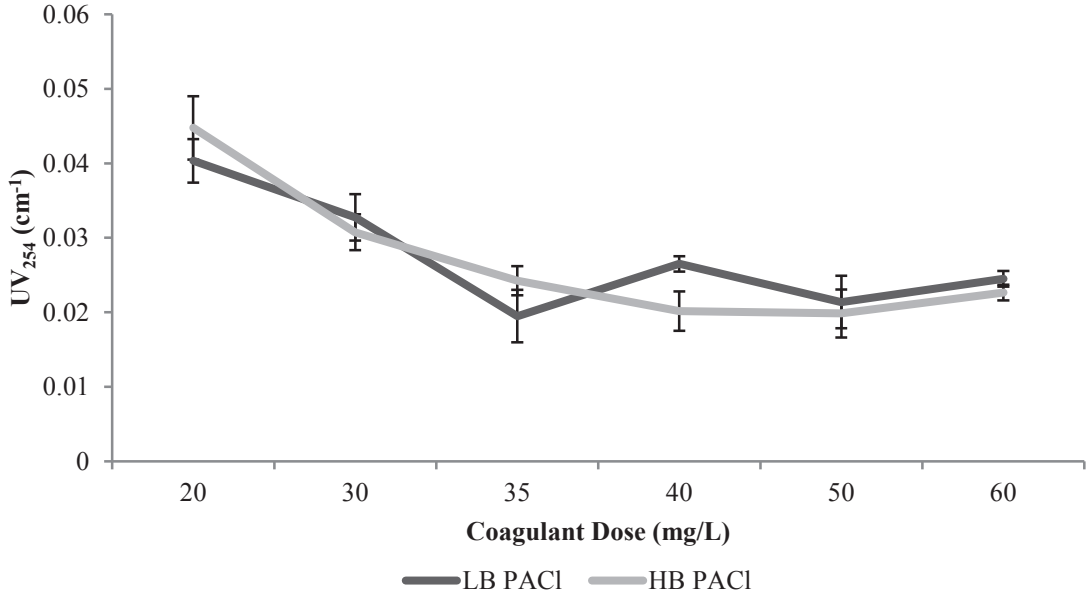

Figure B16. Effect of basicity on clarified water UV_{254} during synthetic challenge raw water trials.

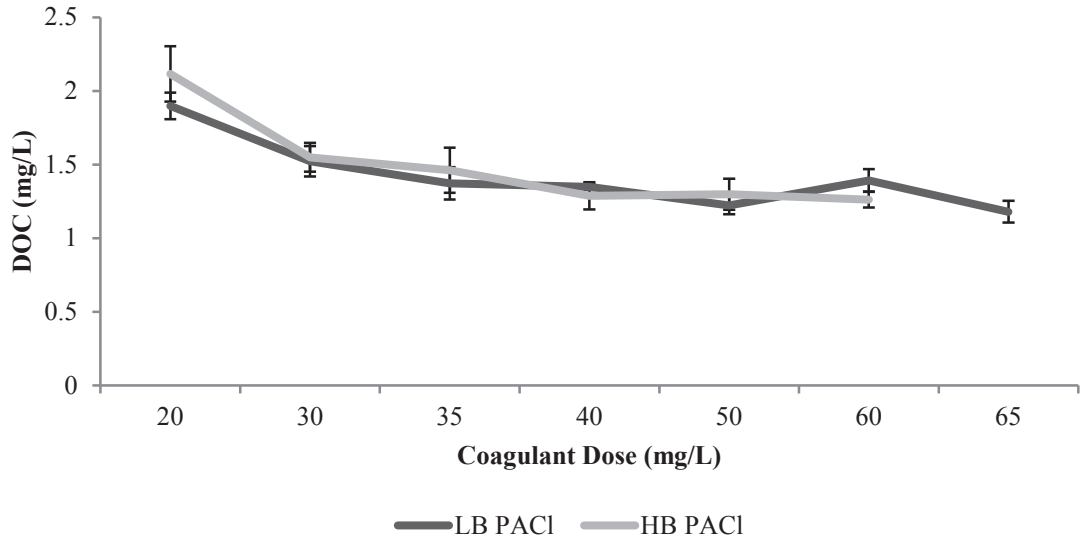

Figure B17. Effect of basicity on clarified water DOC during synthetic challenge raw water trials.

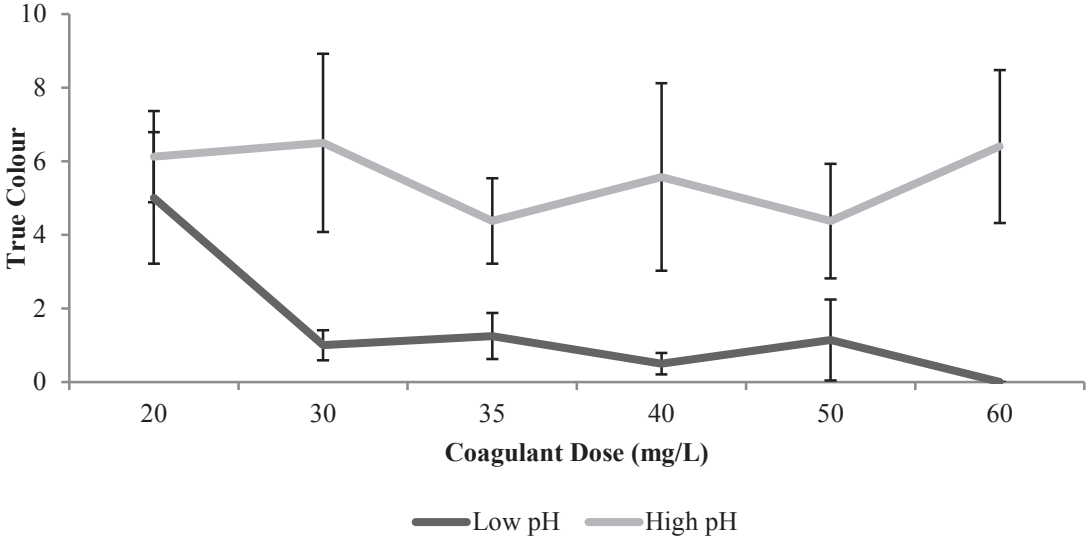

Figure B18. Effect of pH on clarified water true colour during synthetic challenge raw water trials.

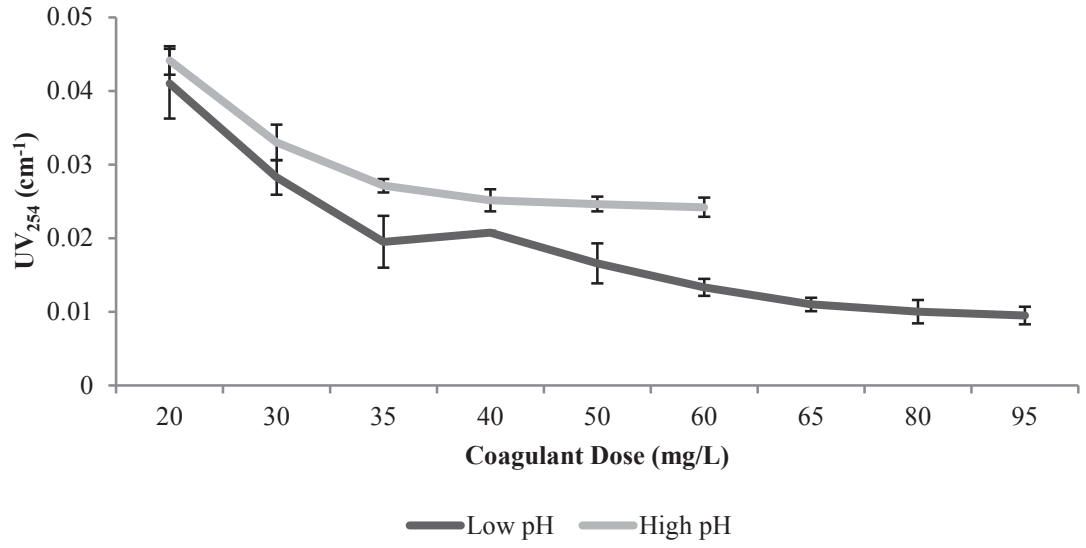

Figure B19. Effect of pH on clarified water UV_{254} during synthetic challenge raw water trials.

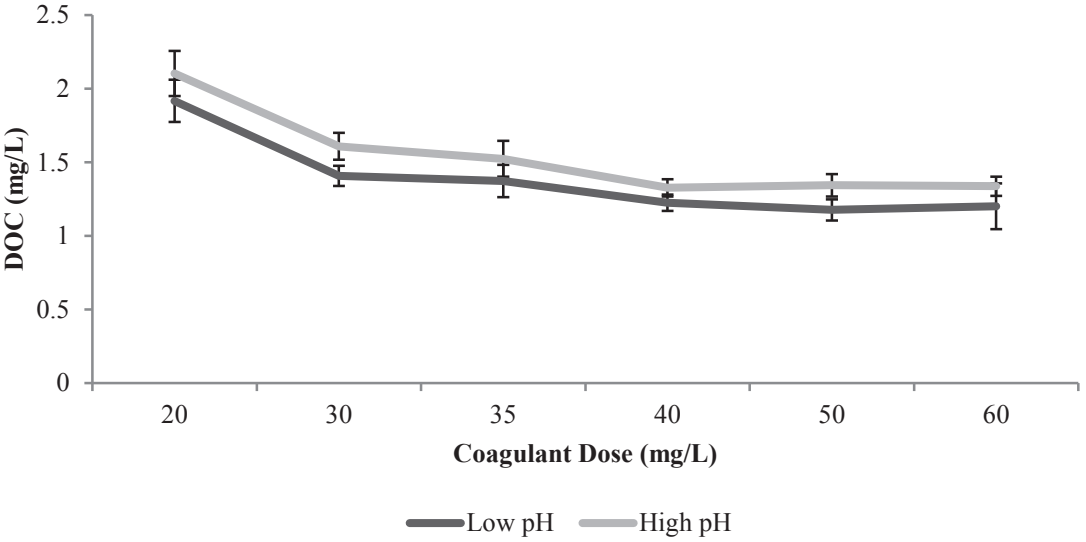

Figure B20. Effect of pH on clarified water DOC during synthetic challenge raw water trials.

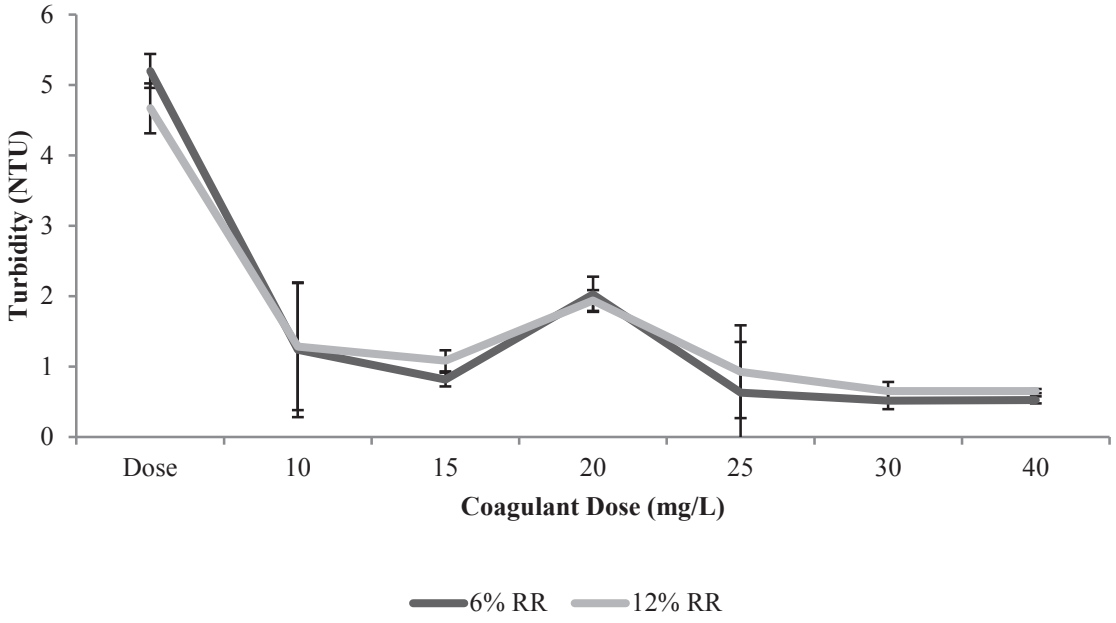

Figure B21. Effect of recycle rate on clarified water turbidity during baseline raw water trials.

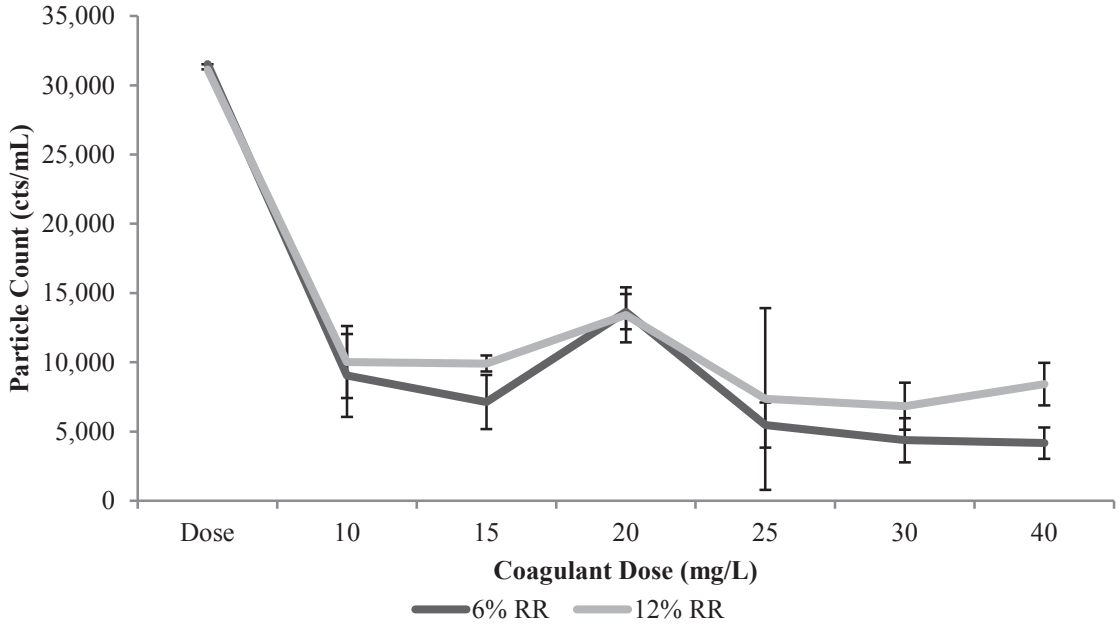

Figure B22. Effect of recycle rate on clarified water particle count during baseline raw water trials.

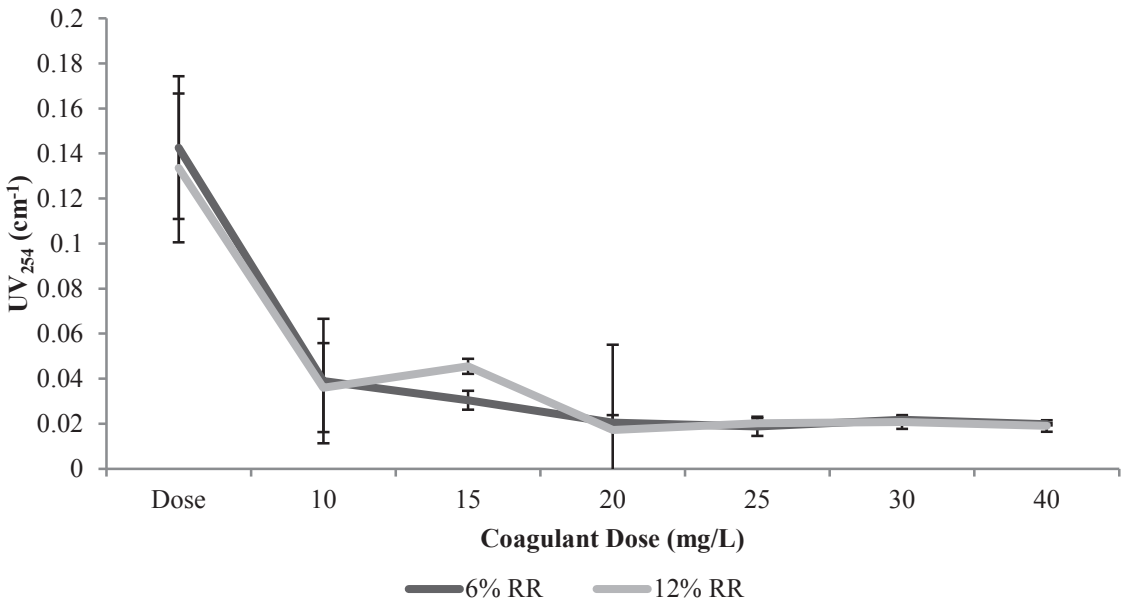

Figure B23. Effect of recycle rate on clarified water UV_{254} during baseline raw water trials.

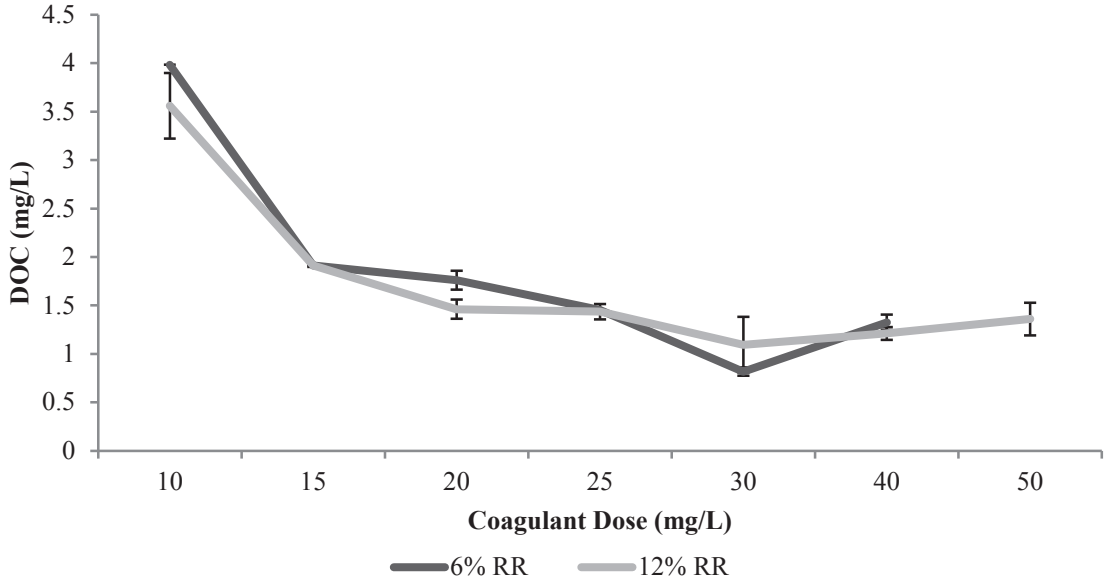

Figure B24. Effect of recycle rate on clarified water DOC during baseline raw water trials.

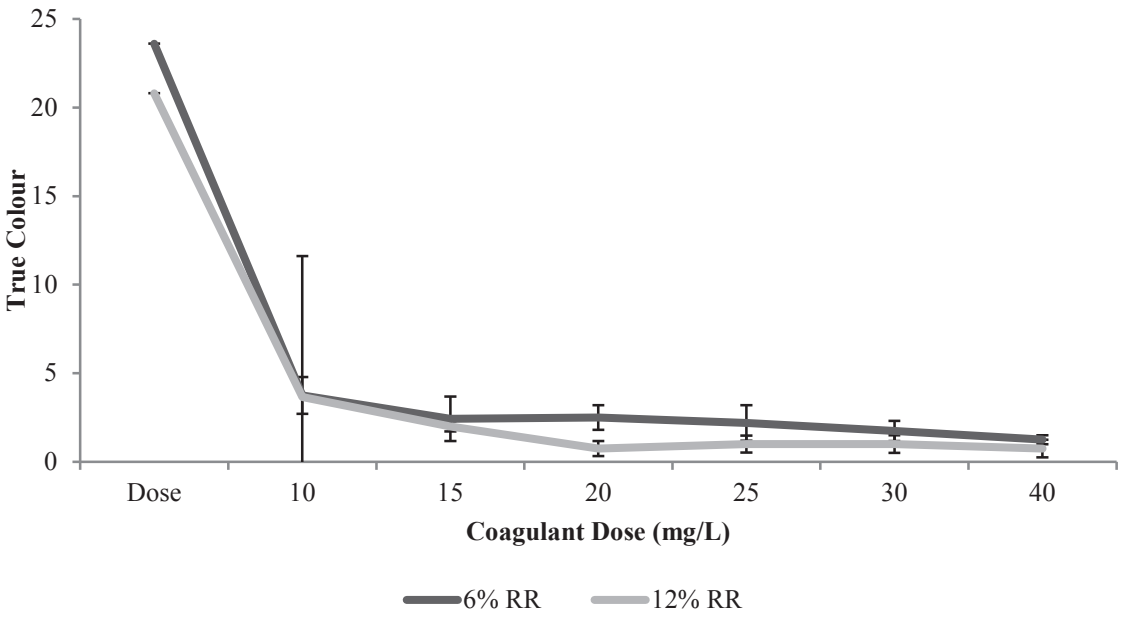

Figure B25. Effect of recycle rate on clarified water true colour during baseline raw water trials.

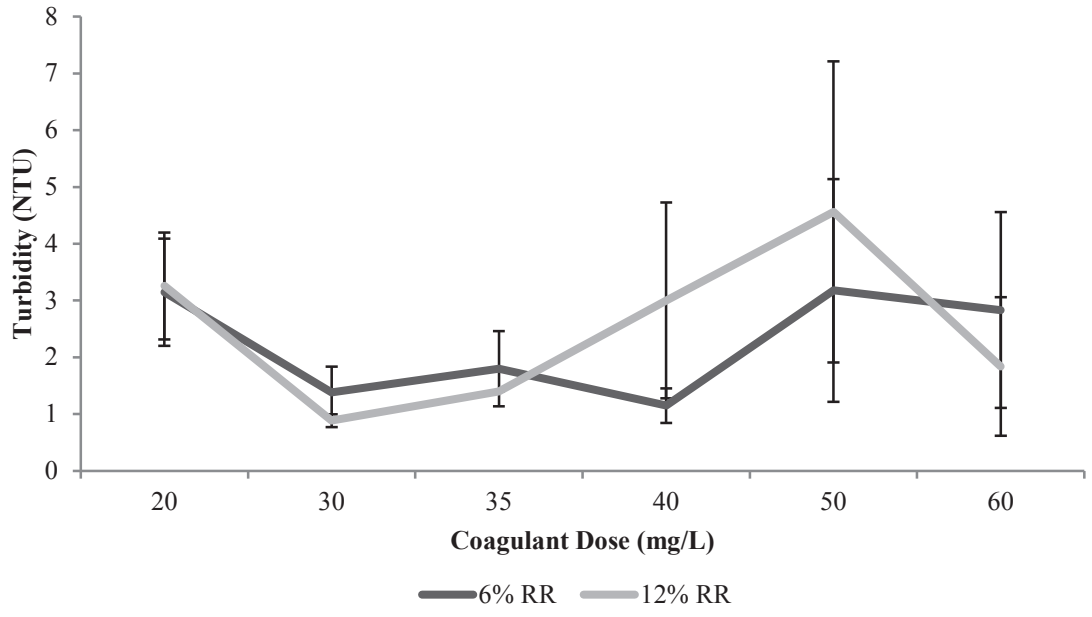

Figure B26. Effect of recycle rate on clarified water turbidity during synthetic challenge raw water trials.

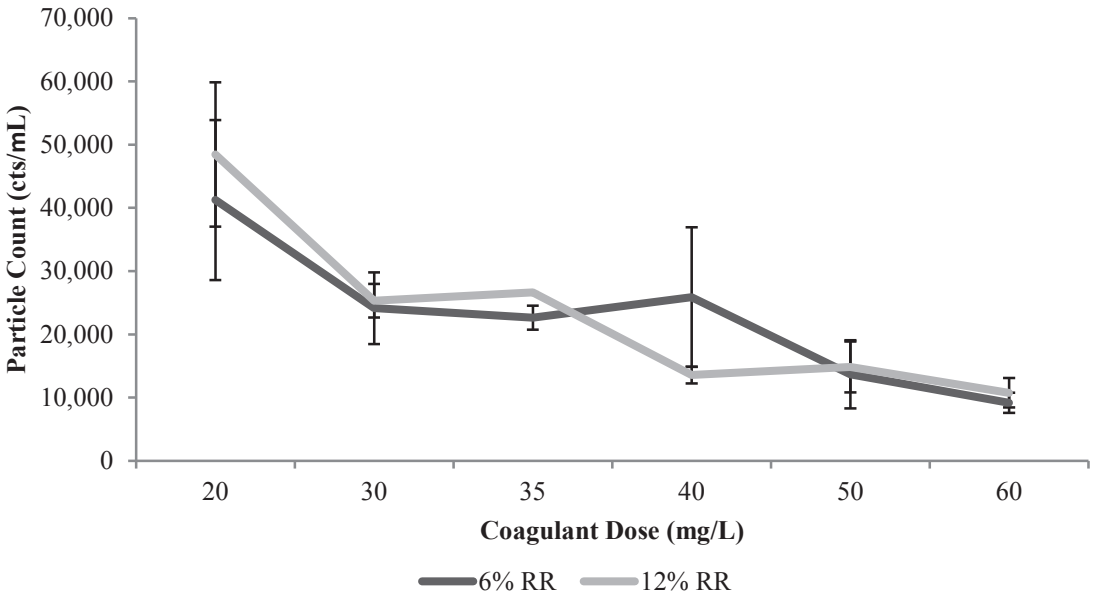

Figure B27. Effect of recycle rate on clarified water particle count during synthetic challenge raw water trials.

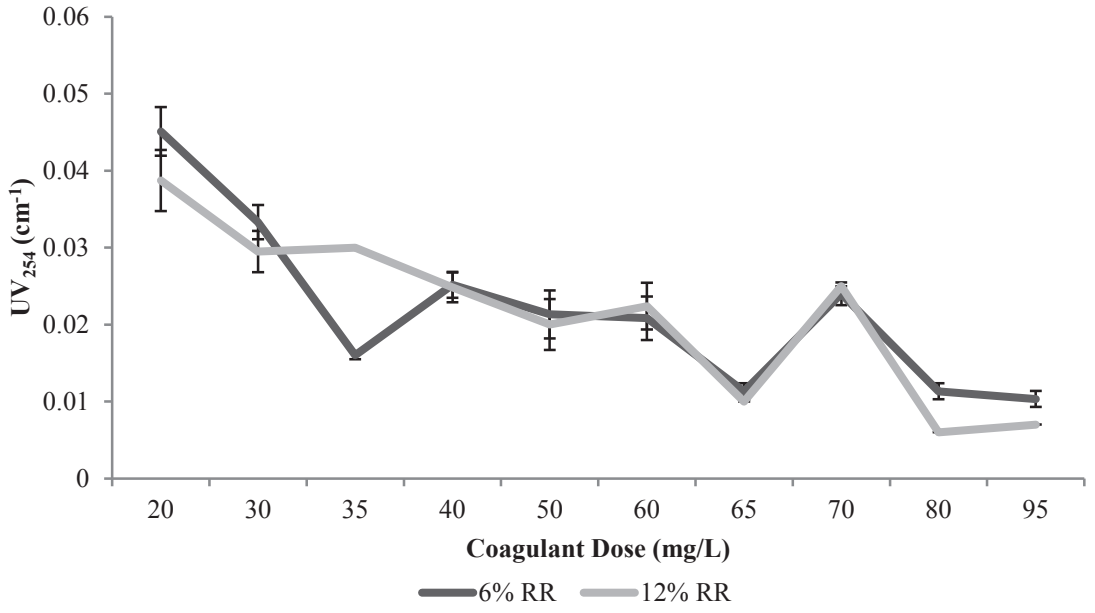

Figure B28. Effect of recycle rate on clarified water UV_{254} during synthetic challenge raw water trials.

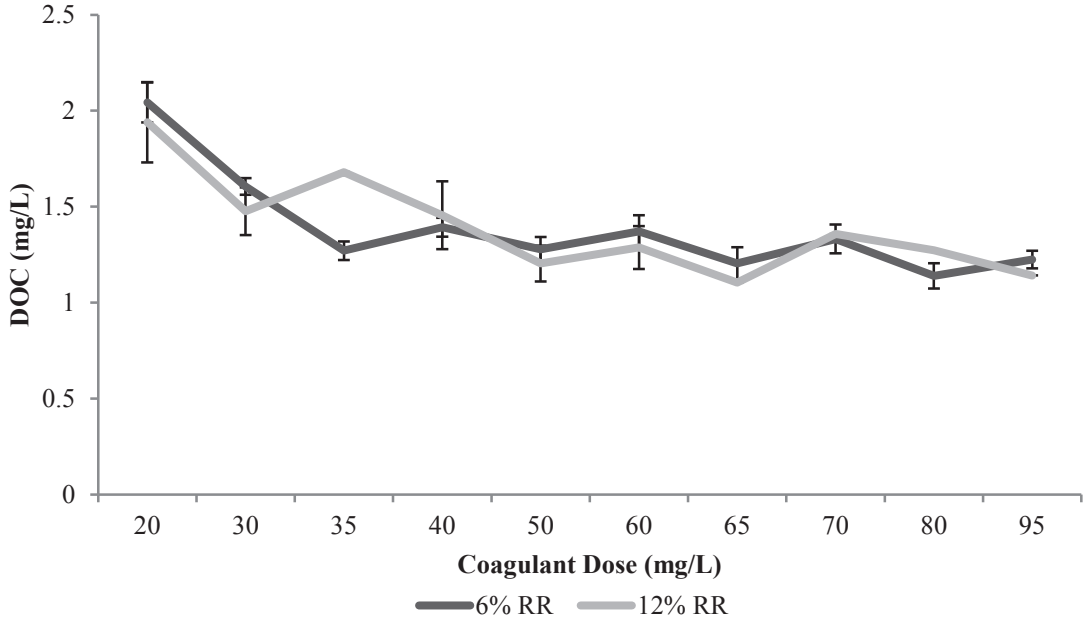

Figure B29. Effect of recycle rate on clarified water DOC during synthetic challenge raw water trials.

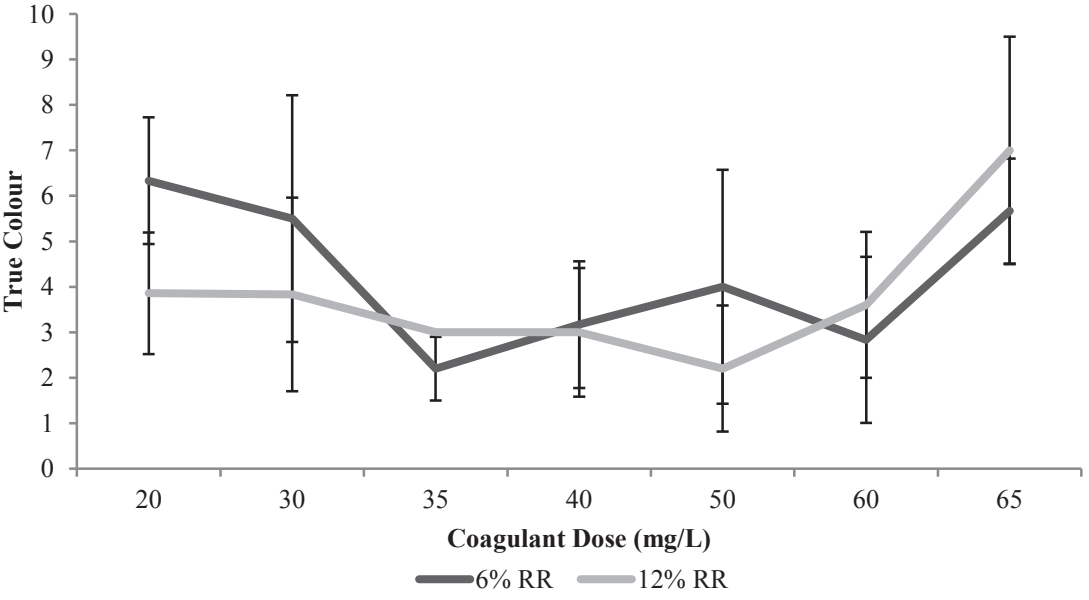

Figure B30. Effect of recycle rate on clarified water true colour during synthetic challenge raw water trials.